GEOBIOLOGICAL FEEDBACKS AND THE EVOLUTION OF THERMOPHILES IN YELLOWSTONE NATIONAL PARK HOT SPRINGS

by

Maria Clara Fernandes Martins

A dissertation submitted in partial fulfillment
of the requirements for the degree

of

Doctor of Philosophy

in

Microbiology and Cell Biology

MONTANA STATE UNIVERSITY
Bozeman, Montana

May 2024

DEDICATION

This thesis is dedicated to my late grandfather, Waldyr Fernandes, and to my late best friend, Anaïs Fiorani. Your lives and lights will always guide me, and I will forever honor you.

ACKNOWLEDGEMENTS

I would like to acknowledge all the teachers I have encountered in my life, especially a few of them who showed me unconditional care, support, and inspiration. First, my mom, Elisabeth F. Fernandes, who is always able to live life in a beautiful, sunshine light that doesn't stop beaming. Her infinite strength, courage, happiness, creativity, and love has been the road I've been walking and collecting stones for my own path. As she always had a strong demand for education, I hope this is proof that I have been listening.

The second is Dr. Demison Motta, a theoretical physicist who was my cosmology teacher during my undergraduate course in Brazil. Being exposed to the mysteries of the Universe by Dr. Motta made me want to go on my own quest related to the mysteries of the origin and distribution of life on Earth and elsewhere. The third and fourth are Dr. Robson Leão and Dr. Elizabeth Marques, both professors and researchers, that gave me the opportunity to learn the fundamentals of microbiology research with an extremely dedicated and supportive team during my undergraduate course in Brazil.

The fifth is Dr. Eric Boyd, who has been my biggest inspiration for the past eight years of undergraduate and graduate work. Dr. Boyd's holistic approach in advising his students and in pursing questions in environmental microbiology has shaped me both personally and professionally. I'm immensely grateful for his belief in me and support over all these years. I'm also grateful to everyone in the Boyd lab and my committee members for all the exchanges and productive discussions. In addition, I thank the Molecular Bioscience Program, and the family of Beverly Ferguson for financial aid during my graduate work. Finally, Luna (cat) and Astro (dog), your warmth and silliness are a source of life I've been lucky and honored to be around.

TABLE OF CONTENTS

TABLE OF CONTENTS CONTINUED

TABLE OF CONTENTS CONTINUED

LIST OF TABLES

Table Page

LIST OF FIGURES

Figure Page

LIST OF FIGURES CONTINUED

ABSTRACT

This dissertation focuses on identifying the geobiological feedbacks that shaped the evolutionary ecology of thermophiles in Yellowstone National Park (YNP) hot springs. Hot springs can generally be grouped as acidic, moderately acidic, and neutral to alkaline. Although the geochemistry and microbiology of YNP hot springs have been studied for over a century, fundamental gaps in the understanding of the feedbacks between them remain. Here, the influence of fluid mixing regime on geochemistry, microbial diversity, and productivity was investigated in three geographically co-localized springs whose communities are supported by chemical energy. The results indicate that a higher degree of disequilibrium in electron donor/acceptor pairs due to mixing of highly reduced volcanic gases and oxidized near surface waters was present in the moderately acidic hot spring, which supported higher biodiversity and primary productivity. In contrast, the acidic hot spring had the lowest biodiversity and productivity. Interestingly, acidic springs are generally dominated by members of the archaeal order Sulfolobales which have been suggested to mediate the acidification of these environments through aerobic elemental sulfur (S_8^0) oxidation that produces sulfuric acid (H_2SO_4).

Intriguingly, Sulfolobales encode the protein sulfide:quinone oxidoreductase (SQR), proposed to catalyze the oxidation of sulfide (H_2S). However, this metabolism has yet to be demonstrated. Five novel Sulfolobales strains were isolated under H_2S-oxidizing conditions from YNP. This activity was coupled to growth and H_2SO_4 production, expanding the role of Sulfolobales in the oxidative sulfur cycle. S_8^0 oxidation in these strains was also investigated due to the observation that nearly half of Sulfolobales don't encode sulfur oxidoreductase (SOR), the canonical pathway of S_8^0 oxidation in Sulfolobales. Two Sulfolobales strains were selected, one of which encoded SOR and the other of which did not. SOR disproportionates S_8^0, yielding H_2S as a product. Since H_2S can react with S_8^0, promoting its solubilization, it was hypothesized that the strain encoding SOR could grow via indirect contact to the mineral while the non-SOR encoding would need direct contact. This was confirmed through experiments where S_8^0 was sequestered in dialysis membranes. Interestingly, the non-SOR strain was able to grow via indirect contact when H_2S was added to the culture media to mimic SOR mechanism. The results shown here provide new insight into the geological and biological feedbacks that shaped the evolution, ecology, and physiology of thermophiles.

CHAPTER ONE

GENERAL INTRODUCTION

Continental Volcanic Hydrothermal Environments

Continental volcanic hydrothermal environments occur when a source of heat derived from hot spots or from plate boundaries (i.e., divergent, or convergent formation) and a source of water (i.e., deep aquifers and/or groundwater, both of which are recharged by snowmelt and/or rainfall) interact (Heasler et al., 2009). The largest surface expression of an active continental hydrothermal system on Earth is in Yellowstone National Park (YNP), Wyoming, USA (Huang et al., 2015) and thus, it has been one of the most studied. The current location of YNP and its surface expression is part of what is known as the age progressing Yellowstone-Snake River Plain (YSRP) volcanic chain system. The YSRP has moved in the SW-NE direction for the last ~ 17 Ma as a result of a hot spot in the mantle and displacement of the North America plate (Christiansen, 2001; Christiansen et al., 2007). The current location of the YSRP, which sits in YNP, is the youngest manifestation of a bimodal basalt-rhyolite magma expression, with the first eruption happening ~ 2 Ma and the last one ~ 0.6 Ma (Christiansen, 2001; Christiansen et al., 2007; Smith et al., 2009; Farrell et al., 2014).

The YNP hydrothermal system is sustained by infiltration of groundwater along faults and fissures. The chemical and isotopic composition of water is altered through water-rock interactions as it percolates through the bedrock to ultimately form the deep aquifer reservoir or parent fluid that is heated by magma (Truesdell and Fournier, 1976; Rye and Truesdell, 1993). These fluids have residence times, estimated to be hundreds to thousands of years (Sturchio et

al., 1993; Sims et al., 2023). Ultimately, the low density, hot fluid (estimated to be ~350ºC; (Fournier, 1989)) rises to the surface through convection and is further altered by water-rock interactions, mixing, and phase separation resulting from decompressional boiling of ascending fluids. Decompressional boiling results in the separation of fluids into a liquid phase that inherits most of charged species, such as chloride (Cl^-), and a vapor phase that inherits most of the volatile species such as hydrogen sulfide (H_2S), carbon dioxide (CO_2), methane (CH_4), and hydrogen (H_2). Both phases eventually discharge at the surface (separately or mixed) and can further interact with shallow groundwater to yield the >10,000 mudpots, hot springs, fumaroles, and geysers that can be found in YNP (Allen and Day, 1935; Truesdell and Fournier, 1976; White, 1988; Fournier, 1989; Rye and Truesdell, 1993; Nordstrom et al., 2005b; Nordstrom et al., 2009b; Lowenstern et al., 2012; Hurwitz and Lowenstern, 2014; Lowenstern et al., 2015).

More than 150 years of study are beginning to manifest in a robust understanding of the complexity of the hydrothermal system in YNP, which can be applied to our understanding of hydrothermal processes more generally (Davis, 1897). For example, the bimodal pH distribution of hot springs occurs across hydrothermal environments on Earth but has been extensively studied in YNP (Allen and Day, 1935; Brock, 1971; Nordstrom et al., 2005b; Nordstrom et al., 2009b). In YNP, nearly half of hot springs can be classified as acid-sulfate (AS) or acid-sulfate-chloride (ASC) waters with a pH < 4, because they are mainly influenced by the vapor phase and are buffered by sulfuric acid. Alternatively, neutral to alkaline waters exhibit pH > 6.5. These can be either alkaline-siliceous (AS) waters or calcium-carbonate (CC) waters. Within and near the boundaries of YNP last caldera formation, AS waters can be formed because they are mainly influenced by the liquid phase (e.g., carrying anions), are saturated in silica due to water-rock

interactions involving rhyolitic bedrock (silicate-rich), and are primarily buffered by dissolved bicarbonate from deep magmatic gases. Outside of the caldera boundary, CC waters can be found, and these are influenced by groundwater being heated in the subsurface and becoming enriched in calcium and carbonate through dissolution of carbonate bedrock (Fournier, 1989; Chafetz and Guidry, 2003; Fouke, 2011; Hurwitz and Lowenstern, 2014).

Alongside the continued exploration of the physical and chemical processes that dictate the composition of hot spring fluids in YNP, a growing interest in the biology supported by hot springs arose, with the first scientific article about microbiology in YNP hot springs published 121 years ago (Setchell, 1903). This interest was re-established in the 1960s with the groundbreaking work of a graduate student at Montana State University, James Brierley (Brierley, 1966), and the pioneering work from a professor of bacteriology at the University of Wisconsin, Thomas Brock (Brock, 1967; Brock and Freeze, 1969). Since then, much has been learned about how diverse these communities can be, how connected microbial activity (i.e., transformation of elements and compounds) is to complex geochemical cycles, and how microbial activities can impact the environment (e.g., precipitation of minerals) (Stetter et al., 1990; Amend, 2001; Meyer-Dombard et al., 2005; Nordstrom et al., 2005b; Spear et al., 2005; Inskeep et al., 2010; Shock et al., 2010; Boyd et al., 2012; Inskeep et al., 2013; Lindsay et al., 2018; Colman et al., 2019b).

More recent research into the biology of YNP hot springs has been motivated by an interest to better understand life's limits, environmental drivers of its evolution, and the potential for hydrothermal environments on other planets to support life. This is because the poly extreme conditions in hydrothermal environments resemble what was likely occurring on early Earth and

it's a suitable natural laboratory to examine the habitability limits of life (Shock and Holland, 2007). Indeed, many microorganisms in hot springs are deep branching on taxonomic phylogenies and have short branch lengths, indicating that they have evolved little relative to the Last Universal Common Ancestor (LUCA) and relative to more derived lineages (Pace, 1997; Bhattacharya et al., 1999; Giulio, 2003; Schwartzman and Lineweaver, 2004; Ciccarelli et al., 2006). Further, representatives of many of these early diverging and thermophilic lineages are dependent on inorganic compounds supplied by the hydrothermal environment to fix CO_2 and support growth (chemolithoautotrophy), a microbial process that is inferred to be ancestral (Thauer et al., 1977). In addition to the astrobiology community, thermophilic microorganisms are of keen interest to the field of biotechnology, where breakthroughs have been achieved, with possibly many more applications still to be discovered (Mehta et al., 2016). A classic example was the isolation of *Thermus aquaticus* and the industrialization of its DNA polymerase I enzyme, known as *Taq* polymerase, which revolutionized molecular biology and diagnostic medicine with the polymerase chain reaction (PCR) (Brock and Freeze, 1969; Chien et al., 1976; Saiki et al., 1985; Ishino and Ishino, 2014).

Although each of the >10,000 thermal features in Yellowstone are unique, patterns in the distribution of microorganisms and their functions can generally be predicted based on geochemical factors (e.g., pH and temperatures) that govern microbial fitness by influencing nutrient and energy availability and/or biochemical compatibility. A prime example is the absence of photosynthetic microorganisms that derive energy from light to drive primary production in high temperature hot springs at temperatures exceeding ~70°C in moderately acidic to alkaline springs (pH >4.0) and 54°C in acidic springs (pH <4.0). This is due to a combination

of temperature inhibition of a yet to be defined component(s) of photosynthetic metabolism, sulfide inhibition of photosystem II, and taxonomic differences delineated by the pH 4.0 boundary (algae only at pH <4.0, combination of Cyanobacteria and algae at pH >4.0 (Boyd et al., 2010a; Cox et al., 2011; Boyd et al., 2012; Hamilton et al., 2012). Above these temperature limits, primary productivity is supported by chemoautotrophy (chemical energy to drive primary production) only. The work described in this thesis builds on these studies and is aimed at better understanding the geobiological feedbacks between microbial activity and geochemistry. The focus of this thesis is on non-photosynthetic zones of hot springs because the influence of photosynthesis (production of organic carbon) can decouple microbial life from the volcanically influenced inorganic chemical environment that support cellular energy metabolism.

Microbial Ecology of High Temperature Hot Springs

The distribution and ecology of microorganisms in hot springs is dependent on the geochemistry of the environment (i.e., temperature, pH, dissolved gases and metals, minerology) and on the within-spring differentiation of these nutrients in the aqueous and solid phases (i.e., planktonic vs sediment communities) (Reysenbach et al., 2000; Amend, 2001; Meyer-Dombard et al., 2005; Boyd et al., 2010a; Inskeep et al., 2010; Hamilton et al., 2011; Boyd et al., 2012; Inskeep et al., 2013; Hamilton et al., 2014; Colman et al., 2016; Lindsay et al., 2018; Colman et al., 2019a). This is especially true for chemoautotrophy-based microbial communities that are dependent on inorganic electron donors and acceptors to generate energy (Amend, 2001; Shock et al., 2010). The patterns in the distribution of microorganisms and their functions observed in these chemoautotrophy-based communities (temperature ~>70°C) will be discussed on the acid-sulfate-chloride and alkaline-siliceous hot spring formations only.

Geomicrobiology of Neutral to Alkaline Hot Springs

Neutral to alkaline hot springs (pH > 6.5, temperature >70°C) are sourced by liquid-phase fluids (thought to be largely analogous to the parental hydrothermal aquifer (Fournier, 1989)). These waters can be further modified by mixing with near surface groundwater or by injection with vapor-phase gas. However, these hot springs are often formed solely by the liquid-phase input and are therefore buffered primarily by dissolved bicarbonate from deep magmatic gases. This is because the dissolved silica present in the liquid-phase can precipitate as sinters as it ascends to the surface and cools, which is hypothesized to seal the plumbing systems of these hot springs, limiting the input of nutrient-rich groundwater and vapor-phase (Vitale et al., 2008; Gibson and Hinman, 2013). This hydrological limitation results in decreased availability of dissolved organic carbon (DOC), fixed nitrogen compounds (i.e., ammonia/ammonium, nitrate (NO_3^-)) and O_2, for example, which tend to be surface derived. Therefore, neutral to alkaline hot springs are generally depleted of nutrients and tend to depend on the input of atmospheric gases (i.e., O_2, CO_2, H_2) and exogenous input of nutrients (e.g., dust, soil, plant matter) to support microbial metabolism.

Interestingly, although neutral to alkaline springs tend to have low nutrient availability, they can harbor unique macroscopic microbial biofilms, usually in the flow/outflow channel, known as “streamers”, due to the hair-like flowing structures (Reysenbach et al., 1994). Studies of these springs have therefore largely been focused on the streamers (Reysenbach et al., 1994; Huber et al., 1998; Reysenbach et al., 2000; Takacs-vesbach et al., 2013), although more recent studies have focused on the microbial communities associated with the water column (i.e., planktonic) and the sediment (Meyer-Dombard et al., 2005; Inskeep et al., 2010; Inskeep et al.,

2013; Colman et al., 2016; Lindsay et al., 2018; Fernandes-Martins et al., 2021; Sims et al., 2023). Based on 16S rRNA gene and metagenome sequencing, members of the bacterial order Aquificales (e.g., *Thermocrinis*, *Sulfurihydrogenibium*) tend to dominate the streamer and planktonic communities and are usually the only chemolithoautotrophs (primary producers) in those communities (Reysenbach et al., 1994; Reysenbach et al., 2000; Blank Carrine et al., 2002; Meyer-Dombard et al., 2005; Reysenbach et al., 2005; Inskeep et al., 2013; Colman et al., 2016). Members of the bacterial order Thermales/Deinococcales (e.g., *Thermus aquaticus*) are also found in association with the streamers and in the planktonic community but are heterotrophs and thus, thought to depend on the byproducts of the primary producers (e.g., cross-feeding of organic carbon, nitrogen compounds) (Brock and Freeze, 1969; Munster et al., 1986; Blank Carrine et al., 2002; Meyer-Dombard et al., 2011). Representatives of these bacterial orders and others (e.g., mostly uncharacterized members of Chloroflexota and the Proteobacteria phylum) as well as a few archaeal orders, such as the Desulfurococcales and Thermoproteales (e.g., uncharacterized members, *Ignisphaera*, *Pyrobaculum*, and *Thermofilum*) and members of the Korarchaeota phylum (mostly uncharacterized) are generally found in the sediment community and usually are not primary producers and depend on cross-feeding (Reysenbach et al., 1994; Reysenbach et al., 2000; Meyer-Dombard et al., 2005; Inskeep et al., 2010; Miller-Coleman et al., 2012; Inskeep et al., 2013; Colman et al., 2016; Jay et al., 2016; Lindsay et al., 2018; Sims et al., 2023).

Based on genomic inference and cultivation approaches, the dominant chemolithoautotrophs in the streamer and planktonic communities are usually supported by the aerobic oxidation of gases such as H_2 and H_2S, but also encode the ability to oxidize compounds

such as thiosulfate ($S_2O_3^{2-}$) and arsenite [(As(III)] and conduct anaerobic metabolism such as sulfur (e.g., SO_4^{2-}, S_8^0) or arsenate [As(V)] reduction with H_2, for example (Kawasumi et al., 1984; Huber et al., 1998; Nakagawa et al., 2005a; Hamamura et al., 2009). In the sediment, the communities are thought to be mostly supported by the limited mineral availability and organic byproducts of the overlaying planktonic community and, generally, are thought to conduct anaerobic metabolism based on heterotrophy, chemoorganoherotrophy (e.g., reduction of NO_3^-, SO_4^{2-} or [As(V)] compounds with organic carbon oxidation), and on some occasions, chemolithoautotrophy as well (e.g., reduction of sulfur compounds with H_2 oxidation) (Kawasumi et al., 1984; Huber et al., 1998; Jay et al., 2015; Jay et al., 2016; Lindsay et al., 2018). A lingering question of these systems relates to how these communities obtain fixed forms of nitrogen, since input of these fixed sources is limited, and homologs of genes for N_2 fixation (i.e., *nif)* are not abundant in these hot springs (Hamilton et al., 2011).

Geomicrobiology of Moderately Acidic Hot Springs

Moderately acidic hot springs ($4 > pH < 6.5$) are thought to form by the mixing of different fluid inputs: vapor-phase, liquid-phase, and groundwater (Stefánsson et al., 2016; Colman et al., 2019a). Importantly, not all three inputs need to be present for this end-result, but a vapor-phase input is typically associated with this spring type. Generally, vapor-phase input is increased in higher elevations due to the ease of gas separation from the water table along the fractures and faults present in the area (Hurwitz and Lowenstern, 2014) and thus, moderately acidic hot springs are usually found in higher elevations or in a higher elevation than nearby hot springs and are not widespread (Brock, 1971). Therefore, the investigation of these systems and associated microbial communities are less common and much less is known about the processes

that support microbial communities inhabiting these systems (Colman et al., 2019a). Because of this, the feedbacks between microbial activity in these environments and their geochemistry are less well understood.

Many of the community members found in weakly acidic hot springs are divergent and have yet to be fully characterized (Inskeep et al., 2013; Colman et al., 2019a). This is also true for differences in the composition of planktonic and sediment communities, which may be expected to be more divergent than acidic or alkaline springs based on differences in gas inputs. Recent 16S rRNA and metagenomic sequencing have indicated that representatives of novel and known bacterial and archaeal orders (e.g., characterized and uncharacterized members of Aquificales, Sulfolobales, Desulfurococcales and Thermoproteales), can be found in these high temperature communities (Meyer-Dombard et al., 2005; Inskeep et al., 2010; Inskeep et al., 2013; Colman et al., 2016; Jay et al., 2016). Metagenomic-based analyses have highlighted an enrichment of genes encoding proteins that are involved in the oxidation of gases (e.g., H_2, H_2S, carbon monoxide (CO) and methane (CH_4)) in moderately acidic hot springs (Colman et al., 2019b; Colman et al., 2019a), and this is reflected in the presence of representatives of *Thermocrinis, Hydrogenobacter, Sulfurihydrogenibium,* and members of the Sulfolobales which are known to encode metabolic flexibility and conduct aerobic oxidation of H_2 and/or H_2S, for example (Huber et al., 1998; Nakagawa et al., 2005a; Sato et al., 2012; Liu et al., 2021).

In addition, aerobic S_8^0 oxidation and facultative anaerobic metabolisms (e.g., H_2 oxidation with S_8^0, ferric iron (Fe^{3+}) or NO_3^- reduction, organic carbon oxidation with S_8^0 reduction) are encoded and have been shown to be conducted by these representatives, as well as members of the Sulfolobales (Kawasumi et al., 1984; Nakagawa et al., 2005a; Suzuki et al.,

2006; Kozubal et al., 2012; Amenabar and Boyd, 2018; Liu et al., 2021). Interestingly, the archaeal order Sulfolobales is known to dominate high temperature acidic hot springs and to be responsible for the oxidation of S_8^0, which contributes to the acidification of hot springs (discussed more below), however, the factors that influence the buffering capacity of moderately acidic hot springs (e.g., degassing, O_2 availability, minerals, physiology) need further investigation. Although little can be said about the formation of these systems and patterns that shape these microbial communities, it has been suggested that the increased disequilibrium in electron donor and electron acceptors as a result of reduced and oxidized fluid mixing, could provide a higher availability of nutrients, which in turn, could increase biodiversity through niche partitioning (Colman et al., 2019a). If these hot springs systems have higher disequilibrium in redox pair and higher biodiversity, it's reasonable to expect that the rates of primary productivity could also be higher. However, to date, little research has been conducted to evaluate the factors that control chemosynthetic primary productivity across YNP hot springs (Urschel et al., 2015; Jennings et al., 2017).

Geomicrobiology of Acidic Hot Springs

Acidic hot springs (pH > 4) are sourced by reduced volcanic gases (vapor-phase) that mix with oxygenated groundwater (acid-sulfate springs) and can be further influenced by mixing with reduced hydrothermal liquid-phase fluids (acid-sulfate-chloride springs) (Nordstrom et al., 2009b). The main factor leading to the acidification of these hot springs is the abiotic oxidation of H_2S (from the vapor-phase) by O_2 (from near surface groundwaters). This generates S_8^0 that is stable at temperatures below 100°C but results in no net production of acidity (Nordstrom et al., 2009b; Sims et al., 2023). This is why vapor-phase influenced springs tend to have high sulfur

contents. It is the oxidation of S_8^0, which is microbially-mediated, that generates SO_4^{2-} and protons (H^+) (i.e., sulfuric acid, H_2SO_4) (Schoen, 1969; Brock et al., 1972; Mosser et al., 1973). The production of acid can leach metals out of the bedrock and often acid hot spring waters are enriched in metals not found in abundance in the other hot spring types, such as ferrous iron (Fe^{2+}), trace elements like nickel (Ni), toxic metals like lead (Pd) as well as rare Earth elements (McCleskey et al., 2004; Nordstrom et al., 2005b; Nordstrom et al., 2009b; McCleskey et al., 2014; McCleskey et al., 2022).

Previous 16S rRNA and metagenomic studies have shown that the microbial communities in high temperature acidic hot springs are dominated by few lineages in contrast to the other hot spring systems (Inskeep et al., 2013; Colman et al., 2018; Lindsay et al., 2018). In the range of 70-75°C, representatives of the bacterial order Aquificales, such as *Hydrogenobaculum* can be dominant in the planktonic and sediment communities (D'Imperio et al., 2008; Boyd et al., 2009; Inskeep et al., 2013; Colman et al., 2016). However, at >75°C, archaeal orders dominate the planktonic and the sediment communities, with differentiation between these niches. For example, representatives of Sulfolobales (e.g., the uncharacterized Yellowstone group "Sulfolobales Acd1") are usually found at 60-90% abundance in planktonic communities (Colman et al., 2018; Lindsay et al., 2018; Colman et al., 2021; Colman et al., 2022; Sims et al., 2023). While Sulfolobales can dominate sediment communities at >80°C, other members of the order Thermoproteales, such as *Vulcanisaeta, Thermoproteus,* and *Caldivirga*, and members of the order Desulfurococcales, such as *Acidilobus*, can also be found in these springs (Colman et al., 2016; Jay et al., 2016). Of these, Aquificales and Sulfolobales' representatives are generally facultative chemolithoautotrophs (with few exceptions such as

some *Thermoproteus*) (Jay et al., 2016) and thus, this agrees with the consistent distribution of these primarily chemoorgonoheterotrophs in >70°C hot springs (i.e., *Vulcanisaeta*, *Caldivirga* and *Acidilobus*) while the primary producers shift at temperature range (i.e., Aquificales <75°C, Sulfolobales >75°C).

The hydrothermal sources of inorganic electron donor and acceptors in acidic hot springs are sulfur (i.e., S_8^0, H_2S and intermediates species, such as polysulfides), H_2, iron (i.e., Fe^{2+} and Fe^{3+}), and to some extent, arsenic compounds (e.g., As(III), As(V)) (Nordstrom et al., 2005b; Nordstrom et al., 2009b). Based on genomic inference and cultivation approaches, the metabolic abilities of members of the Aquificales and Sulfolobales that tend to dominant acidic high temperature springs reflect the availability of these substrates. The Aquificales genus *Hydrogenobaculum* is known to aerobically oxidize H_2, H_2S, and As(III) (D'Imperio et al., 2007; D'Imperio et al., 2008). Many cultivars of Sulfolobales members that are found in YNP hot springs, as well as strains isolated from YNP, have been shown to aerobically oxidize H_2, S_8^0, disproportionate S_8^0, and a few (e.g., *Metallosphaera*) can oxidize Fe(II) (Brock et al., 1972; Kozubal et al., 2012; Lewis et al., 2021; Liu et al., 2021). Interestingly, although genomic analysis highlight that Sulfolobales almost universally encode the enzyme sulfide:quinone oxidoreductase (SQR), thought to allow for H_2S oxidation (Brito et al., 2009), this metabolic ability has not been clearly demonstrated (Plumb et al., 2007; Morales et al., 2011; Morales et al., 2012). Members of the Sulfolobales can also conduct the anaerobic oxidation of H_2 coupled to the reduction of S_8^0 or Fe(III) and the oxidation of S_8^0 coupled with the reduction of Fe(III). In addition, aerobic and anaerobic heterotrophic growth has been demonstrated in members of the

Sulfolobales (e.g., *Acidianus, Sulfolobus*) (Amenabar and Boyd, 2018; Counts et al., 2021; Lewis et al., 2021; Liu et al., 2021).

Due to Sulfolobales high temperature niches, notable metabolic flexibility, and being the first isolated S_8^0 oxidizing thermoacidophile, members of the order became a model to understand hyperthermoacidophiles and how the oxidation of S_8^0 is microbially mediated. Further, their contribution to acidification of natural waters has made them the premier example of the ecological process of niche construction (through acidification), whereby an organism modifies its environment in such a way as to increase the fitness of its offspring (Colman et al., 2018). Notably, hot spring acidification is a microbially mediated process that is dependent on O_2 and thus, it's likely that this process of niche construction through acidification would not have occurred on the anoxic early Earth. Thus far, only one pathway of S_8^0 oxidation is described for the Sulfolobales, which involves the protein sulfur oxidoreductase (SOR) that disproportionates S_8^0 to H_2S, HSO_3^- and $S_2O_3^{2-}$. Intriguingly, about half of Sulfolobales representatives do not encode this protein, many of which have been demonstrated to oxidize S_8^0 (Counts et al., 2021; Liu et al., 2021), highlighting a gap in the understanding of Sulfolobales physiology and ecology in acidic hot springs and in the creation of these environments.

Scope of Thesis

The relationships between spring geochemistry, microbial composition, and microbial activity are the focus of this thesis, with particular emphasis placed on Sulfolobales and their physiology, ecology, and evolution. In Chapter 2, I focus on how different mixing regimes that form hot springs influence nutrient availability (electron donors/acceptors), microbial community composition and chemosynthetic primary productivity. Through geochemical and biological

analyses of three co-localized hot springs of different mixing regimes, it is shown that mixing of reduced and oxidized fluids results in increased disequilibrium in redox pairings, higher biodiversity, and higher rates of chemosynthetic primary productivity. In Chapter 3, I investigate the physiology of Sulfolobales, the dominant microorganisms in high temperature acidic hot springs. Given that Sulfolobales almost universally encode the ability to oxidize H_2S through SQR, target-enrichment under aerobic H_2S-oxidizing conditions was performed from select hot springs where Sulfolobales dominated. Five novel strains were isolated and shown to accelerate the aerobic oxidation of H_2S, coupling this activity to growth and SO_4^{2-} production. In Chapter 4, I focus on the mechanisms of S_8^0 oxidation by Sulfolobales. The only described pathway of S_8^0 oxidation utilizes the protein SOR, which is lacking in nearly half of Sulfolobales representatives. Two of the five novel strains described in Chapter 3 were used to investigate differences in the physiology of SOR-encoding versus non-SOR-encoding Sulfolobales, as one encoded SOR and the other did not. Microscopic observations pointed to different mineral-associations in these strains, with the non-SOR-encoding strain regularly found in direct contact with S_8^0, while the SOR-encoding strain was not found in direct association. It was hypothesized that this behavior was due to H_2S formed through SOR disproportionation, likely solubilizing S_8^0 through nucleophilic attack, ultimately generating nanoparticles of S_8^0 that are more bioavailable and allow for S_8^0 oxidation without the requirement for direct contact. This hypothesis was probed in experiments where direct contact with S_8^0 was not allowed through sequestration in dialysis membranes. The hypothesis was confirmed as only the SOR-encoding Sulfolobales was able to grow. Interestingly, when low concentrations of H_2S were added to the cultures of the non-SOR-encoding Sulfolobales in sequestered S_8^0 conditions to mimic the proposed

mechanisms of SOR, growth and activity was recovered. Finally, in Chapter 5, I provide a summary of these major findings and their implications, as well as multiple future directions that can be developed based on the results of this dissertation.

CHAPTER TWO

RELATIONSHIPS BETWEEN FLUID MIXING, BIODIVERSITY, AND CHEMOSYNTHETIC PRIMARY PRODUCTIVITY IN YELLOWSTONE HOT SPRINGS

Contribution of Authors and Co-Authors

Manuscript in Chapter 2

Author: Maria C. Fernandes-Martins

Contributions: Conducted fieldwork. Carried out laboratory experiments and performed bioinformatics analyses. Contributed to the writing of the manuscript.

Co-Author: Dan R. Colman

Contributions: Conducted field work and oversaw bioinformatics analyses. Contributed to the writing of the manuscript.

Co-Author: Eric S. Boyd

Contributions: Design the study. Conducted field work and oversaw the study. Contributed to the writing of the manuscript.

Manuscript Information

Maria C. Fernandes-Martins, Dan R. Colman, and Eric S. Boyd

Environmental Microbiology

Status of Manuscript:
☐ Prepared for submission to a peer-reviewed journal
☐ Officially submitted to a peer-reviewed journal
☐ Accepted by a peer-reviewed journal
☒ Published in a peer-reviewed journal

Applied Microbiology International and John Wiley & Sons Ltd.
January 18th, 2023, DOI: 10.1111/1462-2920.16340

Originality-Significance

For much of Earth history, microbial life was supported by chemosynthetic metabolism. This remains true today in environments where light is not available (subsurface) or where geochemical conditions preclude photosynthetic metabolism (e.g., high temperature). In such ecosystems, microbial production should be, at first order, dependent on the variation in and availability of electron donors/acceptors (redox pairs) in the environment. Environments with greater variation in and availability of electron donors/acceptors should support greater biodiversity that, in turn, should promote primary production. The variation in and availability of redox pairs in hydrothermal environments are dictated largely by mixing of reduced subsurface and oxidized surface fluids. However, it's unclear if these relationships play out in hydrothermal environments. Here, we investigate the relationships between fluid mixing, biodiversity, and productivity in three co-localized springs in Yellowstone National Park that have different geochemistry. Using geochemical proxies, we characterized the source(s) of fluids to each spring and their mixing regime, determined the taxonomic, genomic, phylogenetic, and functional biodiversity of the communities, and quantified the rates of primary productivity. The results indicate that among these springs, those sourced by reduced volcanic fluids mixed with oxidized groundwater promote increasingly biodiverse communities that are more productive. These results help shed light into factors that may have influenced and sustained microbial biodiversity and productivity in hydrothermal ecosystems on early Earth and in contemporary chemosynthetic systems where photosynthesis is excluded.

Summary

The factors that influence biodiversity and productivity of hydrothermal ecosystems are not well understood. Here we investigate the relationship between fluid mixing, biodiversity, and chemosynthetic primary productivity in three co-localized hot springs (RSW, RSN, and RSE) in Yellowstone National Park that have different geochemistry. All three springs are sourced by reduced hydrothermal fluid, but RSE and RSN receive input of vapor phase gas and oxidized groundwaters, with input of both being substantially higher in RSN. Metagenomic sequencing revealed that communities in RSN were more biodiverse than those of RSE and RSW in all dimensions evaluated. Microcosm activity assays indicate that rates of dissolved inorganic carbon uptake were also higher in RSN than in RSE and RSW. Together, these results suggest that increased mixing of reduced volcanic fluid with oxidized fluids generates additional niche space capable of supporting increasingly biodiverse communities that are more productive. These results provide insight into the factors that generate and maintain chemosynthetic biodiversity in hydrothermal systems and that influence the distribution, abundance, and diversity of microbial life in communities supported by chemosynthesis. These factors may also extend to other ecosystems not supported by photosynthesis, including the vast subterranean biosphere and biospheres beneath ice sheets and glaciers.

Introduction

The relationship between species biodiversity and primary productivity is a central topic in ecological studies and has been widely studied from experimental, observational, and theoretical approaches of herbaceous and forest ecosystems (Willig, 2011). In these studies,

positive correlations have generally been observed between various dimensions of community biodiversity (taxonomic, functional, and/or phylogenetic) and primary productivity (e.g., (Tilman et al., 2012; Grace et al., 2016; Liang et al., 2016; Brun et al., 2019; Liang et al., 2019)). These positive relationships have been suggested to result from interactions between organisms and their environment that, over geological time and through evolutionary adaptation, have shaped populations and their communities toward more efficient use of available resources. This, in turn, is thought to promote greater biomass production (productivity) given a finite supply of those resources.

Far less is known of biodiversity-productivity relationships in microbial ecosystems, despite the fundamental role of microorganisms in global biogeochemical cycles, as major reservoirs of organic carbon, and as modulators of critical ecosystem processes that directly influence plant, animal, and environmental health (Falkowski et al., 2008; Cavicchioli et al., 2019). The few studies that have been conducted on microbial communities, or mixed microbial and macro communities, also generally reveal positive biodiversity-productivity relationships. For example, the phylogenetic diversity of plant root-associated fungi was positively correlated to plant phylogenetic diversity and species richness in a subtropical forest (Liang et al., 2019). Since plant phylogenetic diversity was also positively correlated with plant productivity, a connection was suggested between root-associated fungal diversity and plant productivity. Similarly, a study of 23 lakes in Japan showed that phytoplankton diversity increased with cell density, ultimately reaching stable diversity values at different cell densities that were dependent on the trophic status of the lake (Ogawa and Ichimura, 1984). Yet, when phytoplankton diversity in these lakes was plotted as a function of chlorophyll *a* concentration (as a proxy for

phytoplankton biomass), a humped relationship was observed where biodiversity increased linearly with productivity only to level off or even decrease at higher productivity levels (Ogawa and Ichimura, 1984). This decrease in diversity was observed in communities inhabiting (hyper)eutrophic lakes and was attributed to increased dominance of one or more phytoplankton taxa that produced biomass but that likely competitively excluded other taxa, rendering the community less productive.

A more recent compilation of data of microbial diversity-productivity relationships from 70 natural, experimental, and engineered aquatic ecosystems revealed a variety of relationships between biodiversity and productivity including positive (28% of total studies), negative (35%), and humped shaped (23%) patterns. Differences in these patterns could be attributed to the method used to quantify biodiversity and productivity, limits associated with the gradients in, and scale of, the productivity of ecosystems that could be sampled, or the trophic status of the lakes at the time they were sampled (Smith, 2007). Nonetheless, that similar relationships were identified in microbial and macro ecosystems points to a comparable set of principles governing diversity–productivity curves among all forms of life. Further, these studies highlight the connection between resource availability, resource partitioning among diverse species, and biomass production. Importantly, the aforementioned studies were conducted on ecosystems supported by photosynthesis where energy (light) is essentially in excess supply and where nutrient availability (i.e., nitrogen, phosphorus, and/or iron) typically underpins or limits primary production (Chapin et al., 2011). Far less is known of biodiversity-productivity relationships and their geological/geochemical underpinnings in communities supported by chemosynthesis.

Chemosynthetic organisms are sustained by chemical energy rather than light energy. During chemosynthetic dissimilatory metabolism, reduced and oxidized chemical species (electron donor and acceptors) that are in disequilibrium are reacted (in pairs) to release energy that can be used to power biomass synthesis. Chemoautotrophy, or chemosynthesis, that drives CO_2 fixation, supported microbial life on Earth prior to the advent of photosynthesis ~2.8-3.0 Ga (Marais, 2000) and supports life in contemporary environments that exclude photosynthesis or that exclude photosynthetic products. Examples of such environments include the pore spaces and fractures of subsurface igneous rocks (Colman et al., 2017; Goordial et al., 2021; Fones et al., 2022), caves (Porter et al., 2009), and the subsurface of glaciers or ice sheets (Christner et al., 2014; Dunham et al., 2021). In one such study of four cave ecosystems, a positive relationship was observed between the diversity of 16S rRNA gene phylotypes (richness) and primary productivity (Porter et al., 2009). This relationship was suggested to be related to sulfide availability, a key substrate supporting dark chemoautotrophic metabolism, pointing to the importance of redox disequilibrium in supporting biodiverse chemosynthetic communities. It is unclear if this relationship extends to other dimensions of biodiversity (genomic, phylogenetic, functional) in other chemosynthetic ecosystems.

In addition to subsurface environments where light is not available to support photosynthesis, surface environments exist that exclude photosynthesis, including high temperature hot springs (Boyd et al., 2010b; Cox et al., 2011; Boyd et al., 2012; Hamilton et al., 2012). In these environments, the availability of energy to sustain chemosynthetic organisms and their activities are dependent on the processes that maintain chemical disequilibrium in a system. In hot springs in Yellowstone National Park (YNP), Wyoming, U.S.A., chemical disequilibrium

is largely attributed to mixing of anoxic and reduced subsurface fluids with more oxidized near surface fluids (Shock et al., 2010; Colman et al., 2019a; Fernandes-Martins et al., 2021). It stands to reason that chemical disequilibrium in other chemosynthesis ecosystems is also dependent on mixing of different fluid types, such as has been demonstrated in several marine hydrothermal vent environments (Huber et al., 2002; Huber et al., 2003; Schrenk et al., 2003; Nakagawa et al., 2005b; Reysenbach et al., 2020).

Processes that influence the availability of, and disequilibrium in, electron donors/acceptors and other nutrients in YNP hot springs can best be understood by examining the prevailing geochemical model that describes the functioning of the system (Truesdell and Fournier, 1976; Fournier, 1989; Nordstrom et al., 2009a; Lowenstern et al., 2012). Briefly, infiltration of meteoric water (rain, snowmelt) into the subsurface of YNP allows for water-rock interaction during its descent, heating at depth, and further alteration by input of volatiles. These waters form the ~350 °C hydrothermal aquifer in YNP that is enriched in dissolved CO_2, H_2S, Cl^-, and SO_4^{2-}. This is the parent fluid discharged in YNP springs and it is anoxic (Truesdell and Fournier, 1976). However, prior to its surface discharge as hot springs, geysers, mudpots, or fumaroles, the parent fluid can be modified by *i*) additional water-rock reactions that enrich the fluid with solutes or that deplete the fluid of solutes due to mineral precipitation, *ii*) decompressional boiling and generation of steam through a process termed phase separation (described in more detail below), *iii*) mixing with cold, dilute, and oxidized groundwater, and *iv*) infusion of atmospheric or additional volcanic gas (Nordstrom et al., 2009a; Lowenstern et al., 2012; Hurwitz and Lowenstern, 2014). To this end, the hot springs in YNP provide a unique model system to examine the relationship between *a*) fluid sources and mixing regime, *b*)

taxonomic, functional, and phylogenetic diversity of chemosynthetic microbial communities, and *c*) their productivity.

Here, the relationships between fluid sources and mixing regime, biodiversity, and productivity are examined in three springs ("Roadside West", "Roadside North" and "Roadside West") that are co-localized (within ~100 m of each other) in the Roadside Springs area, Nymph Lake, YNP. Previous studies of two of the three springs ("Roadside West" and "Roadside East") indicate that their geochemical composition is influenced by processes *i*-*iv* above and that this likely influences their taxonomic diversity (Lindsay et al., 2018). In the present work, we further this study through an integrated analysis of aqueous- and gas-phase geochemical data that is used to identify the most plausible mixing regime responsible for each spring's unique geochemical composition. Planktonic and sediment-associated microbial communities from each spring were collected and subjected to DNA extraction and metagenomics sequencing and analysis to determine community taxonomic, functional, and phylogenetic diversity. Further, radiotracer assays were used to quantify the rate of chemosynthetic primary production [dissolved inorganic carbon (DIC) assimilation] in both planktonic and sediment-associated microbial communities. The results provide perspective into the influence of fluid sourcing and mixing regime on community biodiversity and productivity in chemosynthetic ecosystems.

Materials and Methods

Site Description

'Roadside West' (RSW), 'Roadside North' (RSN), and 'Roadside East' (RSE) hot springs are located in the Nymph Lake area along the Norris-Mammoth Corridor (N 44°45'12.7"; W 110°43'30.8"), Yellowstone National Park (YNP), Wyoming, U.S.A. These springs are all located

within ~100 m of each other and were chosen because they are likely hosted in similar bedrock, considering their geographical proximity. The Nymph Lake area is located just north of the caldera rim in what has been termed the “ring fracture zone”, where bedrock is extensively fractured and fissured due to increased seismic activity in this area (Christiansen, 2001). Increased fracturing and fissuring of bedrock is thought to allow for gases to rise to the surface more easily (Lowenstern et al., 2015). RSE and RSW are located at slightly different elevations (2,285 m and 2,283 m, respectively, as estimated via Google Earth using GPS coordinates) and have outflow channels that drain into Nymph Lake (Fig. 1). In contrast, RSN is located at a slightly higher elevation (2,288 m) than RSW and RSE and its outflow channel doesn’t reach Nymph Lake. Roughly 100 m to the east and 100 m in elevation above RSN is an active fumarole vent (Fig. 1).

Sample Collection and Geochemical Analyses

Temperature, conductivity, and pH were measured in the field with temperature-compensated probes (model YSI EC300, YSI Inc., Yellow Springs, OH, U.S.A. or model WTW 3100, WTW Weilheim, Germany) on November 5th, 2020. Dissolved Fe(II) and total sulfide (S^{2-}) concentrations were measured in the field using Hach reagents (ferrozine pillows and sulfide reagents 1 and 2) and a Hach DR/890 spectrophotometer (Hach, Loveland, CO). Spring waters were filtered in the field (0.22 μm) and stored at 4°C for determination of sulfate (SO_4^{2-}), chloride (Cl^-), and nitrate (NO_3^-) concentrations that were measured via Dionex ICS-2100 (Thermo Scientific, Waltham, MA), DIC concentrations via a Shimadzu TOC-VSH instrument (Shimadzu Scientific Instruments, Columbia, MD), and water isotopes ($\delta^{18}O$ and δD) via Liquid Water Isotope Analyzer (LWIA) (Los Gatos Research, San Jose, CA). Samples for SO_4^{2-}, Cl^- and

NO_3^- were collect in glass serum vials with caps and septa, samples for DIC and water isotope analyses were collected in glass serum vials capped with butyl rubber stoppers with no headspace. These samples were measured at the Environmental Analytical Lab at Montana State University. Isotopes were measured in triplicate and are presented relative to the Vienna Standard Mean Ocean Water (VSMOW) standard.

Samples for determination of dissolved gas concentrations were collected using the bubble strip method, as described previously (Chapelle et al., 1997). Ten mL of the gas bubble was injected into a gas chromatograph (model SRI 8610C, SRI instruments, Torrance, CA) and gases were measured as previously described (Lindsay et al., 2018). Helium was used as a carrier gas for all analyses. Gas concentrations were calculated using a standard curve (1 to 10,000 ppm calibration range) (American Gas Group, Toledo, OH) and were converted to dissolved aqueous phase concentrations according to Henry's law, as previously described (Spear et al., 2005). All values are presented as the average and standard error of the mean of three replicates.

Sampling, DNA Extraction, Metagenomic Sequencing, and Data Processing

Roughly 0.5 g sub-samples of sediment were collected from each spring in triplicate using flame sterilized spatulas and were transferred to sterile 1.5 mL polypropylene tubes. Planktonic biomass was collected from ~ 2 to 10 L (contingent on biomass loading) of spring water via 0.22 μm Pall (Fort Washington, NY) membrane filters and a Geotech (Denver, CO) peristaltic pump and polypropylene tubing. Prior to sample collection, ~ 10 L of water were run through the tubing to flush contents. Filters and their contents were transferred aseptically using flame-sterilized forceps to sterile 15 mL polypropylene tubes. Tubes containing sediments and

filters were frozen on dry ice in the field and were transported frozen to the laboratory where they were kept at -80°C.

DNA was extracted from filtered biomass and sediment-associated biomass with the FastDNA Spin Kit for Soil (MP Biomedicals, Irvine, CA) following the manufacturer's instructions. Genomic DNA was quantified fluorometrically via the high sensitivity Qubit assay (Thermo Fisher Scientific, Waltham, MA) and was subjected to paired-end sequencing (2 x 151 bp) with the Illumina NovaSeq platform at the Department of Energy Joint Genome Institute (JGI; Walnut Creek, CA) following the Illumina regular fragment (300 bp) method of library preparation (Clum et al., 2021). Read processing, metagenome assembly, and binning of contigs into metagenome-assembled-genomes (MAGs) were performed as previously described (Fernandes-Martins et al., 2021). The planktonic metagenomes from 'Roadside West', 'Roadside North' and 'Roadside East' are available on JGI-IMG under the identifiers 3300033894, 3300036346, 3300033892, respectively. The sediment metagenomes from 'Roadside West' and 'Roadside North' are available on JGI-IMG under the identifiers 3300033893 and 3300036468, respectively.

Calculation of MAG Phylogenetic Biodiversity

Open reading frames and proteins encoded by MAGs were inferred with PROKKA (v.1.14.5) (Seemann, 2014). Marker genes (n = 30) for both Bacteria and Archaea were identified, aligned, and concatenated with Markerfinder (https://github.com/faylward/markerfinder#markerfinder). The alignment block was subjected to phylogenetic reconstruction using IQ-Tree (v.1.6.11) (Nguyen et al., 2015) specifying the LG model for substitution rates and 1000 'ultra-fast' bootstraps.

The total number of reads that mapped to MAGs in each metagenome was normalized to estimated genome size and these values were used to calculate the relative abundance of each MAG in each community using CheckM (v.10.5) (Parks et al., 2015). Normalized MAG abundances for planktonic and sediment-associated communities for a given spring were then combined to provide an estimate of the taxonomic diversity of the hot spring community. Only planktonic MAGs from RSE were included since quantifiable genomic DNA was not recovered from the sediment community, preventing library construction and metagenomic sequencing. The tree file (generated above) and whole-community relative abundances were imported into R (Team, 2018) and the Picante package (Kembel et al., 2010) was used to calculate the mean pairwise distance (MPD) metric. MPD calculates the mean pairwise phylogenetic distance between all MAGs in a community and is useful in identifying patterns in tree-wide phylogenetic structure of communities (Kembel et al., 2010). MPD calculations accounted for MAG relative abundance ("abundance.weighted" parameter). The standardized effect size (ses.MPD) was implemented to compare the calculated MPD values to a null model that randomizes branches and lineages in the phylogenetic tree. For ses.MPD, positive values of the observed standardized effect (obs.z.) and high *p*-values (obs.p > 0.95) of sample communities versus the randomized (null) community indicate greater phylogenetic distance between individuals in the community than expected by chance (phylogenetic evenness). In contrast, negative values of obs.z and low *p*-values (< 0.05) indicate smaller phylogenetic distance between individuals in the community than expected by chance (phylogenetic clustering).

To estimate the genomic diversity independent of genome-binning approaches, the Nonpareil index of sequence diversity (N_d) was calculated from the quality filtered metagenomic

reads of each sample. The N_d metric represents the diversity of a community in sequence space as a function of read diversity redundancy within a given metagenomic read dataset (Rodriguez et al., 2018). The metric empirically provides similar diversity estimates as the commonly used Shannon diversity index that is often used to estimate taxonomic diversity, but importantly, is calculated without potential methodological biases introduced by database referencing or genome-binning (Rodriguez et al., 2018). The N_d metric was calculated by first estimating the read redundancy of raw reads using the Nonpariel program (v. 3.3.0) using the Kmer based approach (k-mer size of 24) and the Nonpariel.curve function of the Nonpareil package for R (Team, 2018).

Calculation of MAG Functional Diversity

The functional diversity of MAGs comprising a given community was calculated by uploading inferred proteins encoded by MAGs to the Kyoto Encyclopedia of Genes and Genomes (KEGG) function database (Kanehisa and Goto, 2000) using the KEGG Automatic Annotation Server (KAAS) (Moriya et al., 2007). Annotations were mapped through bidirectional best hit (BBH) searches against the KAAS system metabolic pathways. The homolog counts identified for each protein (KEGG Ortholog or KO) in the 'energy metabolism' category (KOs related to photosynthesis and eukaryotic cell machinery, if identified, were not considered) in KEGG (n = 841) for each MAG were exported in a table and were normalized to total homolog counts per MAG to account for unequal genome sizes, MAG incompleteness, and relatedness to the protein database available in KEGG. Fifteen MAGs of the total 96 MAGs from all communities that were identified as putative ectoparasites (i.e., *Nanopusillis* sp.) or that had a combination of low homolog counts [fewer homologs counts than the standard deviation (SD);

median = 82, SD = 35] and low completeness (~50-70% completeness) were excluded from the analysis. Tables describing the KOs for each MAG and the relative abundance of each MAG matrix were imported into R (Team, 2018) and the 'Functional Diversity (FD)' package was used to calculate abundance-weighted function dispersion (FDis) (Sébastien, 2008; Laliberté and Legendre, 2010) of the communities. These values were then plotted as a principal coordinate (PCO) plot.

FDis measures the mean distance of individual MAGs from the centroid (average in PCO space) of all MAGs within each community in functional space (defined based on the KO and MAG abundances) created by the FD package. Lower FDis values correspond to MAGs in a community that encode a similar distribution of KOs (encoded functions) that cluster together in functional (PCO) space. In contrast, higher values correspond to MAGs within a community that encode more dissimilar KOs and that plot distantly from each other in functional (PCO) space.

Inferred Metabolic Functionalities of MAGs

Autotrophic pathways encoded by MAGs were assessed based on KO mapping to the 'carbon fixation' pathways group within the 'energy metabolism' module. The six known autotrophic pathways evaluated here were (1) the Calvin-Benson-Bassham (CBB) cycle, (2) the reductive tricarboxylic acid (rTCA) cycle, (3) the Wood-Ljungdahl (WL) pathway, (4) the 3-hydroxypropionate (3HP) bicycle, (5) the 3-hydroxypropionate/4-hydroxybutyrate (3HP/4HB) cycle, and (6) the dicarboxylate/4-hydroxybutyrate (DC/4-HB) cycle (Berg et al., 2010; Berg, 2011). The identification of homologs of marker proteins for each of these pathways were used to ascribe autotrophic capability to the MAGs. These marker proteins were: ribulose 1,5-bisphosphate carboxylase/oxygenase (RuBisCO; enzyme category (EC) 4.1.1.39) and

phosphoribulokinase (PRK; EC 2.7. 1.19) for the CBB cycle and citryl-CoA synthetase (Ccs; EC 6.2.1.18) and citryl-CoA lyase (Cit; EC 4.1.3.34) or ATP-citrate lyase (ACLY; EC 2.3.3.8) for the rTCA cycle. Homologs of carbon monoxide dehydrogenase/acetyl-CoA synthase (CODH/ACS; EC 1.2.7.4) and formate-tetrahydrofolate ligase (Fhs; 6.3.4.3) were used to evaluate MAGs for the presence of the WL pathway while homologs of propionyl-CoA carboxylase (PCC; EC 6.4.1.3), malonyl-CoA reductase (Mcr; EC 1.2.1.75), malyl-CoA/B-methylmalyl-CoA/citranyl-lyase (Mcl; EC 4.1.3.24), and acetyl-CoA carboxylase (ACC; EC 6.4.1.2) were used to identify evidence for the 3HP pathway. The 3HP/4HB pathway was identified by examining MAGs for homologs of 4-hydroxybutyrl-CoA dehydratase (AbfD; EC 4.2.1.120) and the DC/4-HB pathway was identified by the presence of homologs of 4-hydroxybutyrl-CoA dehydratase (AbfD; EC 4.2.1.120) and pyruvate synthase (Por; EC 1.2. 7.1). MAGs that encoded homologs of a marker gene for an autotrophic pathway but also had evidence for glycolysis and tricarboxylic acid cycle (TCA) were assigned as facultative autotrophs while MAGs that lacked homologs of these autotrophic marker proteins and that encoded homologs for glycolysis, the TCA cycle, or fermentation were assigned as heterotrophs.

To evaluate potential electron donor and acceptors utilized by populations, MAGs were screened for homologs of proteins involved in dissimilatory nitrate reduction (NarABG, EC 1.7.5.1 287 and NapAB, EC 1.9.6.1), sulfate/sulfite reduction (Sat, EC 2.7.7.4; AprAB, EC 1.8.99.2; DsrAB, EC 1.8.99.5), elemental sulfur/polysulfide reduction (DMSO reductases, EC 1.8.5.3; SreABC, no EC), sulfite/tetrathionate reduction (Asr, no EC), thiosulfate reduction (PhsABC, EC 1.8.5.5), arsenate reduction (ArrA, EC 1.20.99.1), hydrogen metabolism ([NiFe]- and [FeFe]-hydrogenases, EC 1.12.1.2 or 1.12.99.6), arsenite oxidation (AioA, EC:1.20.9.1),

iron oxidation (FoxABC, no EC) sulfide oxidation (Sqo, EC 1.8.5.8), thiosulfate/sulfur oxidation (Sox, EC 2.8.5.2), and methane oxidation or production (MmoX, EC 1.14.13.25; McrA, EC 2.8.4.1) were investigated, as previously described (Fernandes-Martins et al., 2021).

Dissolved Inorganic Carbon (DIC) Assimilation Assays

Rates of dissolved inorganic carbon assimilation were determined for planktonic and sediment-associated communities as a measure of community primary production using microcosm assays, as previously described (Boyd et al., 2009). Briefly, acid-washed 24 mL serum bottles were sealed with butyl rubber stoppers and purged with N_2 that had been passed over heated (>200°C) and H_2-reduced copper shavings for 5 min. before autoclaving. In the field, 10 mL of spring water was added directly to twelve serum vials at each of the three springs site; the gas phase in the vials was equalized to atmospheric pressure using a sterile needle and syringe. In the case of sediment assays, the 10 mL of spring water that was injected was filtered (0.1 μm). A roughly 1:10 ratio of sediment and spring water (0.1 μm filtered) slurry was prepared in autoclaved 24 mL vials sealed with butyl rubber stoppers and aluminum caps. All microcosm vials and sediment slurry vials prepared in the field were immediately placed on ice and in the dark for the 2 hrs transport back to the laboratory.

In the laboratory, one mL of each sediment slurry vial from each spring was added to six microcosm vials. Three of the sediment slurry-containing microcosms (sediment) and three microcosms without added sediment (planktonic) were subjected to a single 20 min. autoclave cycle (121 °C, 20 psi) for use as abiotic controls. Microcosm vials were brought to room temperature (~21 °C) and five μCi of [^{14}C] sodium bicarbonate ($NaH^{14}CO_3$) was added to each vial. Microcosms were placed in a sealed bag (secondary containment) and incubated in the dark

at the measured temperature of hot spring waters (*see* Table 1) for six hrs given that preliminary experiments indicated DIC uptake was linear up to that time point (data not shown). After incubation, microcosms were placed in a second sealed bag (tertiary containment) and stored at -20 °C until they were processed, as previously described (Lindsay et al., 2018).

In a fume hood, microcosm vials were thawed at room temperature. Vials were unsealed and acidified to pH of < 2 by adding 200 µL of 12 N HCl to volatilize unassimilated DIC. After two hrs of degassing in the fume hood, microcosm contents were filtered onto 0.22 µm white polycarbonate filters, washed with sterile deionized water, placed in scintillation vials, and dried overnight in the fume hood. Filters were then overlaid with 10 mL of CytoScint ES liquid scintillation fluid (MP Biomedicals, Solon, OH). Radioactivity associated with filtered biomass was measured as counts per minute (CPM) on a Beckman LS 6,500 liquid scintillation counter (Beckman Coulter, Inc., Indianapolis, IN) and converted to disintegrations per minute (DPM) using a quench curve. DPMs were converted to total DIC assimilated using DIC values measured in each spring (described above). Total DIC uptake values were normalized to per unit volume of water for planktonic microcosms or to grams dry weight (gdw) for sediment microcosms. All the values are presented as the average and standard deviation of the mean of three replicate assays.

Results and Discussion

Identifying The Source of Fluids to 'Roadside' Springs and Possible Mixing Regimes

The geochemical and environmental measurements made on 'Roadside West (RSW)', 'Roadside North (RSN)' and 'Roadside East (RSE)' (Fig. 1) are summarized in Table 1. The concentrations of Cl^- and SO_4^{2-} and the isotopic composition ($\delta^{18}O$ and δ^2H) of waters measured

in RSE, RSW, and RSN were used to characterize the source of fluids to each of these springs, using a previously described geochemical model (Nordstrom et al., 2009a) (Fig. 2). The deep hydrothermal aquifer in YNP (~350 °C) is thought to contain ~ 330 mg L^{-1} Cl^- and ~30 mg L^{-1} SO_4^{2-} (Fournier, 1989; Nordstrom et al., 2009a). Waters with concentrations of Cl^- and SO_4^{2-} that are less than these are interpreted to be diluted with ground (recently precipitated meteoric) water whereas those with concentrations exceeding these are interpreted to have undergone evaporation and/or infusion with sulfide (H_2S)-containing volcanic gas, that when oxidized, can contribute SO_4^{2-} but not Cl^-. This geochemical model is founded on the geological process of phase separation (Fournier, 1989; Nordstrom et al., 2009a), whereby parent hydrothermal waters infused with volcanic gases rise toward the surface due to density differences (Fournier, 1989; Nordstrom et al., 2009a). Rapid ascension of these fluids can lead to decompression boiling, allowing volatiles to exsolve from hydrothermal waters resulting in a volatile-rich steam phase and a solute-rich liquid phase (Fournier, 1989; Rye and Truesdell, 1993; Nordstrom et al., 2005a; Nordstrom et al., 2009a; Hurwitz and Lowenstern, 2014). Such volatiles can include hydrogen (H_2), carbon dioxide (CO_2), methane (CH_4), and H_2S. Condensation of volatile-rich steam with oxygen-rich near surface water can result in the oxidation of H_2S, leading to the production of elemental sulfur (S^0), sulfate (SO_4^{2-}), and acidity (Nordstrom et al., 2005a; Nordstrom et al., 2009a). As such, vapor phase influenced springs tend to be acidic (pH <4), have high SO_4^{2-} concentrations, and can be enriched in sulfur and iron compounds due to weathering of local bedrock (Nordstrom et al., 2009a; Amenabar and Boyd, 2019; Sims et al., 2023). In contrast, liquid-phase influenced waters (hydrothermal-only) tend to be neutral to alkaline in pH (pH >6.5), are enriched in solutes such as Cl^-, and generally have lower concentrations of H_2, S^0,

SO_4^{2-}, CH_4, and Fe(II). Hydrothermal-only waters are thought to best reflect the geochemical composition of the parent aquifer, minus dissolved gases (Fournier, 1989; Nordstrom et al., 2009a).

Hot springs with moderately acidic pH (pH 4.0-6.5) can form by mixing regimes other than those mentioned above (White, 1988; Nordstrom et al., 2005a; Nordstrom et al., 2009a; Lowenstern et al., 2012; Amenabar et al., 2015). For example, hydrothermal only waters can mix with *i*) volcanic gases, *ii*) near surface ground (relatively recently precipitated meteoric) , or *iii*) near surface ground waters that have been infused with volcanic gases (Nordstrom et al., 2009a; Lowenstern et al., 2012). Such mixing regimes can begin to be deconvoluted based on distinct geochemical signatures in the form of ratios of SO_4^{2-}/Cl^- in spring waters, the isotopic composition of waters (δ^2H and $\delta^{18}O$), the amount and types of dissolved gases in those waters, along with spring pH and temperature (Nordstrom et al., 2009a; Lowenstern et al., 2012; Colman et al., 2021). Further, nitrate (NO_3^-) is a common component of near surface ground waters (Fernandes-Martins et al., 2021) and can provide an additional metric to describe the input of said waters to a hot spring.

Application of the above framework to RSW, RSN, and RSE indicates that they were all sourced by hydrothermal-only waters at the time of sampling, with those of RSE and RSN being further influenced by dilution with ground water and/or input of volcanic gas (Fig. 2a). Specifically, the Cl^- and SO_4^{2-} concentrations in RSW were 451 and 21 mg L^{-1}, consistent with this being hydrothermal-only water that has undergone evaporation. Importantly, RSW has measurable sulfide indicating that separation of the volatile gas rich phase and the liquid phase in waters sourcing this spring were incomplete or that biological reduction of an oxidized sulfur

compound (e.g., SO_4^{2-}) may be taking place (Truesdell et al., 1977; Nordstrom et al., 2009a; Lindsay et al., 2018). In contrast, the Cl^- and SO_4^{2-} concentrations in RSE were 154 and 92 mg L^{-1}, respectively, which suggests dilution of the HO waters sourcing the spring by ground water (i.e., based on lower Cl^- concentrations) and infusion of H_2S-rich gas that, when oxidized, contributed SO_4^{2-}. Like RSE, the Cl^- and SO_4^{2-} concentrations in RSN were 132 and 99 mg L^{-1}, again suggesting dilution of hydrothermal-only waters with ground water and infusion of these waters with H_2S-rich gas. Both RSE and RSN had detectable NO_3^- (0.26 and 0.28 mg L^{-1}, respectively), which is consistent with input of near surface ground water. The $\delta^{18}O$ and δ^2H of RSW, RSE, and RSN (Fig. 2b) all plot along a previously reported trend line for heated (near-boiling) waters evaporating under non-equilibrium conditions (Craig et al., 1963; Giggenbach, 1978; Nordstrom et al., 2009a). The observation that RSE and RSN waters are less depleted in $\delta^{18}O$ and δ^2H than RSW waters is also consistent with these waters being influenced by mixing with near surface ground water and RSW being influenced to a greater extent by evaporation.

To further examine the waters sourcing each spring, pH and conductivity were compared. The pH of RSW waters was 6.6, consistent with the hypothesized circumneutral to alkaline pH of hydrothermal-only type parent fluids (Fournier, 1989). The pH of RSE was 3.2, consistent with the acidic pH of waters that are infused with H_2S-rich volcanic gas that, when oxidized, contributes SO_4^{2-} and acidity (Fournier, 1989; Nordstrom et al., 2009a). The conductivities of RSW (3.62 mS) and RSE (2.55 mS) were also consistent with hydrothermal-only type water influenced springs, with the latter being lower likely due to dilution with near surface ground water (Nordstrom et al., 2009a; Amenabar et al., 2015). Despite RSN having similar Cl^- and SO_4^{2-} as RSE, its pH was comparatively less acidic (pH 5.1). Typically, springs with pH of 4.0-

6.5 have lower conductivities than more acidic or more alkaline springs, a finding that has been attributed to this spring type often resulting from dilution of hydrothermal-only waters (Amenabar et al., 2015). However, the conductivity of RSN water was 2.65 mS, which is higher than RSE indicating that the source of waters in RSN cannot be attributed solely to dilution of hydrothermal-only water.

To test the possibility that the geochemical composition of RSN was due to mixing of RSE and RSW source waters, two-component mixing models were developed based on pH and conductivity of spring waters. A two-component mixing model based on the conductivity of RSE and RSW water indicated that RSN waters would need to comprise 36 parts RSE water for each part of RSW water. This finding is incompatible with a two-component mixing model for RSN waters based on the pH of RSE and RSW, which would require one-part RSW and 55 parts RSE. Further, the Cl^- concentration in RSN was less than RSW and RSE and the SO_4^{2-} concentration in RSN was greater than RSW and RSE. These observations indicate that RSN waters cannot derive from simple mixing of waters that source RSE and RSW.

RSE and RSW are at slightly lower elevations than RSN, which presumably limits the ability of the liquids sourcing the former springs to source the latter spring. However, a large fumarole is located nearby, but at higher elevation than RSN, consistent with the general notion that volcanic gases tend to form surface expressions (fumaroles) at higher elevations than hot springs due to the ease by which gases can ascend to the surface (Fig. 1) (Hurwitz and Lowenstern, 2014). Therefore, the concentration of select dissolved gases (H_2, CH_4, CO_2) in RSE, RSN, and RSW was examined. Concentrations of H_2, CH_4, and CO_2 were substantially higher in RSN than in RSE and RSW (Fig. 2c), indicating a higher input of volcanic gas into

RSN. Likewise, the concentration of H_2S in RSN was also ~ 50% higher than in RSE, which when combined with the higher SO_4^{2-} concentration (Table 1), is also consistent with a higher flux of volcanic gas into RSN. Potentially reconciling these observations, it is suggested that both RSE and RSN are sourced with hydrothermal-only waters that are diluted with near surface ground water (i.e., based on lower Cl^- concentrations). Both springs had higher SO_4^{2-} concentrations, reflecting injection of waters with reduced volcanic gases containing H_2S. However, RSN, which sits at a higher elevation than RSE and RSW and which is intermediate in elevation between RSE/RSW and an active fumarole, receives a higher input of reduced, hot volcanic gas and this also contains substantial amounts of CO_2. The elevation of RSN may help to facilitate this interaction, as has been suggested for other hot springs systems (Bergfeld et al., 2011; Lowenstern et al., 2012; Lindsay et al., 2019). The higher input of volcanic CO_2 into RSN waters leads to a greater disequilibrium with atmospheric CO_2 concentrations, and subsequent degassing likely buffers the acidity generated by H_2S oxidation, helping to explain the moderately acidic pH of the spring (5.1). The greater input of reduced, hot volcanic gas into RSE and RSN may also help to explain their higher temperatures (85.5°C and 86.2°C, respectively) when compared to RSW (68.5°C).

The different mixing regimes result in geochemical variation among the springs (Table 1, Fig. 2c). In particular, the availability of electron donors and acceptors in RSN, which is sourced by a combination of reduced HO waters, oxidized near surface ground waters, and reduced volcanic gases likely results in increased niche space when compared to RSW and RSE. For example, concentrations of H_2, CO_2, CH_4, H_2S, SO_4^{2-}, and NO_3^- are higher in RSN waters than in RSW or RSE (Table 1, Fig. 2c) which suggests a greater disequilibrium in the availability of

electron donors and acceptors in RSN. While mineral analysis revealed that mineral composition between sites varied, all of the detected minerals were silicates that are not known to be involved in microbial redox reactions (data not shown). Based on precedent studies of other ecological systems (Ogawa and Ichimura, 1984; Smith, 2007; Tilman et al., 2012; Grace et al., 2016; Liang et al., 2016), it is possible that this greater chemical disequilibrium in RSN could support a greater taxonomic, phylogenetic, genomic, and functional biodiversity that, in turn, could promote greater primary production.

Comparison of Community Taxonomic, Phylogenetic, and Genomic Diversity

Based on inferred fluid sources and mixing regime in 'Roadside Springs' and the apparent increased disequilibrium in electron donor and acceptor data in RSN relative to RSE and RSW (Table 1, Fig. 2c), it was hypothesized that the microbial communities inhabiting RSN would exhibit higher biodiversity than those from RSW and RSE. To begin to assess patterns of biodiversity in the community structure, a rank-abundance plot was generated of MAGs that comprised >1% abundance of the total community (Fig. 3). For RSW, RSE, and RSN planktonic communities, a total of 91.3, 71.1, and 60.2% of contigs were binned into MAGs (Supp. Tables 2a, 2b, and 2c). In the RSW planktonic community, a MAG (RSWP_1) closely related to the bacterium *Sulfurihydrogenibium yellowstonense* [97.8% average nucleotide identity (ANI)] was dominant (82.6% of total community). The second most abundant MAG (RSWP_2), which is closely related to a *Thermus* sp. (96.5% ANI), comprised only 4.0% of the total community. The same trend was observed in RSE, where a MAG (RSEP_1) closely related (95.8% ANI) to an uncharacterized archaeon within the order Sulfolobales comprised 55.8% of the planktonic community, while the second most abundant MAG (RSEP_2), also closely related (97.3% ANI)

to an uncharacterized Sulfolobales, comprised 10.0% of the total community. In contrast, the dominant MAG (RSNP_1) in RSN's planktonic community is closely affiliated (96.3% ANI) to an uncharacterized archaeon of the Sulfolobales order and represented 33.0% of the total community while the second MAG (RSNS_2) that was closely related (97.7% ANI) to *Thermocrinis ruber*, was estimated to comprise 16.3% of the total community.

For RSW and RSN sediment communities (detectable DNA was not obtained from RSE sediments), a total of 67.0 and 64.5% of contigs were binned into MAGs (Supp. Tables 2a and 2c). For the sediment communities, RSW had a total of 5 MAGs that were >1% of the total community (Fig. 3). The RSW sediment community was dominated by a MAG (RSWS_1) affiliated with an uncharacterized member of the Bipolauricaeae family (69.5% ANI; 52.0% of total community). The second most abundant MAG (RSWS_2; 10.0% of community) was closely affiliated with *Thermus* sp. (97.6% ANI) while the third most abundant MAG (RSWS_3; 8.0% of community) was related to *Thermoflexus* (85.2 % ANI). Both the fourth and the fifth most abundant MAGs in RSW sediment community were archaea; RSWS_4 was affiliated with *Thermofilales* (85.2% ANI) and RSWS_5 was affiliated with Hadesarchaea (99.1% ANI), and they shared the same abundance (1.2% of the community). RSN had a total of 14 MAGs in the sediment that were >1% of total community, nearly triple the number when compared to RSW. In RSN, a MAG (RSNS_1) related to *Ignisphaera* (98.2 % ANI) and a MAG (RSNS_2) closely related (97.7% ANI) to *Vulcanisaeta* sp., comprised 19.0% and 10.3% of the total community, respectively (Supp. Table 2b, Fig. 3). The third most abundant MAG (RSNS_3) was closely related to *Pyrobaculum* sp. (95% ANI) and comprised 5.0% of the total community. As

mentioned previously, insufficient DNA was obtained from RSE sediments for metagenomic library construction and sequencing, thereby preventing an analysis of this community.

The rank abundance-plots revealed that the structure of RSN communities (planktonic and sediment) was more evenly distributed than those of RSW and RSE. In addition, while RSN was found to support abundant archaeal and bacterial MAGs (Fig. 3), RSW primarily supported bacterial MAGs and RSE only supported archaeal MAGs. This is consistent with previous findings indicating that microbial communities inhabiting neutral to alkaline hot springs (i.e., RSW) host microbial communities that are often dominated by Bacteria whereas acidic springs (i.e., RSE) tend to be dominated by Archaea (Inskeep et al., 2013; Colman et al., 2018).

Quantitative comparison of community diversity (Supp. Table 2) was conducted by evaluating phylogenetic biodiversity via the relatedness of pairs of MAGs based on their phylogenetic distances in trees constructed using taxonomic marker genes. Such metrics provide information on the phylogenetic structure and diversity of communities. Phylogenetically even communities are expected to be prevalent in environments with a greater spectrum of available nutrients and energy sources since such conditions should support more metabolically differentiated taxa thereby minimizing niche overlap and reducing competition among taxa (Meuser et al., 2013). Further, since the metabolic similarity of taxa is related to their phylogenetic similarity, communities comprising metabolically differentiated taxa should be phylogenetic less related than those harboring less metabolically differentiated taxa (Prosser et al., 2007). In contrast, phylogenetically clustered communities are expected to be prevalent in environments where the spectrum of available nutrients and energy sources is more limited. This

is due to increased competition for the limited nutrients and energy sources, resulting in communities dominated by taxa most adapted to utilize those substrates (Prosser et al., 2007).

The mean pairwise distance (MPD) (Kembel et al., 2010) [i.e., the phylogenetic distance separating pairs of taxa (MAGs)], was calculated for planktonic and sediment communities in RSE, RSN, and RSW (Table 2). The MPD for the RSN sediment MAGs was 1.37 while the MPD for the RSW sediment MAGs was 0.82. The MPD for the RSN planktonic MAGs was 1.85, whereas the MPD for the RSW and RSE planktonic MAGs were 0.56 and 0.45, respectively. This indicates that the phylogenetic distance between any two MAGs comprising the RSN communities is greater than that of any two MAGs comprising the RSW and RSE communities. To this end, RSN supports a microbial community that is more phylogenetically diverse than RSW and RSE.

Like MPD estimates, the standardized effect size (SESmpd) indicates that MAGs comprising the RSN community were more phylogenetically even than expected by chance based on the positive SESmpd values for both planktonic and sediment MAGs (1.09 and 0.28, respectively) and *p*-values higher than 0.05 (0.81 and 0.75, respectively). In contrast the SESmpd and *p*-values for MAGs comprising the RSW planktonic and sediment communities (SESmpd= -0.98 and -0.82, respectively; *p*-values = 0.01 and 0.002, respectively) and for MAGs comprising the RSE planktonic community (SESmpd = -1.19; *p*-value = 0.04) suggest that these communities are more phylogenetically clustered (Table 2). This supports the hypothesis that MAGs comprising the RSN community are phylogenetically more even when compared to those comprising RSE and RSW communities, consistent with the RSN community structures when visualized as a rank-abundance plot (Fig. 2).

Importantly, the rank-abundance plot, taxonomic assignments, and the phylogenetic diversity metrics (Fig. 3, Table 2) described above are based on a necessarily incomplete assessment of the metagenomes of each hot spring (range of binned contigs = 60.2 to 91.3%) to meet high quality requirements for MAG analyses. To estimate the biodiversity of the hot springs with a less biased metric, whole metagenome diversity analyses were conducted using the nonpareil index of diversity (N_d) (Rodriguez et al., 2018) that represents the diversity of a community in sequence space as a function of read diversity redundancy within a given metagenomic read dataset. In agreement with the previous metrics of biodiversity described above, N_d estimates for RSN were higher for both planktonic (15.9) and sediment (16.6) communities than that for RSW (planktonic = 15.3, sediment =16.0) and RSE communities (planktonic = 15.5) (Table 2). Thus, the genomic diversity encoded by the RSN community members was higher than in the RSW and RSE communities based on several independent metrics.

Taken together, the different metrics of biodiversity calculated herein collectively indicate that RSN supported greater taxonomic, phylogenetic, and genomic diversity than RSW and RSE. That the moderately acidic RSN spring harbors sediment and planktonic communities comprising both Archaea and Bacteria and that these communities are phylogenetically and taxonomically more diverse than RSE and RSW is consistent with a recent metagenomic investigation of a community inhabiting a moderately acidic (pH 5.4) hot spring (SJ3) in the Smoke Jumper Geyser Basin of YNP. In this study, the sediment community was shown to contain representatives of >50% of major archaeal and bacterial lineages (Colman et al., 2019a) and it was suggested that the extreme disequilibrium in electron donor/acceptors in this spring

due to mixing of reduced volatiles in volcanic gas with oxidized near surface ground water supported high taxonomic biodiversity (Colman et al., 2019a). This relationship does not appear to be limited to the YNP hydrothermal system given that previous studies of marine hydrothermal ecosystems in the Juan de Fuca Ridge (Huber et al., 2003; Rika E. et al., 2013) and in the 'Brothers' sub-arc volcanic system (Reysenbach et al., 2020) reveal that fluid mixing influences taxonomic biodiversity in these systems as well. Further, data from several cave ecosystems suggest that higher sulfide levels were associated with higher levels of biodiversity (Porter et al., 2009), which may point to increased redox disequilibrium and energy availability being an important driver of the biodiversity in these subsurface ecosystems as well.

Comparison of Community Functional Diversity

The higher taxonomic, phylogenetic, and genomic diversity associated with RSN relative to RSE and RSW would be expected to also lead to higher functional diversity. To compare the functional diversity of planktonic and sediment communities, total protein content from the MAGs present in each community was used to calculate Functional Dispersion (FDis), a metric that describes the average distance of MAGs from the centroid of a PCO ordination describing the dissimilarity in KOs encoded in a community of MAGs. A high FDis value is associated with higher functional diversity of a community of MAGs. For the planktonic communities, FDis values were 0.08 for RSW, 0.29 for RSN, and 0.19 for RSE (Table 2). For the sediment communities, FDis values were 0.20 for RSW and 0.38 for RSN. As such, FDis was higher for both planktonic and sediment RSN communities which suggests that the MAGs in these communities encode more dissimilar functions, on average, than MAGs in the RSW and RSE communities. The observation that the most biodiverse communities (RSN planktonic and

sediment) are also the most functionally diverse is consistent with community assembly acting to maximize the use of available resources and redox couples, which are likely higher in RSN due to mixing of reduced and oxidized end member fluid types, while minimizing niche overlap.

Comparison of Chemosynthetic Primary Productivity and Metabolic Profiles

The apparently greater availability and disequilibrium in redox couples capable of driving chemosynthetic metabolism, combined with diversity estimates that suggest the potential to more effectively utilize those redox couples, would be expected to lead to higher levels of primary production. To test this hypothesis, microcosm assays measuring dark dissolved inorganic carbon (DIC) assimilation were conducted using waters and sediments from RSE, RSN, and RSW. DIC assimilation attributable to planktonic communities was detected in all three springs (Fig. 4). However, DIC assimilation attributable to for sediment communities was only detected in RSW and RSN (Fig. 4); rates in RSE microcosms were not significantly different from abiotic controls or background radiation levels (data not shown). Statistically insignificant differences in DIC assimilation between biotic and abiotic controls and background levels of radiation in sediments from RSE is potentially consistent with low amounts of biomass in these sediments, as evidenced by the inability to extract quantifiable DNA from the sediments.

Rates of biotic DIC assimilation varied among planktonic and sediment communities and across springs. DIC assimilation was similar in the planktonic communities for RSW (3.8 ± 2.0 nmol DIC h^{-1} mL^{-1}) and RSN (3.6 ± 1.9 nmol DIC h^{-1} mL^{-1}) and both were significantly higher than RSE (0.2 ± 0.08 nmol DIC h^{-1} mL^{-1}). The fact that RSW and RSN had similar DIC assimilation in the planktonic communities, despite the fact that the communities' structures are fairly different (Fig. 3) could be due to a deficiency in essential nutrient (e.g., phosphorus, fixed

nitrogen) in spring waters. However, for the sediment communities, DIC assimilation in RSN (18.9 ± 1.5 μmol h^{-1} $gdws^{-1}$) was significantly higher than for RSW (3.5 ± 0.9 μmol h^{-1} $gdws^{-1}$) and RSE (0.03 ± 0.006 μmol h^{-1} $gdws^{-1}$). This indicates that, together, the RSN communities are more productive than the RSE and RSW communities, even though RSW was ~20°C cooler than RSN, which, theoretically, should have negatively impacted or limited biodiversity and productivity in RSN when in comparison to RSW.

To identify taxa that are likely contributing to CO_2 fixation in planktonic and sediment communities, we analyzed MAGs at >1% abundance of the total community (Fig. 2) for genes encoding key proteins involved in the six major CO_2 fixation pathways as well as for homologs of key proteins that allow for use of key electron donors and acceptors (Supp. Table 3). The two bacterial MAGs in the planktonic community of RSW (*Sulfurihydrogenibium* and *Thermus*) encode key proteins putatively allowing for autotrophic CO_2 fixation. While *Sulfurihydrogenibium* is known for its autotrophic capabilities and encodes key proteins involved in the rTCA cycle (Huber and Eder, 2006), *Thermus* are traditionally considered to be heterotrophs (Williams and Da Costa, 1992). The RSW planktonic *Thermus* MAG encodes form I RuBisCO (RbcSL) homologs and these have been previously identified in the genomes of *Thermus* strains isolated from high temperature environments that also have high concentrations of bicarbonate (Müller et al., 2016). However, to our knowledge, no isolated *Thermus* strain has been shown to fix CO_2 in laboratory settings. In the RSW sediment community, two of three bacterial MAGs encode key proteins putatively allowing for autotrophic CO_2 fixation. The most abundant RSW sediment MAG (52.0% of the community), which was affiliated with an uncharacterized member of the Bipolaricaulaceae family (69.5% ANI) encoded the WL pathway.

The second most abundant RSW sediment MAG (4.0% of the community), was affiliated with *Thermus* and was inferred to have the ability to fix CO_2 via the CBB pathway, as indicated above. In addition to RbcSL, this MAG also encoded a homolog of phosphoribulokinase (Prk), adding support to the ability of this organism to fix CO_2 via the CBB pathway. Since the sediment and planktonic *Thermus* MAGs shared 98.1% AAI, it is possible that the absence of a homolog of Pgk in the planktonic MAG was due to assembly or binning biases (i.e., incompleteness).

In the RSN planktonic community, two of the five MAGs (Sulfolabaceae and *Thermocrinis*) encoded CO_2 fixation pathways. The most abundant MAG, affiliated with a Sulfolobaceae archaeon encoded 4-hydroxybutanoyl-CoA dehydratase (AbfD), a key protein for the 3HP/4HB pathway. The second most abundant MAG, affiliated with *Thermocrinis*, encoded key enzymes for the rTCA pathway. Intriguingly, in the RSN sediment community, the ability to fix CO_2 was not observed in the most abundant MAGs. Out of the 14 MAGs present in the RSN sediment community, three (*Thermocrinis*, Sulfolobaceae and *Thermoproteus* MAGs) encoded for CO_2 fixation pathways and they all had similar abundances (~2.5 to 3.5% abundance of total community). The *Thermocrinis* MAG (3.5% abundant) encoded for the rTCA pathway, the Sulfolobaceae MAG (3.2% abundant) encoded for the 3HP/4HB pathway, and the *Thermoproteus* MAG (2.5% abundant) encoded for DC/4HB pathway. The fact that only three MAGs with similar but lower abundances were identified as potentially having autotrophic capabilities in RSN sediment, even though this community had the high rates for DIC assimilation (Fig. 4), could be explained by their absolute abundance (number of cells) being higher than what the relative abundance from sequence based analyses revealed (Fig. 3, Supp.

Table 2b) and/or the sediment matrix containing mineral sources of electron donors/acceptors (e.g., iron oxides, elemental sulfur) not identified through our analysis and observations. Finally, in the RSE planktonic community, the two most abundant MAGs, both archaea from the Sulfolobaceae family, encoded the potential to fix CO_2 via the 3HP/4HB pathway (Supp. Table 3). In total, four of the seven most abundant (>1% abundance) MAGs in RSW, six of the 20 most abundant MAGs in RSN, and two of the three most abundant MAGs in RSE encoded the potential to fix CO_2.

MAGs encoding putative autotrophic capabilities were examined for protein homologs allowing for use of electron donors and acceptors (Fig. 5; Supp. Table 3). All RSW planktonic and sediment MAGs (*Sulfurihydrogenibium* sp. (RSWP_1), *Thermus* sp. (RSWP_2), and *Thermus* sp. (RSWS_2), with the exception of Bipolaricaulaceae (RSWS_1), encoded homologs allowing for potential use of H_2S, thiosulfate, or S^0 as electron donors (Sqo and Sox homologs) and O_2 as electron acceptor (Cox or CydBD homologs). One of these MAGs, *Thermus* sp. (RSWS_2), encoded the ability to also utilize thiosulfate as electron acceptor (PhsAB homologs). No pairing of electron donor/acceptor was found for Bipolaricaulaceae (RSWS_1) which could be due to the MAG being only 73.4% complete. Nevertheless, these observations suggest some overlap in the electron donors and acceptors capable of fueling primary production in the RSW communities and suggests competition for nutrients is an important driving force in the assembly of that community.

RSN populations encoded a more diverse pairing of electron donors and acceptors. The two autotrophic MAGs (Sulfolobaceae, RSNP_1; *T. ruber*, RSNP_2) in the planktonic community both encoded the ability to use O_2 as an oxidant (Cox homologs) and H_2S as a

reductant (Sqo homologs). The Sulfolobaceae MAG also had the ability to oxidize H_2 ([NiFe]-hydrogenase homologs) and to disproportionate sulfur (Sor homologs) while the *T. ruber* MAG encoded the ability to also oxidize thiosulfate and/or S^0 (Sox homologs). This indicates that these MAGs could be filling overlapping niches (H_2S and S^0) but also distinct niches due to the potential ability to utilize different electron donors (thiosulfate and H_2). For the sediment community, the *T. ruber* (RSNS_6) and the Sulfolobaceae (RSNS_7) MAGs encoded the same metabolic potential as their closely related planktonic MAGs. The *Thermoproteus* sp. (RSNS_9) MAG encoded homologs for H_2S and H_2 oxidation and O_2 reduction like the Sulfolobaceae MAG (RSNS_7). In addition, the *Thermoproteus* sp. MAG encoded for SO_4^{2-} reduction (Sat, AprAB, DsrAB homologs) that could be paired with H_2-oxidation. To this end, the metabolic potentials of RSN MAGs suggest fewer competitive interactions over electron donor/acceptor pairs, which is consistent with a more even distribution of MAGs in the rank-abundance plot (Fig. 3), SESmpd and FDis calculations (Table 2). This, in turn, may promote higher primary productivity (Fig. 4). Such a positive feedback in the availability of nutrients, microbial biodiversity, and chemoautotrophic-based primary productivity has also been observed in communities inhabiting low temperature sulfidic caves (Porter et al., 2009). Together, these observations suggest that such relationships may extend to other subterranean biospheres such as those beneath glaciers and ice sheets, among others.

Finally, in the RSE planktonic community, both Sulfolobales MAGs (RSEP_1 and RSEP_2) encoded the potential to utilize H_2S and H_2 as reductants (Sqo and [NiFe]-hydrogenase homologs) and to use O_2 as an oxidant (Cox homolog). In addition, the second most abundant MAG, RSEP_2, also encoded the potential to oxidize Fe(II) (Fox homologs), which is consistent

with the acidity of this hot spring (pH = 3), the abundant availability of Fe(II) in the spring (3.91 mg/L) and visible iron (III) oxide deposits along the outflow channel (Table 1, Fig. 1). While this could suggest that RSE communities have more inorganic chemical species available for redox pairing than the RSW communities, the fact that RSE communities weren't as productive could be due to limitation in other nutrients such as bicarbonate for CO_2 fixation given the inherent speciation and outgassing of CO_2 at low pH (Fig. 4, Fig. 2c) or that the low pH itself constrained biomass accumulation and productivity due to constraints that such conditions impose on microbial life (Johnson, 1998; Baker-Austin and Dopson, 2007). The fact that some RSE and RSN MAGs harbored the genetic potential to oxidize H_2 while dominant RSW MAGs did not is also consistent with geochemical observations that RSE and RSN are likely sourced with more H_2 rich volcanic gases, and in the case of RSN, had a higher concentration of H_2 (Fig. 2a, c).

Conclusions

In the present study, we evaluated the hypothesis that more extensive mixing of oxidized and reduced fluids would increase the availability of electron donors, electron acceptors, and nutrients and increase available niche space using three co-localized hot spring environments (RSE, RSN, RSW) with geochemical conditions that preclude photosynthesis. We hypothesized that increased niche space, in turn, would promote higher biodiversity and chemosynthetic-primary productivity. The relationship between biodiversity and primary productivity has been extensively studied in macro- and microbial communities that are supported by photosynthesis (Ogawa and Ichimura, 1984; Smith, 2007; Liang et al., 2019), but is understudied in chemosynthetic-based ecosystems with the sole exception being a study of four cave

communities that showed a positive relationship between 16S rRNA gene taxonomic diversity (richness) and primary productivity (Porter et al., 2009).

Results of our geochemical characterization show that RSW, RSN and RSE hot springs are each impacted by the phase-separation process that occurs as hydrothermal fluids ascend to the surface in YNP, with RSW being primarily sourced by reduced hydrothermal-only waters. RSE is also sourced by hydrothermal waters that are diluted by oxidized ground waters and that is infused with reduced vapor phase gases. RSN is sourced similarly to RSE, with the exception that RSN receives higher gas input likely to due to its location at higher elevation closer to an active fumarole. This high input of volcanic gases in RSN likely buffers its pH to be intermittent relative to the prevailing bimodal distribution of hot spring pH in YNP as acidic (<4.0) or circumneutral to alkaline (pH >6.5). Based on geochemical data, we conclude that the mixing regime sourcing fluids to RSN generates more varied and extensive redox disequilibria and hypothesized that this, in turn, would create more niche space to support more biodiverse communities and to fuel greater microbial chemosynthesis than RSW and RSE.

Metagenomic sequencing and a variety of taxonomic, phylogenetic, genomic, and functional analyses indicate that the RSN community hosts a community with higher biodiversity than RSW and RSE, regardless of whether planktonic or sediment communities were compared across springs. This is consistent with the predictions from geochemical data that indicate RSN likely hosts more complex and extensive niche space than RSW and RSE that should promote more biodiversity than RSW and RSE. Increased taxonomic, phylogenetic, genomic, and functional diversity would be expected to lead to utilization of a greater spectrum of available resources in RSN than RSW and RSE, which should be reflected by measurement of

chemosynthetic (dark) primary production. Microcosm activity assays indicate that rates of dark dissolved inorganic carbon assimilation (chemoautotrophy) were similar for RSN and RSW planktonic communities but were significantly higher than that of RSE planktonic community. For the sediment community, RSN had a significantly higher rate than RSW and RSE communities. Altogether, the results presented here indicate a positive feedback between mixing regimes that promote increased niche space, biodiversity, and chemosynthetic-based primary productivity in high temperature continental hydrothermal systems. Additional research involving more hot spring ecosystems is expected to further identify factors that influence biodiversity-productivity relationships in hot springs. Such factors might include residence times of waters in hot springs, input of allochthonous organic matter (e.g., dust, surface runoff), and the availability of other key nutrients (e.g., fixed nitrogen, phosphorus).

Acknowledgements

This work was supported by a grant from the National Science Foundation (EAR-1820658) to DRC and ESB. The Department of Energy Joint Genome Institute's Community Sequencing Program (CSP 504081 to DRC, and ESB) supported the metagenomic sequence generation. We thank Melody Lindsay for help in DNA extractions. We thank Annie Carlson at the National Park Service for assistance in obtaining the permit (YELL-05544) to conduct this work in YNP and for allowing access to the Roadside Springs area during administrative travel periods.

References

Amenabar, M.J., and Boyd, E.S. (2019) A review of the mechanisms of mineral-based metabolism in early Earth analog rock-hosted hydrothermal ecosystems. *World J Microbiol Biotechnol* 35: 29.

Amenabar, M.J., Urcshel, M.R., and Boyd, E.S. (2015) Metabolic and taxonomic diversification in continental magmatic hydrothermal systems. *In Microbial Evolution under Extreme Conditions ed Corien Bakermans, De Gruyter*.

Baker-Austin, C., and Dopson, M. (2007) Life in acid: pH homeostasis in acidophiles. *Trends Microbiol* 15: 165-171.

Ball, J.W., McCleskey, R.B., Nordstrom, D.K., and Holloway, J.M. (2006) Water-chemistry data for selected springs, geysers, and streams in Yellowstone National Park, Wyoming, 2003–2005. In. U.S. Geological Survey Open File Report.

Berg, I.A. (2011) Ecological aspects of the distribution of different autotrophic CO_2 fixation pathways. *Appl Environ Microbiol* 77: 1925-1936.

Berg, I.A., Kockelkorn, D., Ramos-Vera, W.H., Say, R.F., Zarzycki, J., Hügler, M. et al. (2010) Autotrophic carbon fixation in archaea. *Nat Rev Microbiol* 8: 447-460.

Bergfeld, D., Lowenstern, J.B., Hunt, A.G., Shanks III, W.C.P., and Evans, W. (2011) Gas and isotope chemistry of thermal features in Yellowstone National Park, Wyoming. In. U.S. Geological Survey Report.

Boyd, E.S., Leavitt, W.D., and Geesey, G.G. (2009) CO_2 uptake and fixation by a thermoacidophilic microbial community attached to precipitated sulfur in a geothermal spring. *Appl Environ Microbiol* 75: 4289-4296.

Boyd, E.S., Hamilton, T.L., Spear, J.R., Lavin, M., and Peters, J.W. (2010) [FeFe]-hydrogenase in Yellowstone National Park: evidence for dispersal limitation and phylogenetic niche conservatism. *ISME J* 4: 1485-1495.

Boyd, E.S., Fecteau, K.M., Havig, J.R., Shock, E.L., and Peters, J.W. (2012) Modeling the habitat range of phototrophs in Yellowstone National Park: toward the development of a comprehensive fitness landscape. *Front Microbiol* 3: 221.

Brock, T.D. (1971) Bimodal distribution of pH values of thermal springs of the world. *Geol Soc Am Bull* 82: 1393-1394.

Brun, P., Zimmermann, N.E., Graham, C.H., Lavergne, S., Pellissier, L., Münkemüller, T., and Thuiller, W. (2019) The productivity-biodiversity relationship varies across diversity dimensions. *Nat Commun* 10: 5691.

Cavicchioli, R., Ripple, W.J., Timmis, K.N., Azam, F., Bakken, L.R., Baylis, M. et al. (2019) Scientists' warning to humanity: microorganisms and climate change. *Nat Rev Microbiol* 17: 569-586.

Chapelle, F.H., Vroblesky, D.A., Woodward, J.C., and Lovley, D.R. (1997) Practical considerations for measuring hydrogen concentrations in groundwater. *Environ Sci Tech* 31: 2873–2877.

Chapin, F.S.III., Matson, P.A., and Vitousek, P. (2011) *Principles of Terrestrial Ecosystem Ecology*: New York, NY: Springer Science & Business Media.

Christiansen, R.L. (2001) The quarternary and pliocene Yellowstone plateau volcanic field of Wyoming, Idaho, and Montana. In. U.S. Geological Survey Professional Paper 729-G.

Christner, B.C., Priscu, J.C., Achberger, A.M., Barbante, C., Carter, S.P., Christianson, K. et al. (2014) A microbial ecosystem beneath the West Antarctic ice sheet. *Nature* 512: 310-313.

Clum, A., Huntemann, M., Bushnell, B., Foster, B., Foster, B., Roux, S. et al. (2021) DOE JGI Metagenome Workflow. *mSystems* 6: e00804-00820.

Colman, D.R., Amenabar, M.J., Fernandes-Martins, M.C., and Boyd, E.S. (2022) Subsurface Archaea associated with rapid geobiological change in a model Yellowstone hot spring. *Commun Earth Environ* 3, 205

Colman, D.R., Feyhl-Buska, J., Robinson, K.J., Fecteau, K.M., Xu, H., Shock, E.L., and Boyd, E.S. (2016) Ecological differentiation in planktonic and sediment-associated chemotrophic microbial populations in Yellowstone hot springs. *FEMS Microbiol Ecol* 92(9)

Colman, D.R., Lindsay, M.R., and Boyd, E.S. (2019) Mixing of meteoric and geothermal fluids supports hyperdiverse chemosynthetic hydrothermal communities. *Nat Commun* 10: 681.

Colman, D.R., Poudel, S., Stamps, B.W., Boyd, E.S., and Spear, J.R. (2017) The deep, hot biosphere: Twenty-five years of retrospection. *Proc Natl Acad Sci U S A* 114: 6895-6903.

Colman, D.R., Poudel, S., Hamilton, T.L., Havig, J.R., Selensky, M.J., Shock, E.L., and Boyd, E.S. (2018) Geobiological feedbacks and the evolution of thermoacidophiles. *ISME J* 12: 225-236.

Colman, D.R., Lindsay, M.R., Harnish, A., Bilbrey, E.M., Amenabar, M.J., Selensky, M.J. et al. (2021) Seasonal hydrologic and geologic forcing drive hot spring geochemistry and microbial biodiversity. *Environ Microbiol* 23: 4034-4053.

Cox, A., Shock, E.L., and Havig, J.R. (2011) The transition to microbial photosynthesis in hot spring ecosystems. *Chem Geol* 280: 344-351.

Craig, H., Gordon, L.I., and Horibe, Y. (1963) Isotopic exchange effects in the evaporation of water. *J Geophys Res* 68: 5079-5087.

de la Torre, J.R., Walker, C.B., Ingalls, A.E., Könneke, M., and Stahl, D.A. (2008) Cultivation of a thermophilic ammonia oxidizing archaeon synthesizing crenarchaeol. *Environ Microbiol* 10: 810-818.

Dunham, E.C., Dore, J.E., Skidmore, M.L., Roden, E.E., and Boyd, E.S. (2021) Lithogenic hydrogen supports microbial primary production in subglacial and proglacial environments. *Proc Natl Acad Sci U S A* 118: e2007051117.

Des Marais, D.J. (2000) When did photosynthesis emerge on Earth? *Science* 289: 2.
Falkowski, P.G., Fenchel, T., and Delong, E.F. (2008) The microbial engines that drive Earth's biogeochemical cycles. *Science* 320: 1034-1039.

Fernandes-Martins, M.C., Keller, L.M., Munro-Ehrlich, M., Zimlich, K.R., Mettler, M.K., England, A.M. et al. (2021) Ecological dichotomies arise in microbial communities due to mixing of deep hydrothermal waters and atmospheric gas in a circumneutral hot spring. *Appl Environ Microbiol* 87: e01598-01521.

Fones, E.M., Templeton, A.S., Mogk, D.W., and Boyd, E.S. (2022) Transformation of low-molecular-weight organic acids by microbial endoliths in subsurface mafic and ultramafic igneous rock. *Environ Microbiol*.

Fournier, R.O. (1989) Geochemistry and dynamics of Yellowstone hydrothermal system. *Annu Rev Earth Planet Sci* 17: 13-53.

Giggenbach, W.F. (1978) The isotopic composition of waters from the El Tatio geothermal field, northern Chile. *Geochim Cosmochim Acta* 42: 979-988.

Goordial, J., D'Angelo, T., Labonté, J.M., Poulton, N.J., Brown, J.M., Stepanauskas, R. et al. (2021) Microbial diversity and function in shallow subsurface sediment and oceanic lithosphere of the Atlantis Massif. *mBio* 12: e00490-00421.

Grace, J.B., Anderson, T.M., Seabloom, E.W., Borer, E.T., Adler, P.B., Harpole, W.S. et al. (2016) Integrative modelling reveals mechanisms linking productivity and plant species richness. *Nature* 529: 390-393.

Guo, L., Wang, G., Sheng, Y., Sun, X., Shi, Z., Xu, Q., and Mu, W. (2020) Temperature governs the distribution of hot spring microbial community in three hydrothermal fields, Eastern Tibetan Plateau Geothermal Belt, Western China. *Sci Total Environ* 720: 137574.

Hamilton, T.L., Koonce, E., Howells, A., Havig, J.R., Jewell, T., Torre, J.R.d.l. et al. (2014) Competition for ammonia influences the structure of chemotrophic communities in geothermal springs. *Appl Environ Microbiol* 80: 653-661.

Hamilton, T.L., Vogl, K., Bryant, D.A., Boyd, E.S., and Peters, J.W. (2012) Environmental constraints defining the distribution, composition, and evolution of chlorophototrophs in thermal features of Yellowstone National Park. *Geobiology* 10: 236-249.

Holloway, J.M., Nordstrom, D.K., Böhlke, J.K., McCleskey, R.B., and Ball, J.W. (2011) Ammonium in thermal waters of Yellowstone National Park: Processes affecting speciation and isotope fractionation. *Geochim Cosmochim Acta* 75: 4611-4636.

Hou, W., Wang, S., Dong, H., Jiang, H., Briggs, B.R., Peacock, J.P. et al. (2013) A comprehensive census of microbial diversity in hot springs of Tengchong, Yunnan province, China, using 16S rRNA gene pyrosequencing. *PLOS ONE* 8: e53350.

Huber, J.A., Butterfield, D.A., and Baross, J.A. (2002) Temporal changes in archaeal diversity and chemistry in a mid-ocean ridge subseafloor habitat. *Appl Environ Microbiol* 68: 1585-1594.

Huber, J.A., Butterfield, D.A., and Baross, J.A. (2003) Bacterial diversity in a subseafloor habitat following a deep-sea volcanic eruption. *FEMS Microbiol Ecol* 43: 393-409.

Huber, R., and Eder, W. (2006) Aquificales. In *The Prokaryotes*: Springer New York, pp. 925-938.

Hurwitz, S., and Lowenstern, J.B. (2014) Dynamics of the Yellowstone hydrothermal system. *Rev Geophys* 52: 375-411.

Inskeep, W.P., Jay, Z.J., Tringe, S.G., Herrgard, M.J., Rusch, D.B., and YNP Metagenome project steering committee & working group members (2013) The YNP metagenome project: environmental parameters responsible for microbial distribution in the Yellowstone geothermal ecosystem. *Front Microbiol* 4: 67.

Johnson, D.B. (1998) Biodiversity and ecology of acidophilic microorganisms. *FEMS Microbiol Ecol* 27: 307-317.

Kanehisa, M., and Goto, S. (2000) KEGG: Kyoto Encyclopedia of Genes and Genomes. *Nucleic Acids Res* 28: 27-30.

Kembel, S.W., Cowan, P.D., Helmus, M.R., Cornwell, W.K., Morlon, H., Ackerly, D.D. et al. (2010) Picante: R tools for integrating phylogenies and ecology. *Bioinformatics* 26: 1463-1464.
Kharaka, Y.K., Thordsden, J.J., and White, L.D. (2002) Isotope and chemical compositions of meteoric and thermal waters and snow from the greater Yellowstone National Park region. In. U.S. Geological Survey Open File Report.

Laliberté, E., and Legendre, P. (2010) A distance-based framework for measuring functional diversity from multiple traits. *Ecology* 91: 299-305.

Liang, J., Crowther, T.W., Picard, N., Wiser, S., Zhou, M., Alberti, G. et al. (2016) Positive biodiversity-productivity relationship predominant in global forests. *Science* 354: 12.

Liang, M., Liu, X., Parker, I.M., Johnson, D., Zheng, Y., Luo, S. et al. (2019) Soil microbes drive phylogenetic diversity-productivity relationships in a subtropical forest. *Sci Adv* 5: 8.

Lindsay, M.R., Amenabar, M.J., Fecteau, K.M., Debes, R.V., 2nd, Fernandes Martins, M.C., Fristad, K.E. et al. (2018) Subsurface processes influence oxidant availability and chemoautotrophic hydrogen metabolism in Yellowstone hot springs. *Geobiology* 16: 674-692.

Lindsay, M.R., Colman, D.R., Amenabar, M.J., Fristad, K.E., Fecteau, K.M., Debes, R.V., 2nd et al. (2019) Probing the geological source and biological fate of hydrogen in Yellowstone hot springs. *Environ Microbiol* 21: 3816-3830.

Lowenstern, J.B., Bergfeld, D., Evans, W.C., and Hurwitz, S. (2012) Generation and evolution of hydrothermal fluids at Yellowstone: insights from the Heart Lake Geyser Basin. *Geochem Geophys Geosyst* 13.

Lowenstern, J.B., Bergfeld, D., Evans, W.C., and Hunt, A.G. (2015) Origins of geothermal gases at Yellowstone. *J Volcanol Geotherm Res* 302: 87-101.

McCleskey, R.B., Chiu, R.B., Nordstrom, D.K., Campbell, K.M., Roth, D.A., Ball, J.W., and Plowman, T.I. (2014) Water-chemistry data for selected springs, geysers, and streams in Yellowstone National Park, Wyoming, beginning 2009. In. U.S. Geological Survey Open File Report.

Meuser, J.E., Baxter, B.K., Spear, J.R., Peters, J.W., Posewitz, M.C., and Boyd, E.S. (2013) Contrasting patterns of community assembly in the stratified water column of Great Salt Lake, Utah. *Microb Ecol* 66: 268-280.

Meyer-Dombard, D.R., Shock, E.L., and Amend, J.P. (2005) Archaeal and bacterial communities in geochemically diverse hot springs of Yellowstone National Park, USA. *Geobiology* 3: 211-227.

Miller, S.R., Strong, A.L., Jones, K.L., and Ungerer, M.C. (2009) Bar-coded pyrosequencing reveals shared bacterial community properties along the temperature gradients of two alkaline hot springs in Yellowstone National Park. *Appl Environ Microbiol* 75: 4565-4572.

Moriya, Y., Itoh, M., Okuda, S., Yoshizawa, A.C., and Kanehisa, M. (2007) KAAS: an automatic genome annotation and pathway reconstruction server. *Nucleic Acids Res* 35: W182-W185.

Müller, W.J., Tlalajoe, N., Cason, E.D., Litthauer, D., Reva, O., Brzuszkiewicz, E., and Van Heerden, E. (2016) Whole genome comparison of *Thermus* sp. NMX2.A1 reveals principal carbon metabolism differences with closest relation *Thermus scotoductus* SA-01. *G3-Genes Genom Genet* 6: 2791-2797.

Nakagawa, S., Takai, K., Inagaki, F., Chiba, H., Ishibashi, J.-I., Kataoka, S. et al. (2005) Variability in microbial community and venting chemistry in a sediment-hosted backarc hydrothermal system: impacts of subseafloor phase-separation. *FEMS Microbiol Ecol* 54: 141-155.

Nguyen, L.T., Schmidt, H.A., von Haeseler, A., and Minh, B.Q. (2015) IQ-TREE: a fast and effective stochastic algorithm for estimating maximum-likelihood phylogenies. *Mol Biol Evol* 32: 268-274.

Nordstrom, D.K., Ball, W.J., and McCleskey, R.B. (2005) Ground water to surface water, chemistry of thermal outflows in Yellowstone National Park. In *Geothermal Biology and Geochemistry in Yellowstone National Park*. Inskeep, W.P., and McDermott, T. (eds). Bozeman, MT: Thermal Biology Institute, Montana State University, pp. 73-94.

Nordstrom, D.K., McCleskey, R.B., and Ball, J.W. (2009) Sulfur geochemistry of hydrothermal waters in Yellowstone National Park: IV Acid-sulfate waters. *Appl Geochem* 24: 191-207.
Nurk, S., Meleshko, D., Korobeynikov, A., and Pevzner, P.A. (2017) metaSPAdes: a new versatile metagenomic assembler. *Genome Res* 27: 824-834.

Ogawa, Y., and Ichimura, S. (1984) Phytoplankton diversity in inland waters of different trophic status. *Japanese J Limnology* 45: 173-177.

Parks, D.H., Imelfort, M., Skennerton, C.T., Hugenholtz, P., and Tyson, G.W. (2015) CheckM: assessing the quality of microbial genomes recovered from isolates, single cells, and metagenomes. *Genome Res* 25: 1043-1055.

Porter, M.L., Engel, A.S., Kane, T.C., and Kinkle, B.K. (2009) Productivity-diversity relationships from chemolithoautotrophically based sulfidic karst systems. *Int J Speleol* 38: 13.

Power, J.F., Carere, C.R., Lee, C.K., Wakerley, G.L.J., Evans, D.W., Button, M. et al. (2018) Microbial biogeography of 925 geothermal springs in New Zealand. *Nat Commun* 9: 2876.

Prosser, J.I., Bohannan, B.J.M., Curtis, T.P., Ellis, R.J., Firestone, M.K., Freckleton, R.P. et al. (2007) The role of ecological theory in microbial ecology. *Nat Rev Microbiol* 5: 384-392.

Reysenbach, A.-L., St. John, E., Meneghin, J., Flores, G.E., Podar, M., Dombrowski, N. et al. (2020) Complex subsurface hydrothermal fluid mixing at a submarine arc volcano supports distinct and highly diverse microbial communities. *Proc Natl Acad Sci U S A* 117: 32627-32638.

Rika E., A., Mónica T., B., Steven J., H., and John A., B. (2013) Microbial community structure across fluid gradients in the Juan de Fuca Ridge hydrothermal system. *FEMS Microbiol Ecol* 83: 324-339.

Rodriguez, R.L., Gunturu, S., Tiedje, J.M., Cole, J.R., and Konstantinidis, K.T. (2018) Nonpareil 3: Fast estimation of metagenomic coverage and sequence diversity. *mSystems* 3.

Rye, R.O., and Truesdell, A.H. (1993) The question of recharge to the deep thermal reservoir underlying the geysers and hot springs of Yellowstone National Park. In. U.S. Geological Survey Open File Report Vol. 1993.

Schrenk, M.O., Kelley, D.S., Delaney, J.R., and Baross, J.A. (2003) Incidence and diversity of microorganisms within the walls of an active deep-sea sulfide chimney. *Appl Environ Microbiol* 69: 3580-3592.

Sébastien, V. (2008) New multidimensional functional diversity indices for a multifaceted framework in functional ecology. *Ecology* v. 89: pp. 2290-2301-2008 v.2289 no.2298.

Seemann, T. (2014) Prokka: rapid prokaryotic genome annotation. *Bioinformatics* 30: 2068-2069.

Sharp, C.E., Brady, A.L., Sharp, G.H., Grasby, S.E., Stott, M.B., and Dunfield, P.F. (2014) Humboldt's spa: microbial diversity is controlled by temperature in geothermal environments. *The ISME Journal* 8: 1166-1174.

Shock, E.L., Holland, M., Meyer-Dombard, D.A., Amend, J.P., Osburn, G.R., and Fischer, T.P. (2010) Quantifying inorganic sources of geochemical energy in hydrothermal ecosystems, Yellowstone National Park, USA. *Geochim Cosmochim Acta* 74: 4005-4043.

Sims, K.W.W., Messa, C.M., Scott, S.R., Parsekian, A.D., Carr, B.J., Lowenstern, J.B. et al. (2022) A tale of two pools: the dynamic impacts of reactive transport, phase separation and shallow mixing on the geochemistry and microbiology of a coupled Yellowstone hydrothermal system. *Sci Adv*. *In Press*.

Smith, V.H. (2007) Microbial diversity-productivity relationships in aquatic ecosystems. *FEMS Microbiol Ecol* 62: 181-186.

Spear, J.R., Waker, J.J., McCollom, T.M., and Pace, N.R. (2005) Hydrogen and bioenergetics in the Yellowstone geothermal ecosystem. *Proc Natl Acad Sci U S A* 102: 2555-2560.

R Core Team (2018) R: A language and environment for statistical computing. *R Foundation for Statistical Computing, Vienna, Austria*.

Tilman, D., Reich, P.B., and Isbell, F. (2012) Biodiversity impacts ecosystem productivity as much as resources, disturbance, or herbivory. *Proc Natl Acad Sci U S A* 109: 10394-10397.

Truesdell, A.H., and Fournier, R.O. (1976) Conditions in the deeper parts of the hot spring systems of Yellowstone National Park, Wyoming. In. U.S. Geological Survey Open-File Report 76-428.

Truesdell, A.H., Nathenson, M., and Rye, R.O. (1977) The effects of subsurface boiling and dilution on the isotopic compositions of Yellowstone thermal waters. *J Geophys Res* 82: 3694-3704.

Uritskiy, G.V., Diruggiero, J., and Taylor, J. (2018) MetaWRAP—a flexible pipeline for genome-resolved metagenomic data analysis. *Microbiome* 6.

Wang, S., Hou, W., Dong, H., Jiang, H., Huang, L., Wu, G. et al. (2013) Control of temperature on microbial community structure in hot pprings of the Tibetan Plateau. *PLOS ONE* 8: e62901.

White, D.E., Hutchinson, Roderick A., and Keith, Terry E.C. (1988) The geology and remarkable thermal activity of Norris Geyser Basin, Yellowstone National Park, Wyoming, U.S. In. U.S. Geological Survey Professional Paper p. 84.

Williams, R.A.D., and Da Costa, M.S. (1992) The Genus *Thermus* and Related Microorganisms. In *The Prokaryotes*: Springer, New York, NY., pp. 3745-3753.

Willig, M.R. (2011) Biodiversity and productivity. *Science* 333: 1709-1710.

Tables

Table 1. Physical and chemical measurements made on waters collected from Roadside Springs, Norris-Mammoth Corridor, Yellowstone National Park, on November 5th, 2020.

Site	GPS	Temp. (˚C)	pH	Cond. (mS)	Water Isotopes (‰)		SO_4^{2-}	Cl^-	NO_3^-	S^{2-}	Fe(II)	DIC
					δ^2H	$\delta^{18}O$	(mg L^{-1})					
RSW	N 44.4512 W 110.4340	68.5	6.6	3.62	-130.3	-12.5	21.3	451.4	BD	0.26 ± 0.01	BD	32.1 ± 3.2
RSN	N 44.4514 W 110.4332	86.2	5.1	2.65	-132.6	-14.5	99.1	132.6	0.28 ± 0.05	0.46 ± 0.02	BD	6.0 ± 0.6
RSE	N 44.4512 W 110.4329	85.5	3.2	2.55	-138.1	-15.9	92.6	154.2	0.26 ± 0.06	0.18 ± 0.02	3.91 ± 0.08	2.1 ± 0.2

Abbreviations: GPS, Global Positioning System coordinates (WGS 84 datum); BD, Below Detection (<0.02 mg L^{-1}); Temp., Temperature; Cond., Conductivity; ‰, per mil; SO_4^{2-}, Sulfate; Cl^-, Chloride, NO_3^-, Nitrate; S^{2-}, Total Sulfide; Fe(II), Ferrous Iron; DIC, Dissolved Inorganic Carbon

Table 2. Calculated biodiversity metrics for metagenome assembled genomes (MAGs) or assembled contigs for each planktonic and sediment community in specified sites.

	Roadside West		Roadside North		Roadside East
	Planktonic	Sediment	Planktonic	Sediment	Planktonic
Number of MAGs	22	20	20	25	9
Number of MAGs (>1%)	2	5	4	14	3
Mean pairwise distance (mpd)	0.56	0.82	1.85	1.37	0.45
Standardized effect (SESmpd)	-0.98	-0.82	1.09	0.28	-1.19
p-value	0.01	0.002	0.81	0.75	0.04
Non-pareil diversity (N_d)	15.34	16.02	15.94	16.61	15.50
Functional Dispersion (FDis)	0.08	0.19	0.28	0.38	0.19

Figures

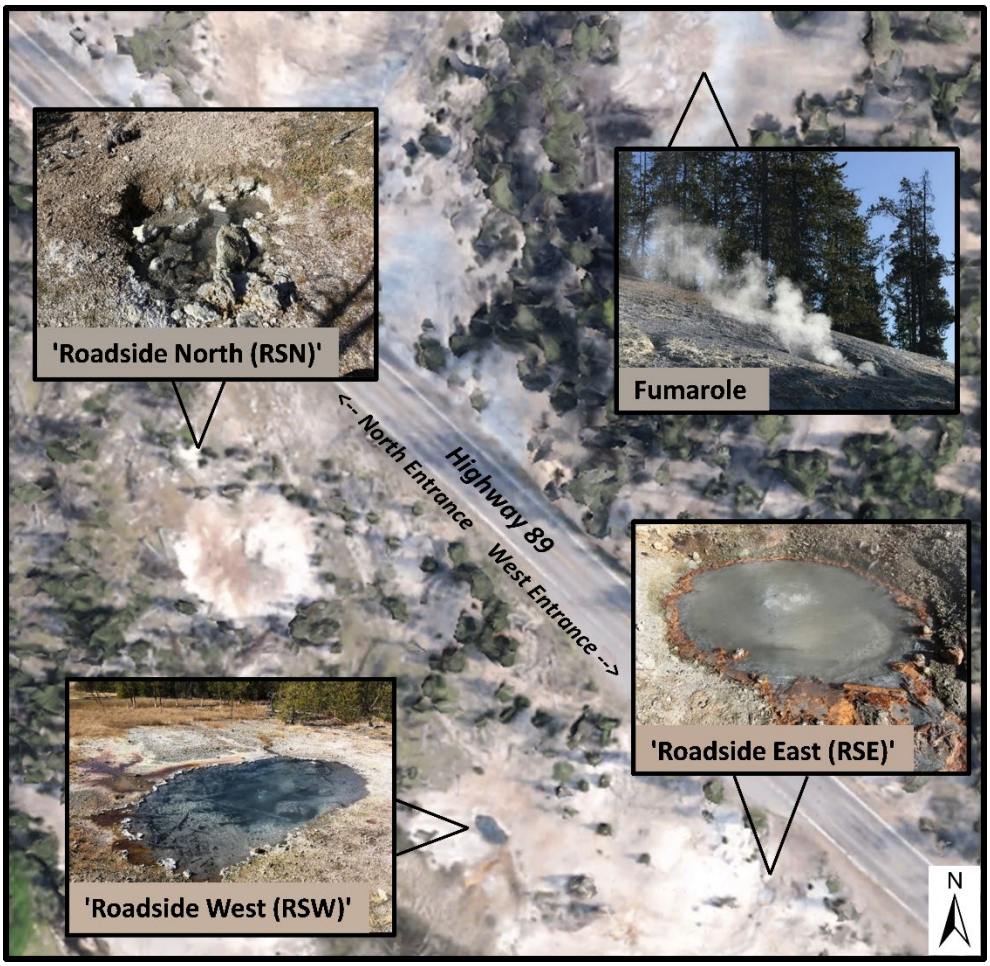

Figure 1. 'Roadside springs' are located in the Nymph Lake area in Yellowstone National Park (YNP). Roadside North (RSN), Roadside West (RSW), and Roadside East (RSE) hot springs, as well as the location of a large fumarole, are highlighted on a satellite image of the local obtained from Google Earth. YNP entrances and north arrow are indicated for reference.

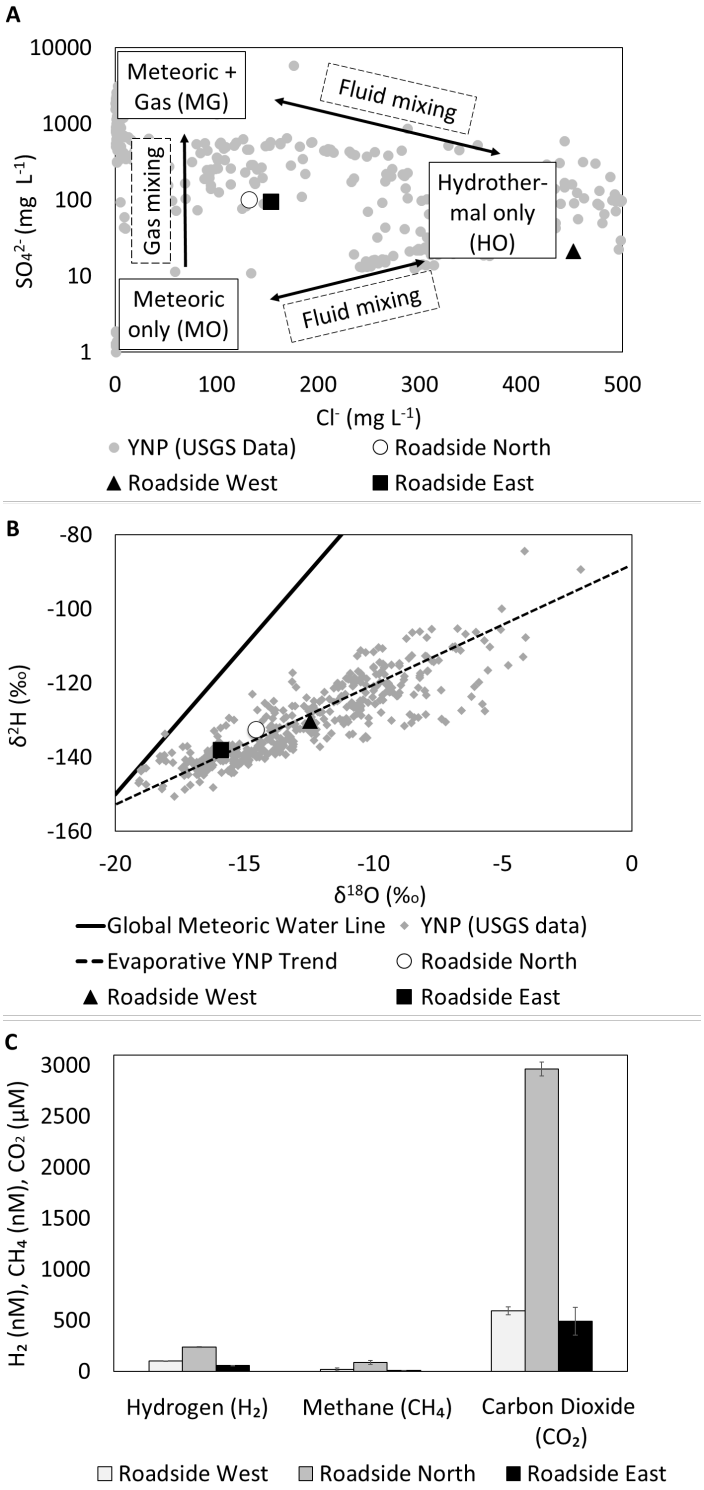

Figure 2. (A) Sulfate (SO_4^{2-}) (shown in log scale) and chloride (Cl^-) concentrations in hot spring waters. Data from 'Roadside Springs' are plotted in reference to data collected from a variety of Yellowstone National Park (YNP) hot springs generated by the United State Geological Survey

(USGS) as reported in (Ball et al., 2006) and (McCleskey et al., 2014) (grey dots). End-member water compositions, as defined by (Nordstrom et al., 2005b), are hydrothermal water only (HO), meteoric water only (MO), meteoric water with gas (MG). The vertical arrow shows increasing gas input into MO waters and angled arrows show mixing signatures. (B) The isotopic composition of hot spring waters ($\delta^{18}O$ and $\delta^{2}H$) in YNP. The $\delta^{18}O$ and $\delta^{2}H$ of Roadside waters are indicated alongside those of hot spring waters collected by the USGS as reported (Ball et al., 2006) and (McCleskey et al., 2014) (grey symbols). For reference, the black line and the dashed line are the Global Meteoritic Water Line (GMWL) (slope of ~2.8) and the inferred evaporative trend (slope of 5) at the $\delta^{18}O$ and $\delta^{2}H$ values for estimated recharge water for the hydrothermal system in YNP, at the $\delta^{18}O$ and $\delta^{2}H$ values for estimated recharge water, respectively, as defined previously (Kharaka et al., 2002; Nordstrom et al., 2005b) (C) Concentrations of dissolved hydrogen (H_2), methane (CH_4), and carbon dioxide (CO_2) measured in 'Roadside Springs' waters. The average and standard deviation of three replicate measurements are shown.

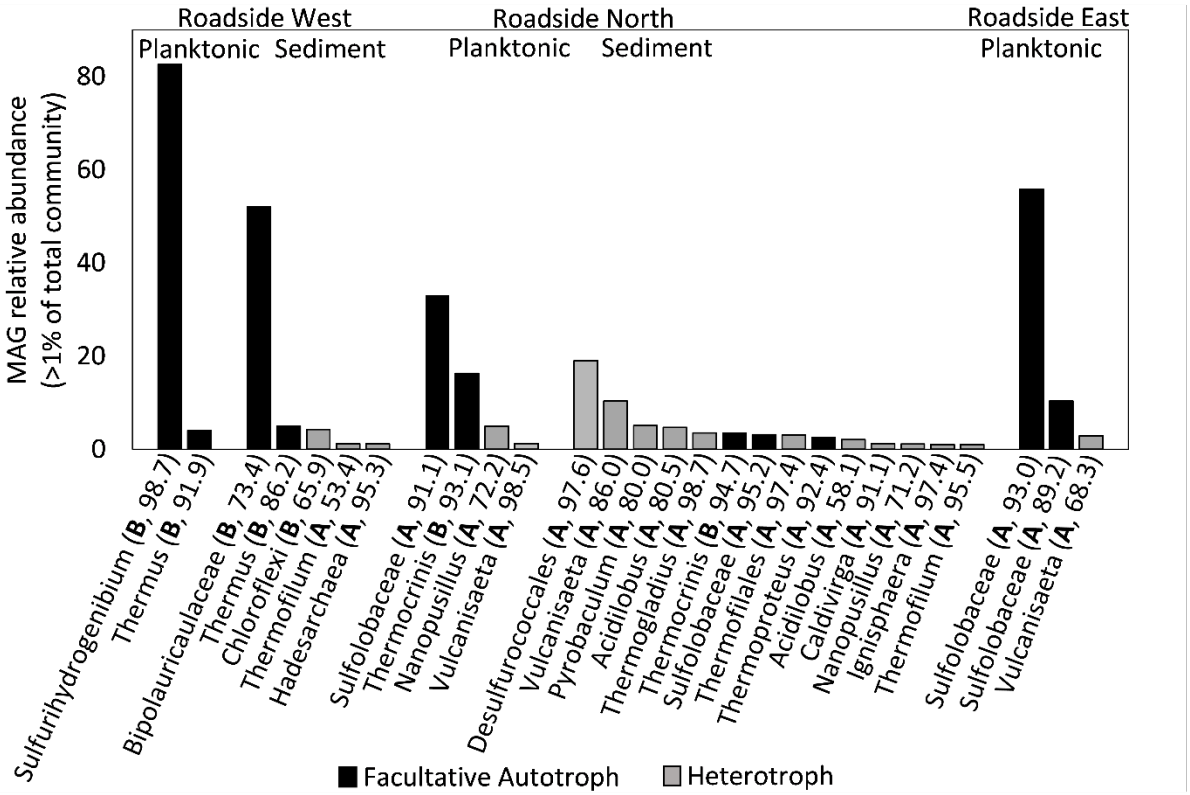

Figure 3. Rank abundance plot for metagenome assembled genomes (MAGs) (>50% complete and with a relative abundance cut-off of >1% of total community). Spring names are shown at the top of the legend and planktonic and sediment communities are depicted below. Black bars indicate MAGs that encode homologs for key proteins involved in one of the 6 primary carbon fixation pathways as well as glycolysis and TCA cycle (facultative autotroph). Grey bars indicate MAGs that didn't encode for key proteins involved in one of those carbon fixation pathways (heterotroph). The taxonomy of MAGs is indicated and in parenthesis is labeled with an 'A' denoting archaeal MAGs or a 'B' denoting bacterial MAGs, followed by the estimated completeness of each MAG. Taxonomic assignments were based on GTDBTK classification (Supp. Table 2).

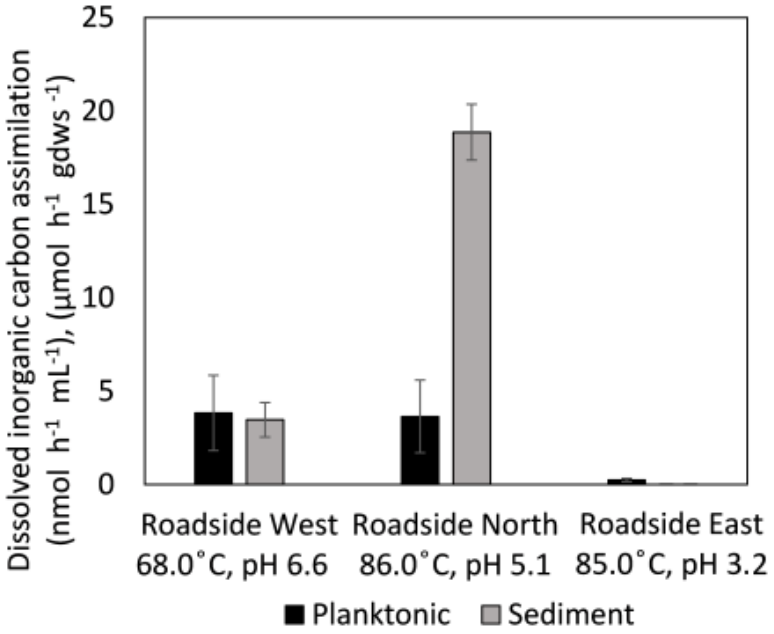

Figure 4. Rates of dissolved inorganic carbon (DIC) assimilation attributable to planktonic (black bars) or sediment (grey bars) communities in 'Roadside Springs'. Assays containing sediments and/or spring water and a ^{14}C-bicarbonate tracer were incubated in the dark for 6 hours at 68°C (Roadside West), 86°C (Roadside North), and 85°C (Roadside East). Abiotic (autoclave-killed) controls were subtracted from biotic controls to arrive at the values attributed to biology, which are depicted. The average and standard deviation for the triplicate assays is shown as nmol DIC per hour per mL for planktonic communities and as µmol DIC per hour per gram dry weight sediment (gdws) for sediment communities.

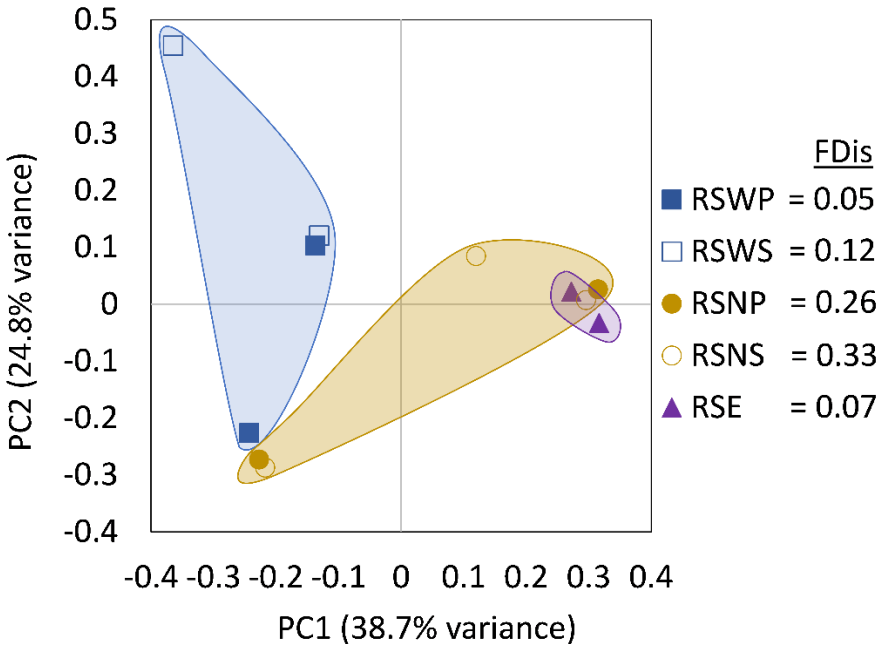

Figure 5. Principal coordinate analysis (PCoA) of the variation in the functional potential of metagenome-assembled genomes (MAGs) associated with putatively facultative autotrophs that represent >1% of the total community. The PCoA was based on a dissimilarity matrix of orthologs of proteins annotated in the 'dissimilatory pathways' under the 'energy metabolism' category in the Kyoto Encyclopedia of Genes and Genomes (Kanehisa and Goto, 2000). A total of 11 autotrophic MAGs were considered from all communities, with MAGs recovered from sediment indicated in closes symbols and MAGs recovered from filtered spring water (planktonic) in open symbols. The ordination was used to calculate functional dispersion (FDis) using the 'fdisp' function in the FD package (Sébastien, 2008; Laliberté and Legendre, 2010) in R. these values are shown alongside the FDis values obtained through the calculation.

CHAPTER THREE

SULFIDE OXIDATION BY MEMBERS OF THE SULFOLOBALES

Contribution of Authors and Co-Authors

Manuscript in Chapter 3

Author: Maria C. Fernandes-Martins

Contributions: Design the study. Conducted fieldwork. Carried out laboratory experiments and performed bioinformatics analyses. Contributed to the original writing and editing of the manuscript.

Co-Author: Dan R. Colman

Contributions: Conducted field work and oversaw bioinformatics analyses. Contributed to the editing of the manuscript.

Co-Author: Eric S. Boyd

Contributions: Design the study. Conducted field work and oversaw the study. Contributed to the original writing and editing of the manuscript.

Manuscript Information

Maria C. Fernandes-Martins, Dan R. Colman, and Eric S. Boyd

Proceedings of National Academy of Science Nexus

Status of Manuscript:
☐ Prepared for submission to a peer-reviewed journal
☐ Officially submitted to a peer-reviewed journal
☒ Accepted by a peer-reviewed journal
☐ Published in a peer-reviewed journal

Oxford University Press

Abstract

The oxidation of sulfur compounds drives the acidification of geothermal waters. At high temperatures (>80°C) and in acidic conditions (pH <6.0), oxidation of sulfide has historically been considered an abiotic process that generates elemental sulfur (S^0) that, in turn, is oxidized by thermoacidophiles of the model archaeal order Sulfolobales to generate sulfuric acid (i.e., sulfate and protons). Here, we describe five new aerobic and autotrophic strains of Sulfolobales comprising two species that were isolated from acidic hot springs in Yellowstone National Park (YNP) and that can use sulfide as an electron donor. These strains significantly accelerated the rate and extent of sulfide oxidation to sulfate relative to abiotic controls, concomitant with production of cells. Yields of sulfide-grown cultures were ~2-fold greater than those of S^0-grown cultures, consistent with thermodynamic calculations indicating more available energy in the former condition than the latter. Homologs of sulfide:quinone oxidoreductase (Sqr) were identified in nearly all Sulfolobales genomes from YNP metagenomes as well as those from other reference Sulfolobales, suggesting a widespread ability to accelerate sulfide oxidation. These observations expand the role of Sulfolobales in the oxidative sulfur cycle, the geobiological feedbacks that drive the formation of acidic hot springs, and landscape evolution.

Significance Statement

The oxygen-dependent oxidation of elemental sulfur by members of the model archaeal order Sulfolobales is widely thought to acidify hydrothermal waters. However, the primary source of sulfur in most hydrothermal systems is sulfide, which is widely thought to spontaneously oxidize in the presence of oxygen. Here, we show that sulfide is stable in the

presence of oxygen at low pH and that aerobic Sulfolobales significantly accelerate its oxidation and couple this to cell and acid production. Growth kinetics were significantly enhanced in cultures provided with sulfide relative to elemental sulfur, suggesting sulfide as the preferred electron donor. These results expand the role of Sulfolobales in the geobiological feedbacks that modulates the co-evolution of thermoacidophiles and their acidic habitats.

Introduction

Volcanic hot springs exhibit a bimodal distribution in their pH, reflecting the prevalence of two types of spring waters: acid-sulfate (pH 2-4) and neutral-bicarbonate (pH 7-9), respectively (Brock, 1971). Formation of acid-sulfate waters is initiated by injection of magmatic sulfur dioxide (SO_2) into deep hydrothermal fluids and its subsequent disproportionation as those fluids cool (<400°C) to form either *i*) sulfuric acid (HSO_4^-), elemental sulfur (S^0), and protons (H^+) or *ii*) HSO_4^-, sulfide (HS^-), and H^+ (Eq. 1 and Eq. 2, respectively) (Kusakabe et al., 2000). Reaction 2 is expected to prevail in volcanic systems with lower sulfur concentrations and lower temperatures (Holland, 1965), such as YNP (Nordstrom et al., 2009b). During their ascent to the surface, fluids can undergo the process of decompressional boiling, which allows volatiles (e.g., hydrogen sulfide or H_2S) to partition into the gas phase (Fournier, 1989; Nordstrom et al., 2009b) leaving a volatile poor liquid phase that forms neutral-bicarbonate (pH 7-9) hot spring waters when it surfaces. Low density volatiles can continue to ascend to the surface where they can condense with oxygen (O_2)-rich near surface groundwaters (Allen and Day, 1935; Brock, 1971). Under such conditions, sulfide can react with O_2 to form thiosulfate ($S_2O_3^{2-}$) (Eq. 3) that, in acidic waters (< 6.0), rapidly disproportionates to form S^0 and bisulfite (HSO_3^-) (Eq. 4;

(Nordstrom et al., 2005b)). HSO_3^- is also unstable in acidic and oxygenated waters and oxidizes rapidly to form SO_4^{2-} (Eq. 5).

$$3SO_2 + 3H_2O \rightarrow 2HSO_4^- + S^0 + 2H^+ \quad \text{(Equation 1)}$$

$$4SO_2 + 4H_2O \rightarrow 3HSO_4^- + H_2S + 3H^+ \quad \text{(Equation 2)}$$

$$2HS^- + 2O_2 \rightarrow S_2O_3^{2-} + H_2O \quad \text{(Equation 3)}$$

$$S_2O_3^{2-} + H^+ \rightarrow S^0 + HSO_3^- \quad \text{(Equation 4)}$$

$$HSO_3^- + ½O_2 \rightarrow SO_4^{2-} + H^+ \quad \text{(Equation 5)}$$

$$S^0 + 3/2\ O_2 + H_2O \rightarrow HSO_4^- + H^+ \quad \text{(Equation 6)}$$

At temperatures <100°C, S^0 is stable and thus represents an abundant electron donor and acceptor for microorganisms in hot spring environments (Nordstrom et al., 2005b; Nordstrom et al., 2009b). Reactions 1-5 are generally considered abiotic and do not contribute to net production of acidity (Nordstrom et al., 2005b). However, the oxidation of S^0 is considered biologically mediated, a reaction that is thought to be responsible for the acidification of hot springs (Brock et al., 1972; Mosser et al., 1973; Shivvers and Brock, 1973; White, 1988; Nordstrom et al., 2005b; Nordstrom et al., 2009b).

At temperatures above 80°C, the dominant organisms in acidic hot springs are generally members of the archaeal order Sulfolobales (Urbieta et al., 2015; Jiang et al., 2016; Ward et al., 2017; Colman et al., 2018). While aerobic S^0-oxidation is generally the metabolism associated foremost with members of the Sulfolobales (Brock et al., 1972; Shivvers and Brock, 1973; Counts et al., 2021; Lewis et al., 2021), the group is metabolically diverse and reports of heterotrophic or autotrophic, aerobic or anaerobic, and lithotrophic growth are widespread

among cultivars (Amenabar and Boyd, 2018; Counts et al., 2021; Lewis et al., 2021; Liu et al., 2021). For example, members of the Sulfolobales have been shown to grow via oxidation of ferrous iron (Fe(II)), hydrogen (H_2), and pyrite (FeS_2), via reduction of ferric iron (Fe(III)) and S^0, and via S^0-disproportionation, among other oxidation-reduction reactions. Nevertheless, aerobic S^0 oxidation was long thought to be a unifying feature of Sulfolobales until more recent reports of Sulfolobales strains that are either inhibited by S^0 (*Sulfodiicoccus acidiphilus*) (Sakai and Kurosawa, 2017) or that are strict anaerobes (*Stygiolobus azoricus* (Segerer et al., 1991)).

S^0-oxidation in Sulfolobales is thought to involve the cytoplasmic enzyme sulfur oxidoreductase:reductase (Sor) that catalyzes the O_2-dependent disproportionation of S^0 to yield sulfide, HSO_3^-, and $S_2O_3^{2-}$, a reaction that by itself is not energy conserving (Kletzin, 1989, 1992; Urich et al., 2004; Zeldes et al., 2019; Liu et al., 2021). Sulfide is then oxidized by membrane-associated sulfide:quinone reductase (Sqr) that conserves energy by coupling oxidation to the reduction of quinone in a membrane-associated electron transport chain (Brito et al., 2009), while HSO_3^- and $S_2O_3^{2-}$ are processed downstream through additional energy conserving reactions (Zimmermann et al., 1999; Müller et al., 2004; Liu et al., 2021). As such, any Sulfolobales that can oxidize S^0 via Sor should also be able to oxidize sulfide. Indeed, all Sulfolobales that encode Sor also encode Sqr (Zeldes et al., 2019; Liu et al., 2021). Further, those members of the Sulfolobales that do not encode Sor encode Sqr and a heterodisulfide reductase (Hdr) complex (Zeldes et al., 2019; Counts et al., 2021; Liu et al., 2021), and the latter has been suggested to be an alternative and essential pathway for sulfur oxidation in other thermophiles, including model acidophilic bacteria (Jiang et al., 2014; Boughanemi et al., 2016; Koch and Dahl, 2018; Colman et al., 2022), as well as in the Sulfolobales strain *Metallosphaera cuprina*

(Jiang et al., 2014). Together, these observations raise the question as to whether Sulfolobales can catalyze sulfide oxidation and couple this redox reaction to biomass production as an alternative or preferred strategy over S^0 oxidation.

In potential support of sulfide oxidation by Sulfolobales, a Sqr purified from membranes of a *Acidianus ambivalens* linked sulfide oxidation to O_2-reduction (Brito et al., 2009). Further, Sqr purified from membranes of the archaeon *Caldivirga manquilingensis* was shown to have the same catalytic properties of linking sulfide oxidation to the reduction of quinone (Lencina et al., 2013). In addition, studies of high temperature hot spring communities have interpreted the presence of Sqr homologs in reconstructed Sulfolobales genomes as evidence that they are involved in sulfide oxidation (Colman et al., 2021; Colman et al., 2022; Fernandes-Martins et al., 2023). However, despite 50+ years of study, oxidation of sulfide by members of the Sulfolobales (or more broadly among Archaea) remains an open question (Counts et al., 2021; Liu et al., 2021) since the few papers that have reported oxidation of sulfide by Sulfolobales either did not show the supporting data (Stetter et al., 1990; Kawarabayasi et al., 2001; Morales et al., 2012) or provided debatable results (Plumb et al., 2007; Morales et al., 2011; Silva et al., 2023), as discussed more below. It is also possible that the prevailing notion that sulfide is unstable in the presence of O_2 at high temperature and in acidic conditions (Brock et al., 1972; Nordstrom et al., 2005b; Nordstrom et al., 2009b) may have limited research into whether Sulfolobales can accelerate this oxidative process.

To begin to reconcile these observations, we investigated abiotic and biotic reactions involved in sulfide oxidation at high temperature and acidic pH. We probed the kinetics of abiotic sulfide oxidation with O_2 at varying pH, temperature, and O_2-concentration to identify

conditions where microorganisms could possibly accelerate the kinetics of the reaction and conserve energy from the reaction. This information was then used to guide the enrichment of sulfide-oxidizing organisms from three hot springs in Yellowstone National Park, Wyoming, U.S.A.: Cinder Pool, 'Realgar Pool', and 'Red Bubbler'. We describe the ability of four closely related strains of *Stygiolobus* (Sulfolobales) and a new genus (Sulfolobales) to accelerate the O_2-dependent oxidation of sulfide, generating acidity through SO_4^{2-} and H^+ production. These data expand the role of Sulfolobales in the oxidative sulfur cycle to include sulfide oxidation and further underscore their role in the acidification of hot springs waters.

Materials and Methods

Kinetics of Abiotic Sulfide Oxidation

Abiotic sulfide oxidation assays were conducted in laboratory defined conditions at 80°C and at pH 3.0 or 7.0 and in the presence of varying O_2 concentrations in the headspace (0%, 1%, and 21% vol./vol.). Ten mL of Milli-Q water were distributed in acid-washed 24 mL serum bottles and vials were sealed with grey butyl rubber stoppers. Following autoclave sterilization, vials were purged for 20 min. with N_2 passed over heated (350°C) and H_2-reduced copper shavings. Triplicate vials for each condition were prepared for each time point. An aliquot of anoxic and filter-sterilized (0.22 µm) sodium citrate solution (prepared to final pH of 3.0) or Tris-HCl (prepared to a final pH of 7.0) was added to each serum bottle to a final concentration of 200 µM or 1 mM, respectively. The N_2 headspace of vials was left as is (0% O_2 condition) or was replaced by air at a specific volume to achieve the final concentration of 1% vol./vol O_2, or completely replaced by air to achieve the final concentration of 21% vol./vol O_2. Finally, an aliquot of an anoxic and filter-sterilized (0.22 µm) solution of sodium sulfide (Na_2S) was added

to each serum bottle to a final concentration of 100 μM. The experiments were run for 15 h and the concentration of dissolved total sulfide ($H_2S/HS^-/S^{2-}$) was determined every 3 h via the methylene blue reduction assay (Fogo and Popowsky, 1949) and this was converted to total sulfide using Henry's law as previously described (Boyd et al., 2007).

A second set of abiotic sulfide oxidation kinetic assays was conducted to investigate the reactivity of sulfide with ferric iron ions [added as ferric sulfate $(Fe_2SO_4)_3$]. These experiments were conducted at pH 2.6 and at 80°C, and the vials were prepared as described above (without addition of headspace O_2) to mimic previously described experiments (Plumb et al., 2007). Briefly, Na_2S was added to a final concentration of eight mM in triplicate 70 mL serum bottles containing 30 mL of Milli-Q containing 25 mM $(Fe_2SO_4)_3$. A triplicate set of serum bottles that did not contain $(Fe_2SO_4)_3$ was used as a control. All reactors were buffered with nine mM of an anoxic and filter-sterilized (0.22 μm) sodium citrate solution (prepared to final pH of 2.6). Aqueous sulfide concentrations were measured and converted to total sulfide as described above, and production of ferrous iron was determined via the Ferrozine assay (Viollier et al., 2000).

X-Ray Powder Diffraction Analysis

Precipitates that were observed during abiotic reactions and growth of Sulfolobales strains were concentrated via centrifugation (14,000 × *g*, 20 min., 4°C) from triplicate reactors (~100 mL in total). The supernatant was discarded via pipetting and the pellet was air dried overnight. Precipitates were characterized at the Imaging and Chemical Analysis Laboratory (ICAL) at Montana State University using a SCINTAG X-1 system X-ray powder diffraction (XRD) spectrometer (XRD Eigenmann GmbH, Mannheim, Germany).

Sample Collection and Field Geochemical Assays

In 2018, ~ 1g of sediment from 14 acidic hot springs (Supplemental Table 3) in YNP were aseptically sampled, placed in sterile 15 mL falcon tubes, and frozen on dry ice in the field and stored in a -80°C freezer back in the laboratory until used in DNA extractions. Subsamples of hot spring water for enrichment and cultivation were collected on August 28th, 2020, in autoclaved 70 mL glass serum vials from Cinder Pool (CP; pH 2.6, 87.8°C; 44.732444 N, 110.709779 W) and from the surface of "Realgar Pool" (RP; pH 3.9, T 85.8°C; 44.73558 N, 110.70705 W), both of which are located at Norris Geyser Basin, YNP. On June 3td, 2021, samples of hot spring water were again collected from CP but from 9 m and 21 m below the surface for cultivation. A description of the approach to collect samples from depth at CP is discussed elsewhere (Colman et al., 2022). On June 13th, 2023, samples for cultivation were collected from the surface water of "Red Bubbler" (RB; pH 3.0, T 90°C; 44.72650 N, 110.70900 W), also located at Norris Geyser Basin. Sterile vials for water samples for cultivation were completely filled and capped with sterile butyl rubber stoppers equipped with needles to exclude headspace. The needles were then removed, the bottles capped, wrapped in aluminum foil to exclude light, and kept at room temperature (~20°C) during transport to the laboratory prior to inoculating enrichment medium. Surface water from each hot spring for use as an additive to growth medium (described below) was also collected from each spring and filtered (0.22 μm) in the field into autoclaved polypropylene bottles that were then stored on ice during transport back to the laboratory, followed by storage at 4°C until their use.

The temperature, conductivity, and pH of hot spring waters were measured in the field with temperature-compensated probes (model YSI EC300, YSI Inc., Yellow Springs, OH, U.S.A. or model WTW 3100, WTW Weilheim, Germany). Subsamples of waters for ion

chromatography (IC) and for inductively coupled plasma mass spectrometry (ICP-MS) were filtered in the field (0.22 μm) and stored in polypropylene vials capped with no headspace. Samples for ICP-MS were acidified with trace metal grade nitric acid to a final concentration of 1% vol./vol. Samples of culture medium or supernatant following growth were filtered (0.22 μm) prior to acidification for ICP-MS analyses. IC and ICP-MS analyses of hot spring waters were conducted at the Montana Bureau of Mines and Geology Analytical Laboratory.

Enrichment and Isolation

Enrichment medium was prepared by combining 80% base salt medium with 20% filtered (0.22 μm) water from either CP or RP. Base salt medium comprised $CaCl_2$ (0.33g L^{-1}), NH_4Cl (0.33g L^{-1}), KCl (0.33g L^{-1}), $MgCl_2$ (0.33g L^{-1}), and KH_2PO_4 (0.33g L^{-1}), as previously described (Boyd et al., 2007). The salts were added to Milli-Q water and the pH was adjusted to 2.6 (CP) or 4.0 (RP) using 1N HCl. Twenty-seven mL of base salt/filtered spring water medium was dispensed into 70 mL serum bottles that were then sealed with grey butyl rubber stoppers. Following autoclave sterilization, vials were purged for 20 min. with N_2 passed over heated (350°C) and H_2-reduced copper shavings. Next, the headspace was purged with carbon dioxide (CO_2) for 5 min. and vials were placed in an 85°C incubator. After two h of incubation, the headspace was equilibrated to atmospheric pressure, followed by addition of anoxic and filter-sterilized (0.22 μm) solutions of Wolfe's vitamins (Atlas, 2004) and SL-10 metals (Widdel, 1983) to a final concentration of 1 mL L^{-1} each. Oxygen (O_2) (as air) was added to the headspace to a final concentration of 1.5 % vol./vol. An anoxic and filter-sterilized (0.22 μm) sodium citrate buffer solution, prepared to a final pH of 2.6 (CP) and 4.0 (RP), was added to serum bottles to a final concentration of 200 μM and an anoxic and filter-sterilized (0.22 μm) solution of Na_2S was

added to each serum bottle to a final concentration of 100 µM. Three mL of a sediment/spring water slurry were added to each respective vial as inoculum and vials were incubated at 85°C. For elemental sulfur (S^0) enrichment conditions, serum bottles were prepared as described above with the exception that baked (100°C, 120 min.) S^0 was added to a final concentration of ~450 µM (0.014 g L^{-1}). To better understand why the Sulfolobales strains grow better with filter-sterilized hot spring water additions, cultures were grown under S^0 oxidizing conditions and compared using 100% base salt medium versus 80% synthetic base salt medium with 20% sterile hot spring water. Triplicate cultures were prepared for each condition for the initial time point (TI) and for the final time point (TF) (n = 12). Each culture vial was filtered sterilized (0.22 µm), and the filtrate prepared for ICP-MS analyses, as described above, which were conducted at the Montana Bureau of Mines and Geology Analytical Laboratory.

Monitoring of Growth and Activity in Enrichments

Enrichment progress was evaluated every 5 h by monitoring the concentrations of dissolved sulfide [primarily H_2S at pH 2.6 and 4.0 (Amend, 2001)], SO_4^{2-}, and cells. The concentration of aqueous sulfide ($H_2S/HS^-/S^{2-}$) was determined via the methylene blue reduction assay (Fogo and Popowsky, 1949) and this was converted to total sulfide using Henry's law as previously described (Boyd et al., 2007). The concentration of SO_4^{2-} was determined via a barium chloride turbidity assay (Kolmert et al., 2000). Quantification of sulfite (HSO_3^-) and thiosulfate ($S_2O_3^{2-}$) were probed in spent culture media with assays based on the reduction of fuchsin (Pachmayr, 1960; Urich, 2005) and ion-chromatography (IC), respectively. The concentration of cells in enrichments was determined by removing 0.5 mL aliquots of culture, mixing with 0.1 µL of a 2 mg/mL 4′,6-diamidino-2-phenylindole (DAPI) stock, and incubating

the mixture in the dark for ~30 min. Cells were collected onto black polycarbonate filters with 0.22 μm pores (Millipore Sigma, Billerica, MA) and were enumerated with an Evos fluorescence microscope (Thermo Fisher Scientific, Waltham, MA, U.S.A.). Cultures were transferred until a single morphotype was observed and were maintained by weekly (10% vol./vol.) transfers of log or late log phase cells into fresh growth medium.

DNA Extraction, (Meta)genomic Sequencing, Assembly, and Genome Binning

Genomic DNA was extracted from sediment samples (~ 0.5 g) from the 14 hot springs (Supplemental Table 3) and from enrichment culture biomass using the FastDNA Sping Kit for Soil (MP Biomedicals, Irvine, CA) following the manufacturer's instructions and was quantified fluorometrically via the high sensitivity Qubit assay (Thermo Fisher Scientific). Biomass from cultivation vials for DNA extractions was concentrated via centrifugation (14,000 × *g*, 20 min., 4°C) from 300 mL of enrichment culture that was confirmed via microscopy to have a single morphotype. Genomic DNA from the 14 hot spring sediment samples was subjected to paired-end sequencing (2 x 151 bp) with the Illumina NovaSeq platform at the UW Madison Next-Generation Sequencing Center. Genomic DNA from enrichment cultures was sequenced via the Illumina NovaSeq platform at Microbial Whole Genome Sequencing (MiGs; Pittsburgh, PA, U.S.A.). Read processing, genome assembly, and binning of contigs into metagenome-assembled-genomes (MAGs) was performed as previously described (Fernandes-Martins et al., 2021) using the MetaWRAP pipeline (Uritskiy et al., 2018). MAGs recovered from hot spring metagenomes are deposited at the National Center for Biotechnology Information (NCBI) database (Sayers et al., 2022) under BioProject PRJNA1019763. The partial genome sequence of the isolates is deposited at NCBI database under BioProject PRJNA1019763, together with their

translated protein content, with the exception of Sulfolobales RB85, which can be found in the Supplemental Table 8.

Phylogenetic and Genomic Characterization

Marker genes (n = 30) for Archaea were identified, aligned, and concatenated using Markerfinder (https://github.com/faylward/markerfinder#markerfinder) for 31 reference genomes or MAGs (five representative of outgroups for the Sulfolobales order, 21 type strain of the Sulfolobales order, and the five isolated strains). The alignment block was subjected to phylogenetic reconstruction using IQ-Tree (v.1.6.11) (Nguyen et al., 2015) specifying the LG model and 1000 'ultrafast' bootstrap replicates, as previously described (Fernandes-Martins et al., 2021). Open reading frames and encoded proteins were identified with PROKKA (v.1.14.5) (Seemann, 2014), and the protein annotation for each MAG was then submitted to METABOLIC v 4.0 (Zhou et al., 2019) to identify keys genes for CO_2 fixation and dissimilatory sulfur metabolism. This included 4-hydroxybutyryl-CoA dehydratase (Abfd) for CO_2 fixation and sulfide quinone oxidoreductase (Sqr), sulfur oxygenase:reductase (Sor), heterodisulfide reductase (HdrAB1B2C1C2), and sulfur/polysulfide reductase (SreABC) for dissimilatory sulfur metabolism (Supplemental Table 4). In addition, homologs of Sqr were identified among 51 hot spring metagenomes from our in-house hot spring database (Supplemental Table 3; Supplemental Table 5) using METABOLIC v 4.0 (Zhou et al., 2019). The homologs for sulfite:acceptor oxidoreductase (Suox), thiosulfate:quinone oxidoreductase (Tqo), and tetrathionate hydrolase (TetH) were identified with query from the characterized proteins of *Acidianus ambivalens* using the Basic Local Alignment Search Tool (BLASTp) (Boratyn et al., 2012) at the National Center for Biotechnology Information (NCBI). Parameters used to search for homologs were a E value

cutoff of $1.0e^{-50}$, amino acid identify of >50% and >60% coverage of the query sequence (Fernandes-Martins et al., 2021). BLASTp was also used to determine the percent identify between the biochemically characterized Sqr from *A. ambivalens* and Sqr homologs identified in the genomes of isolates. Homologs that weren't in the publicly available assemblies or were unbinned contigs were submitted in Supplemental Table 7.

Scanning Electron Microscopy (SEM)

Ten mL of the enrichment culture from *Stygiolobus* sp. CP85 – 0m growing on sulfide were harvested during log-phase via centrifugation (14,000 × *g*, 20 min., 4°C) for field emission scanning electron microscope (FE-SEM) analysis. After centrifugation, the supernatant was removed by aspiration and the cell pellet was resuspended in base salt medium containing 2% vol./vol. glutaraldehyde for 2 h at room temperature (~21°C). Fixed cells were collected on an Au-sputtered 0.2 µm black polycarbonate filter and were subjected to dehydration using an ethanol series (25, 50, 70, 85, 95, and 100%), as previously described (Payne et al., 2021). Filtered and dehydrated cells were stored dry at 4°C until imaging in the Imaging and Chemical Analysis Laboratory (ICAL) at Montana State University. Samples were mounted on the FE-SEM holder using double-sided carbon tape and sputtered with a thin film of iridium for conductivity before loading to the FE-SEM chamber, as described previously (Payne et al., 2021). Images were taken using a high-resolution FE-SEM (Supra 55VP, Zeiss, Thornwood, NY, U.S.A.) with a primary electron beam energy of 1 keV at different magnifications.

Energetics Calculations

Available Gibbs free energy (ΔG) at the specific pressure and temperature of growth experiments (1 atm; 80°C) at the time of inoculation was calculated using the package CHNOSZ

as implemented in the R statistical framework (Boyer, 2023). ΔG calculations can be described by Equation 7 (Amenabar et al., 2017):

$$\Delta G = \Delta G° + 2.303RT \log Q \qquad \text{(Equation 7)}$$

$$H_2S\ (aq) + 2\ O_2\ (aq) \rightarrow HSO_4^-\ (aq) + H^+ \qquad \text{(Equation 8)}$$

where ΔG° represents standard conditions (J mol $^{-1}$), R represents the ideal gas constant (~8.314 J mol^{-1} K^{-1}), T indicates temperature in Kelvin (K), and Q is the reactant and product activity quotient. Q was calculated using the balanced equation for aerobic S^0 oxidation (Eq. 6) and for aerobic sulfide oxidation (Eq. 8) at the specific ionic strength of the aqueous solutions.

Determination of Sulfide Toxicity

The *Stygiolobus* CP85 – 0m strain was used to probe the concentration where sulfide becomes toxic. Cultivation medium was prepared as described above but was amended to include different starting concentrations of sulfide, added as Na_2S. This included 100 µM (positive control), 500 µM, 1 mM and 15 mM starting sulfide. All culture vials were amended with citrate buffer at a concentration to sufficiently buffer the medium (pH 2.6) given the amount of Na_2S that was added to achieve the final sulfide concentration (i.e., the 500 µM sulfide treatment included 600 µM citrate buffer). Cultures were monitored every 24 h to monitor the depletion of sulfide via the methylene blue assay (Fogo and Popowsky, 1949) and the production of cells via fluorescent microscopy, as described above.

Dissolved Inorganic Carbon Assimilation Assays

Rates of dissolved inorganic carbon assimilation were determined for planktonic-associated communities recovered from a depth profile (0 m, 9 m, 21 m) in ‘Cinder Pool’ (pH

2.6, T 88°C), as previously described (Fernandes-Martins et al., 2023). Briefly, acid-washed 24 mL serum bottles were sealed with butyl rubber stoppers and purged with N_2 that had been passed over heated (>200°C) and H_2-reduced copper shavings for 5 min. before autoclaving. In the field, 10 mL of spring water from each of the three depth profiles was added directly to twelve serum vials; the gas phase in the vials was equalized to atmospheric pressure using a sterile needle and syringe. All microcosm vials prepared in the field were immediately placed on ice and in the dark for the 2 hr transport back to the laboratory.

In the laboratory, six microcosms from each depth profile were subjected to a single 20 min. autoclave cycle (121 °C, 20 psi) for use as abiotic controls. Microcosm vials were brought to room temperature (~21 °C) and five μCi of [^{14}C] sodium bicarbonate ($NaH^{14}CO_3$) was added to each vial. Microcosms were placed in a sealed bag (secondary containment) and incubated in the dark near the measured temperature of hot spring waters (*see* Table 1) for two and four hrs. After incubation, microcosms were placed in a second sealed bag (tertiary containment) and stored at -20 °C until they were processed, as previously described (Fernandes-Martins et al., 2023). Briefly, in a fume hood, microcosm vials were thawed at room temperature. Vials were unsealed and acidified to pH of < 2 by adding 200 μL of 12 N HCl to volatilize unassimilated DIC. After two hrs of degassing in the fume hood, microcosm contents were filtered onto 0.22 μm white polycarbonate filters, washed with sterile deionized water, placed in scintillation vials, and dried overnight in the fume hood. Filters were then overlaid with 10 mL of CytoScint ES liquid scintillation fluid (MP Biomedicals, Solon, OH). Radioactivity associated with filtered biomass was measured as counts per minute (CPM) on a Beckman LS 6,500 liquid scintillation counter (Beckman Coulter, Inc., Indianapolis, IN). All the values presented are biological values

as the average and standard deviation of the mean of three replicate assays, accounted for the background values measured in abiotic vials.

Results

Kinetics of Abiotic Sulfide Oxidation

The kinetics of abiotic sulfide oxidation was determined at 80°C in MilliQ water buffered at pH of 3.0 and 7.0 pH, in the presence of 0%, 1%, and 21% O_2 (vol./vol.) (Figure 1). The concentration of aqueous sulfide was quantified every 3 h for a period of 15 h. The decrease in aqueous sulfide in the 0% O_2 condition conducted at pH 3.0 and pH 7.0 indicated that it quickly equilibrated with the gas phase, since no other oxidants were available (Figure 1). The equilibration period occurs within the first 6 h in the pH 3.0 assays whereas it occurred throughout the duration of the experiment in pH 7.0 assays. Therefore, the difference observed in the depletion of sulfide between the 0% O_2 (vol./vol.) assays (equilibration only) when compared to those conducted in the presence of 1% and 21% O_2 (vol./vol.) assays (equilibration + oxidation) can be used to isolate the amount of sulfide that was oxidized abiotically by O_2.

In assays conducted at pH 7.0 and in the presence of 1% and 21% O_2 vol./vol, the concentration of sulfide decreased to below the equilibrium concentrations (0% O_2 vol./vol.) within the first 3 h of incubation (Figure 1A). In comparison, assays conducted at pH 3.0 in the presence of 1% and 21% O_2 showed minimal decreases below that of the equilibrium concentration (0% O_2 v vol./vol.) after 3 h (Figure 1B). The rate of abiotic oxidation of sulfide at 1% and 21% vol./vol. O_2 was calculated between 3 h and 15 h by transforming the measured aqueous sulfide concentration (μM) to total sulfide in μmoles (aqueous and gas phase). The rate of abiotic oxidation in assays provided with 1% vol./vol. O_2 was 0.03 ± 0.005 and 0.04 ± 0.005

μmols h^{-1} at pH 3.0 and pH 7.0, respectively. Assays provided with 21% vol./vol. O_2 exhibited an abiotic sulfide oxidation rate of 0.06 ± 0.006 and 0.08 ± 0.002 μmols h^{-1} at pH 3.0 and pH 7.0, respectively.

A second experiment was conducted to investigate the kinetics of abiotic oxidation of sulfide by ferric ions [Fe(III) added as $(Fe_2SO_4)_3$] under anoxic conditions. Abiotic experiments were established to mimic the conditions used in Plumb et al., 2007. Anoxic citric acid-buffered medium containing 25 mM $(Fe_2SO_4)_3$ was reacted with 8 mM of sodium sulfide (Na_2S) at 80°C and at a pH 3.0. A near instantaneous reaction occurred (Supplemental Video 1) as evinced by the immediate formation of black suspended particles that quickly transformed into a white flocculant material that then precipitated. XRD analysis of the precipitated flocs showed a 100% match with S^0 (Supplemental Figure 6). These reactions resulted in an immediate consumption of all added sulfide and the concomitant production of ~12.5 mM Fe(II), which nearly accounts for the 8 mM sulfide if all of it was converted to S^0 (release of 16 mM electrons). These observations are consistent with the results presented by Plumb et al., 2017 wherein the concentration of Fe(II) at the start of the experiment was ~9 mM, despite those authors having not added Fe(II) but rather having added Fe(III).

Isolation of Sulfide-Oxidizing Sulfolobales Strains

Water from the surface (0 m) of two YNP hot springs, RP (pH 4.0) and CP (pH 2.6; Table 1, Supplemental Table 1, Supplemental Figure 1), was used as inoculum for enrichment of aerobic, autotrophic sulfide-oxidizing microorganisms. Additional sampling campaigns were conducted to collect water from 9 m and 21 m depth (pH 2.6) from CP and from the surface of an additional hot spring, RB (pH 3.0), for use as inoculum for enrichment using the same strategy as

above. Initial enrichments failed to produce cells unless a small amount of filter sterilized (0.22 μm) and autoclaved spring water was added to the microcosms. ICP-MS was conducted on culture supernatants to identify elements present in hot spring water that might stimulate cell growth. No trends in metal concentration pre- and post-growth were identified with the exception of iron (Fe), that decreased in concentration (Supplemental Table 6). However, a decrease in Fe was observed in cultures grown with both 100% base salt media and the 4:1 ratio of base salt medium to filtered and autoclaved hot spring water, suggesting that this was unlikely to be what is stimulating growth. Rather, it is possible that an element not part of those analyzed via ICP-MS or an organic substrate present in spring water may be what is stimulating growth. Subsequent enrichments and enrichment transfers therefore contained a 4:1 ratio of base salt medium to filtered and autoclaved hot spring water. Repeated passage of enrichments from 0, 9, and 21 m depth at CP, in addition to those enrichments from surface (0 m) from RP and RB resulted in single morphotypes (coccus) for each of the five samples. SEM images of the YNP strain CP85 – 0m reveal 0.8 to 1.2 μm diameter coccoid cells (Supplemental Figure 2), consistent with results from fluorescent microscopy and with the morphology of Sulfolobales in general (Brock et al., 1972; Liu et al., 2021; Sakai et al., 2022).

Genomic Sequencing, Characterization, and Phylogenomic Analyses

Genomic DNA was extracted and sequenced from each of the five enrichments. Assembly resulted in a single genome for each isolate, adding support to microscopic analyses indicating that each culture hosted a single morphotype. A phylogenomic reconstruction of the five isolate genomes in the context of 26 Sulfolobales metagenome-assembled genomes (MAGs) recovered from 14 acidic YNP hot springs, and 26 reference genomes (21 type strains of the

Sulfolobales order and five outgroup genomes: *Desulfuroccocus amylolyticus*, *Desulfuroccocus mucosus*, *Pyrolobus fumarii*, *Thermogladius calderae*, *Thermosphaera aggregans*) was constructed (Figure 2). The isolates from RP and CP formed a well-supported clade with *Stygiolobus azoricus*, the type strain of this genus. The genomes of cultivars from depth at CP (CP85 – 9m and CP85 – 21m) formed a well-supported and distinct lineage from those of the CP and RP surface strains (CP85 – 0m and RP85 – 0m). The four YNP *Stygiolobus* genomes share 94.0% average nucleotide identity (ANI) with the type strain, *S. azoricus*, and are highly similar to each other (pairwise ANIs of 98.4 to 99.0%) (Supplemental Table 2). The three *Stygiolobus* genomes (CP85 – 0m, CP85 – 9m, and CP85 – 21m) from CP cultivars all had estimated genome sizes of 2.3 Mbp while the *Stygiolobus* RP85 – 0m genome had a genome size of 1.9 Mbp. All genomes were estimated to be >87% complete. Additional details of cultivar genomes, including completeness, contamination, and N50 of contigs, are reported in Supplemental Table 2.

The genome of the RB85 – 0m cultivar formed a well-supported and distinct branch relative to the *Sulfurisphaera* and *Sulfolobus* clades, with an ANI of 74.9%, 76.2% and 73.0% to *Sulfurisphaera tokodaii*, *Sulfurisphaera ohwakuensis and Sulfolobus acidocaldarius,* respectively. The average amino acid identity (AAI) was 66.8% to both *Sulfurisphaera* species and 63.0% to *Sulfolobus acidocaldarius*. Similarly, the 16S rRNA gene from the RB85 – 0m genome shared 95% sequence identity with *S. tokodaii* and *S. ohwakuensis*. This suggests that RB85 – 0m likely represents a separate and new genus or species within the Sulfolobales. The Sulfolobales genome from RB had an estimated genome size of 2.4 Mbp and was estimated to be 99.4% complete. Additional details of cultivar genome, such as contamination and N50 of contigs, are reported in Supplemental Table 2.

To compare metabolic pathways encoded by the RB85 – 0m genome, the YNP *Stygiolobus* genomes (n = 4), reference Sulfolobales genomes (n = 21) and Sulfolobales MAGs recovered from 14 acidic metagenomes in YNP (n = 26), the presence of key homologs related to CO_2-fixation (Abfd), dissimilatory sulfur metabolism (Sqr, Sor, Hrd, Sre), and to O_2 reduction (Cox) were mapped onto the phylogenetic tree (Figure 2). The reference Sulfolobales genomes, the Sulfolobales MAGs recovered from YNP, and all five isolate YNP Sulfolobales genomes (CP85 – 0m, RP85 – 0m, CP85 – 9m, CP85 – 21m and RB85 – 0m) encoded similar metabolic potentials with differences observed mainly in the distribution of homologs of genes encoding two enzyme complexes (Sor and SreABC). All reference Sulfolobales genomes (with the exception of *Sulfodiicoccus acidiphilus*), all Sulfolobales MAGs recovered from YNP (with the exception of *Saccharolobus caldissimus* RB8), and the five new YNP Sulfolobales genomes encoded the ability to fix CO_2 through the 3-hydroxypropionate/4-hydroxybutyrate pathway (3HP/4HB), as indicated by presence of the protein homolog diagnostic for this pathway, Abfd. All Sulfolobales analyzed (reference, YNP recovered MAGs, and isolates) had the ability to reduce O_2, as indicated by the presence of Cox. All reference Sulfolobales genomes, with the exception of *Sulfolobus acidocaldarius*, and all Sulfolobales MAGs recovered from YNP springs encoded homologs of Sqr. Purified Sqr from *A. ambivalens* (Sulfolobales), which commonly inhabit acidic hot springs, was shown to catalyze the oxidation of sulfide coupled to reduction of quinone, with polysulfide as the putative product of oxidation (Brito et al., 2009). These catalytic properties were also subsequently shown in purified Sqr from C. *manquilingensis* (Thermoproteales), that are also common inhabitants of acidic hot springs (Lencina et al., 2013). Reference genomes such as Sulfolobales Acd1 (Yellowstone group), *Sulfolobus acidocaldarius,*

Stygiolobus azoricus, Saccharolobus caldissimus, Saccharolobus solfataricus, Saccharolobus islandicus, Saccharolobus shibatae, Sulfodiicoccus acidiphilus, Metallosphaera yellowstonensis, Metallosphaera hakonensis, and *Metallosphaera cuprina* lacked homologs of Sor but encoded homologs of the Hdr complex (HdrAB1B2C1C2), which is suggested to be important for S^0 oxidation in other thermophiles (Jiang et al., 2014; Boughanemi et al., 2016; Koch and Dahl, 2018). Only nine reference genomes (*Sulfurisphaera ohwakuensis, Stygiolobus azoricus, Saccharolobus caldissimus, Saccharolobus solfataricus, Saccharolobus islandicus, Metallosphaera yellowstonensi, Acidianus brierleyi, Acidianus sulfidivorans* and *Acidianus manzaensis*) and only two of the recovered YNP MAGs (Sulfolobales Acd1 Yellowstone AL7, and OHSP4) encoded homologs of SreABC, indicating an ability to respire S^0 via this pathway. All four *Stygiolobus* genomes (CP85 – 0m, RP85 – 0m, CP85 – 9m, and CP85 – 21m) encoded homologs of Sqr allowing for sulfide oxidation and Sor or the Hdr complex allowing for S^0 oxidation. Sulfolobales RB85 – 0m only encoded Sqr and the Hdr complex (Figure 2; Supplemental Table 4). All the five Sqr present in the isolated strains exhibited >80% sequence identities (100% sequence coverage) to Sqr from *Acidianus ambivalens* (Brito et al., 2009), suggesting that their functions are comparable.

Kinetics of Sulfide Oxidation and Cell Production

Growth curves for the two *Stygiolobus* strains isolated from the surface of CP (CP85 – 0m) and RP (RP85 – 0m) are shown in Figure 3, while data for the *Stygiolobus* strains isolated from depth at CP (CP85 – 9m and CP85 – 21m) and the Sulfolobales strain isolated from RB (RB – 0m) are shown in Supplemental Figure 3 and Supplemental Figure 4, respectively. For both CP85 – 0m and RP85 – 0m abiotic controls, the sulfide that was added at the start of the

experiment quickly equilibrated with the headspace, with 40 μM ± 3.2 μM and 36 μM ± 1.3 μM remaining after 5 h of incubation, respectively (Figure 3A, D). The rate of sulfide equilibration with the gas phase in these reactors was similar to that observed for the initial abiotic experiment controls lacking O_2 (Figure 1B). However, for both strain CP85 – 0m and RP85 – 0m reactors that contained cells, only 9 μM ± 0.4 μM and 9 μM ± 3.0 μM aqueous sulfide remained, respectively, after 5 hr incubation (Figure 3A, D). Sulfide (as Na_2S) was again added to CP85—0m and RP95 – 0m biotic reactors to achieve final concentrations of ~100 μM at 6 h and 12 h time intervals. In both biotic reactors, aqueous sulfide was below detection limits (< 1 μM) within 6 h of each addition, whereas substantial aqueous sulfide remained in abiotic reactors at these time intervals. After 24 h of incubation, the amount of aqueous sulfide in CP85 - 0m abiotic reactors did not change whereas the amount of aqueous sulfide in RP85 – 0m abiotic reactors continued to decrease.

In both CP85 – 0m and RP85 – 0m biotic reactors, the oxidation of sulfide was coupled to production of cells, as indicated by an increase in cell concentrations from 1.1 ± 0.04 x 10^6 cells mL^{-1} up to 7.8 ± 0.4 x 10^6 cells mL^{-1} and an increase from 8.5 ± 0.3 x 10^5 to 4.0 ± 0.07 x 10^6 cells mL^{-1}, respectively (Figure 3B, E). The production of cells and the oxidation of sulfide in the biotic reactors were also accompanied by the production of sulfate (SO_4^{2-}) (Figure 3C, F). The initial SO_4^{2-} concentration in CP85 – 0m cultures (derived from the 20% vol./vol. of CP hot spring water added) was 422 ± 9 μM and this increased to 620 ± 32 μM after 36 hr, yielding a total of 197 μM SO_4^{2-} produced. This accounted for ~70% of the sulfide (total of 280 μM H_2S) that was added to the CP85 – 0m reactors during the course of incubation. The initial SO_4^{2-} concentration in RP85 – 0m cultures (derived from the 20% vol./vol. of RP hot spring water

added) was 310 ± 9 μM, which decreased to 233 ± 13 μM after 5 hr (Figure 3F), possibly due to assimilation by cells. After 24 hr, SO_4^{2-} increased to 377 μM ± 53 μM, yielding a total of 144 μM SO_4^{2-} produced. This accounted for ~51% of the added sulfide (total of 280 μM H_2S). SO_4^{2-} production was not detected in abiotic reactors (Figure 3F). The two *Stygiolobus* strains obtained from depth in CP (CP85 – 9m and CP85 – 21m) and the Sulfolobales strain isolated from RB (RB85 – 0m) exhibited similar cell production, sulfide oxidation kinetics, and SO_4^{2-} production kinetics when compared to the surface strain from CP (Supplemental Figure 3, A-D; Supplemental Figure 4, A-C).

Comparison of H_2S- Versus S^0-Dependent Growth

The growth kinetics of strain CP85 – 0m was examined under sulfide-oxidation and S^0-oxidation conditions. Cultures were grown with the same amount of electron donor [~450 μM of either Na_2S or S^0] and electron acceptor (1.5% O_2 vol./vol.) with shaking (50 rotations per minute) when incubated at 80°C (Figure 4). The density of cells in sulfide-grown CP85 – 0m cultures increased from 7.8 ± 0.4 x 10^5 cells mL^{-1} to 6.6 ± 1.1 x 10^6 cells mL^{-1} during the incubation period whereas the density of S^0-grown cultures increased from 8.3 ± 0.8 x 10^5 cells mL^{-1} to 2.3 ± 0.1 x 10^6 cells mL^{-1}, representing roughly three-fold less growth than the former condition (Figure 4A). The production of SO_4^{2-} also differed among growth conditions, with a total of 411 μM SO_4^{2-} produced in sulfide-grown CP85 – 0m cultures (accounting for ~91% of added H_2S) whereas only 305 μM SO_4^{2-} was produced in S^0-grown CP85 – 0m cultures (accounting for ~68% of added S^0). The cell yields for sulfide-grown cultures was 0.37 cells/picomol SO_4^{2-} produced and for S^0-grown cells was 0.09 cells/picomol SO_4^{2-} produced. The

calculated Gibbs energy ((ΔG) at 80°C and 1 atm) for aerobic sulfide-oxidation was -726 kJ/mol and that for aerobic S^0-oxidation was -513 kJ/mol.

The toxicity of sulfide (added as Na_2S) to *Stygiolobus* CP85 – 0m was also examined (Supplemental Figure 5). The number of cells produced when provided with 500 µM sulfide (2.1 ± 0.7 x 10^6 cells mL^{-1}) was similar to when 100 µM sulfide was provided (2.0 ± 0.2 x 10^6 cells mL^{-1}) over the first 24 h of incubation. However, production of cells leveled off in the control condition after 24 h incubation but continued to increase over 72 h in the 500 µM condition (6.5 ± 1.0 x 10^6 cells mL^{-1}), likely reflecting electron donor limitation in the former condition. Cultures of CP85 – 0m provided with one mM sulfide at the start of the experiment exhibited a lag of 24 h before cell production commenced, ultimately reaching 3.2 ± 1.1 x 10^4 cells mL^{-1}. Like cultures provided with 500 µM sulfide, those provided with one mM sulfide reached their highest densities following 72 h incubation (8.2 ± 0.5 x 10^6 cells mL^{-1}). Cultures provided with 15 mM sulfide did not grow, indicating sulfide becomes toxic to CP85 – 0m at a concentration between one and 15 mM. In abiotic reactors amended with one mM sulfide, and in abiotic and biotic reactors amended with 15 mM H_2S, a white flocculant precipitate started to form after 0.5 hr incubation. The amount of precipitate increased in quantity with incubation time and turned yellowish by the end of the experiment (96 hr). The precipitate was identified as S^0 via XRD (Supplemental Figure 6).

Relevance of Sulfide Oxidation in Yellowstone Hot Springs

The presence of Sqr homologs was investigated using our in-house compilation of MAGs from 51 hot spring sediment community metagenomes that were recovered across a wide range of pH (1.3-9.0) and temperature (60-93°C) conditions (Figure 5A). Of the 51 metagenomes

examined, MAGs from one metagenome from a low-pH spring (pH 2.9, 81.9°C), MAGs from a metagenome from a mid-pH spring (pH 6.2, 83.2°C), and MAGs from two metagenomes from neutral to alkaline pH springs (pH 7.1, 86.0°C; pH 8.7, 77.2°C) lacked homologs of Sqr. The distribution of Sqr among MAGs from the remaining 47 hot springs was uneven, with those from low pH springs (pH 1.3-4.0; n = 24 metagenomes) having significantly (one-way ANOVA 0.019; $p < 0.05$) more Sqr homologs on average than those from mid pH springs (pH 4.1-6.5; n = 12 metagenomes) and neutral to alkaline pH springs (pH 6.6-9.0; n = 14 metagenomes) (Figure 5B). The distribution of Sqr homologs among MAGs differed among the low pH hot springs that they came from, with up to 79% of the total metagenome community (as the sum of MAG relative abundance) encoding homologs in one hot spring (pH 1.6, T 88°C). Communities where >60% of the MAGs encoded Sqr homologs were only from hot springs with pH <2.5. In communities from mid-pH hot springs, the highest percentage of MAGs encoding Sqr homologs was 18% whereas all communities from neutral to alkaline hot springs had <20% of the total MAGs, with the exception of one hot spring (pH 9.0, T 87°C) that had up to 35% of the MAGs encoding Sqr homologs. This same spring had 30 μM (1 mg/L) of aqueous sulfide at the time of sampling.

The concentration of aqueous sulfide across 73 YNP hot springs (pH 1.3-9.0; 60-95°C) (Supplemental Figure 7) shows that it does not differ as a function of pH (Supplemental Figure 7A). However, when SO_4^{2-} is included in the distribution of total sulfur (sulfide + SO_4^{2-}) in YNP hot springs (S^0 is not easily measured nor is it often reported) (Supplemental Figure 7B), the relationship with pH is apparent with acidic springs being enriched in sulfur. This is consistent with sulfuric acid buffering of low pH (pH < 4) hot springs (Nordstrom et al., 2005b).

Chemoautotrophic Primary Production

The isolation of autotrophic *Stygiolobus* strains from the depth at CP prompted experiments to evaluate whether they or other autotrophic members of the community might be active. Chemoautotrophic primary production assays (i.e., dark CO_2-fixation) were conducted on waters collected from 0 m, 9 m, and 21 m depths in CP were conducted using ^{14}C-labeled bicarbonate. The amount of radioactivity (μCi) fixed into biomass was quantified at 2 h and 4 h of incubation at 85°C for abiotic (autoclave sterilized) and biotic assays, and the data shown is that of chemoautotrophic CO_2-fixation (biotic minus abiotic values) (Figure 6). The amount of ^{14}C-labeled bicarbonate fixed into biomass was higher at 2 h than at 4 h for each of the samples collected from depth, suggesting electron donor/acceptor limitation and/or cell lysis occurred during the course of the assay. On average, the surface samples (0 m) had an activity of $3.1 \pm 2.7 \times 10^{-4}$ μCi at 2 h of incubation that decreased to $1.3 \pm 1.1 \times 10^{-4}$ μCi at 4 hr. The 9 m samples had an activity of $8.9 \pm 1.6 \times 10^{-4}$ μCi at 2 h of incubation that decreased to 5.7 ± 1.0 μCi by 4 h. The 21 m samples had an activity $8.0 \pm 5.1 \times 10^{-4}$ μCi at 2 h of incubation and decreased to $5.0 \pm 3.3 \times 10^{-4}$ μCi at 4 h.

Discussion

Current models for the generation of acidic hot springs begins by invoking abiotic oxidation of sulfide at high temperature by O_2, resulting in the formation and accumulation of S^0 as the stable end-product at low temperatures of <100°C (Eqs. 1-5) through a series of reactions that do not generate net acidity (Brock et al., 1972; Mosser et al., 1973; White, 1988; Nordstrom et al., 2005b; Nordstrom et al., 2009b). Rather, it is thought that microbially-mediated aerobic oxidation of S^0 to SO_4^{2-} and H^+ (Eq. 6) by members of the archaeal order Sulfolobales drives the

acidification of hot springs. However, experiments conducted herein suggest that the rate of high temperature aerobic abiotic oxidation of sulfide at acidic pH is substantially slower than at circumneutral pH and is not instantaneous under either condition, even at atmospheric concentrations of O_2. The pH dependence of the oxidation kinetics is likely attributable to the pH-dependent protonation of sulfide (Amend, 2001) that likely protects the S^{2-} from oxidation (Figure 1), as previously suggested (Chen and Morris, 1972). Under suboxic conditions (i.e., 1% O_2 vol./vol.), which are to likely prevail deeper in springs or in spring sediments, abiotic oxidation of sulfide proceeded even slower at circumneutral pH (pH 7.0) and was negligible at acidic pH (pH 3.0). Together, these observations indicated the presence of a kinetic barrier that allowed low concentrations of sulfide and O_2 to coexist in acidic and neutral waters at high temperatures. Thus, the possibility exists that microorganisms inhabiting such environments can contribute to, and possibly accelerate, aerobic sulfide oxidation.

Prior studies have suggested that members of the Sulfolobales can oxidize sulfide. For example, a previous report claimed that *A. sulfidivorans* and *A. brierleyi* can grow by oxidizing sulfide with Fe(III) as oxidant (added as $Fe_2(SO_4)_3$) (Plumb et al., 2007). However, Fe(III) spontaneously react with sulfide, forming S^0 and Fe(II) at acidic pH (Brock and Gustafson, 1976; Amenabar et al., 2017). Further, Fe(II) and S^0 are a suitable redox pair for many members of the Sulfolobales(Amenabar et al., 2017; Liu et al., 2021). In the present study, this reaction was shown to occur nearly spontaneously in abiotic reactors containing sulfide and Fe(III) ions (Supplemental Video 1). S^0 and Fe(II) were identified as products of the reaction. This indicates that the addition of sulfide by Plumb *et al*., 2017 to reactors containing Fe(III) ions drove the formation of Fe(II) and S^0. Thus, *A. sulfidivorans* and *A. brierleyi* were most likely growing via

Fe(II) oxidation coupled with S^0 reduction, rather than via sulfide oxidation coupled with Fe(III) reduction as reported (Plumb et al., 2007).

The lack of characterized thermoacidophiles with the demonstrated ability to catalyze aerobic sulfide oxidation, combined with the demonstration that sulfide and O_2 can co-exist in acidic hot springs and thermodynamic calculations indicating available free energy from this redox couple (Shock et al., 2010), motivated new enrichment experiments to isolate strains capable of accelerating aerobic sulfide oxidation. Here, we report five new Sulfolobales strains from YNP hot springs (*Stygiolobus* CP85 – 0m, *Stygiolobus* CP85 – 9m, *Stygiolobus* CP85 – 21m, *Stygiolobus* RP85 – 0m, and Sulfolobales RB85 – 0m) (Figure 2) that can accelerate the oxidation of sulfide under suboxic conditions (Figure 3; Supplemental Figure 3; Supplemental Figure 4). Each of these strains were shown to oxidize ~300 μM of sulfide over a period of 15 h, bringing the aqueous sulfide concentration to below detection limits (< 2 μM). In contrast, sulfide was still quantifiable in abiotic reactors following 36 hr of incubation. All strains continued to produce cells between 15 h and 24 h incubation after all aqueous sulfide had been consumed, concomitant with the production of SO_4^{2-} (Figure 3B, E, C, F; Supplemental Figure 3; Supplemental Figure 4). This suggests that the cells continue to oxidize sulfur compounds of intermediate oxidation state (e.g., $S_2O_3^-$, SO_3^{2-}) once the provided sulfide was consumed. However, these compounds were not detected in spent medium, which is likely due to 1) their localization in the cytoplasm of cells and/or 2) their inherent instability in oxic and acidic conditions (Nordstrom et al., 2005b).

All four isolated *Stygiolobus* MAGs (CP85 - 0m, 9m and 21m; RP85 – 0m) encoded similar suites of proteins allowing for dissimilatory sulfur metabolism (Figure 2) including the

key proteins Sqr (sulfide oxidation) as well as Sor and Hdr complex (S^0 oxidation) and cytochrome *c* oxidase (Cox) for O_2-reduction, whereas the isolated Sulfolobales MAG from RB (RB85 - 0m) encoded Sqr, the Hdr complex, and Cox (no Sor, a finding that was consistent with the other MAGs of this uncharacterized clade in YNP). Previously, *S. azoricus*, the only species of the genus, was described to be an obligate anaerobe (Segerer et al., 1991) even though its genome encoded Cox. This finding was a departure for the Sulfolobales order, where all characterized members are either obligate or facultative aerobes (Colman et al., 2018). Recently, a new species, *Stygiolobus caldivivus,* was described and shown to be a facultative aerobe (Sakai et al., 2022), restoring agreement with what it's known of members of the Sulfolobales order as well as adding support to our findings that *Stygiolobus* sp. can utilize O_2 as an electron acceptor while oxidizing sulfide via Sqr.

Sqr is thought to create linear chains of sulfur as polysulfides ($^-S\text{-}S_n\text{-}S^-$) in the cytoplasm (Brito et al., 2009) that are then disproportionated by sulfur oxygenase:reductase (Sor) that generates additional sulfide, and HSO_3^-, and ultimately, $S_2O_3^{2-}$ (Kletzin, 1989; Urich et al., 2004; Urich, 2005; Liu et al., 2021). HSO_3^- and $S_2O_3^{2-}$ react in downstream processes through sulfite:acceptor oxidoreductase (Suox) and thiosulfate:quinone oxidoreductase (Tqo), respectively, and are linked to energy conservation and sulfur trafficking (e.g., through tetrathionate hydrolase (TetH) and the Hdr complex), ultimately generating SO_4^{2-}, H^+, and ATP (Zimmermann et al., 1999; Müller et al., 2004; Counts et al., 2021; Liu et al., 2021). However, the sulfide generated from Sor is then re-oxidized by Sqr and the $^-S\text{-}S_n\text{-}S^-$ is again processed by Sor. Thus, a delay in the conservation of energy that can be used to drive biomass production is expected during growth on sulfide until most of the sulfur atoms have travelled through the

"energetic spiral" of ~10 steps following Sqr activity. This is consistent with data shown here (Figure 3B, E; Supplemental Figure 3B), where cells experienced a lag phase (~5-12 h) during the first hours of sulfide-dependent growth. While the Sulfolobales MAG from RB (as well as the whole clade that it belongs to) did not encode homologs of Sor, it encoded homologs of the Hdr complex that has been proposed to be essential for acidophilic and neutrophilic bacteria, and acidophilic archaea (i.e., Sulfolobales) to grow via inorganic sulfur compound oxidation (Jiang et al., 2014; Boughanemi et al., 2016; Koch and Dahl, 2018; Colman et al., 2022). Although the exact mechanism of sulfur oxidation via this pathway remains to be elucidated, the Hdr complex is universally conversed in Sulfolobales (Figure 2) (Zeldes et al., 2019; Counts et al., 2021; Liu et al., 2021), suggesting it is essential and a potential alternative mechanism for intracellular sulfur to be processed after sulfide is oxidized by Sqr. Altogether, these results suggest that the novel Sulfolobales strains isolated in this study and other Sulfolobales in general that encode Sqr, Sor, and/or Hdr can accelerate aerobic sulfide oxidation and conserve energy from this reaction for use in biomass production.

The pKa of sulfide at 80°C is ~ 6.4 (Amend, 2001), suggesting that the majority of the sulfide added to reactors in the present study is in the uncharged form, H_2S, and could freely diffuse across the membrane. H_2S can be toxic to microorganisms (Beauchamp et al., 1984; Kushkevych, 2013; Lv et al., 2016; Kushkevych et al., 2019) due to it interfering with components of electron transport chains and because it can deprotonate once inside the cell (higher pH) and acidify the cytoplasm (Riahi and Rowley, 2014; Lv et al., 2016; Urschel et al., 2016). A previous study by Morales et. al 2011 showed that cultures of *Sulfolobus metallicus* (now called *Sulfuracidifex metallicus*) were tolerant of and able to grow (albeit poorly) on sulfide

when provided as a gas (~1200 mg L^{-1}) in sealed reactors containing 21% O_2 (~250 mg L^{-1}). However, in abiotic reactors from the same study, ~300 mg L^{-1} of H_2S was consumed after 24 hr incubation, consistent with abiotic oxidation by O_2 at near stoichiometric quantities (Morales et al., 2011). Further, a more recent study(Silva et al., 2023) showed S^0 production in aerobic cultures of *S. metallicus* grown with gaseous H_2S (1000 mg L^{-1}) over an incubation period of 250 hrs, with S^0 being generated within the first hrs of the experiment. Further, tetrathionate was also generated early during the incubation, indicating that both are likely produced as intermediates and were likely available to support growth of this strain (Silva et al., 2023). Given the poor solubility of H2S at pH 2.5 (as shown herein through equilibration experiments), it is possible that intermediate S species supported growth in these experiments, rather than H_2S. Indeed, experiments conducted herein also show that sulfide at high concentrations reacted with O_2 to yield S^0 (Supplemental Figure 5; Supplemental Figure 6). Further, sulfide at a concentration of 1 mM was toxic to *Stygiolobus* CP85 – 0m (Supplemental Figure 5). Importantly, sulfide concentrations in YNP surface hot spring waters rarely exceed 100 μM (McCleskey et al., 2004; Ball et al., 2006; McCleskey et al., 2014; McCleskey et al., 2022), and reports of concentrations in the mM range found to be toxic to *Stygiolobus* CP85 – 0m are even more rare (e.g., Boulder Spring (Cox et al., 2011)).

We examined whether *Stygiolobus* CP85 – 0m could grow with S^0 and, if so, whether it grew better with S^0 or sulfide. The strain was grown aerobically (1.5% O_2 vol./vol.) with ~450 μM of either H_2S or S^0. An important caveat however, is that unlike sulfide, S^0 is essentially insoluble (478 nM at 80°C) (Kamyshny, 2009). After incubation for 48 hr, *Stygiolobus* CP85 – 0m cells growing on sulfide (Figure 4A) achieved a much higher cell density and produced more

SO_4^{2-} (Figure 4B) than *Stygiolobus* CP85 – 0m cells growing on S^0, revealing that sulfide-grown cells were 4x more efficient in conserving energy and coupling it to growth than S^0-grown cells. The available free Gibbs energy (ΔG) for both reactions was calculated at a temperature of 80°C and at atmospheric pressure (1 atm). Aerobic sulfide oxidation had a ΔG of -726 kJ/mol while aerobic S^0 oxidation had a ΔG of -513 kJ/mol, suggesting that aerobic sulfide oxidation provided 1.4x more energy for the cells than S^0 oxidation. While it is possible that the rate of sulfide or S^0 oxidation and the ability to couple this to growth could be influenced by their relative availabilities or solubilities, this alone cannot account for the difference in cell yield. Together these results suggested that *Stygiolobus* CP85 – 0m was more efficient at coupling aerobic sulfide oxidation to cell growth than it was at coupling aerobic S^0 oxidation to growth, possibly pointing to sulfide as the preferred substrate in natural systems. If true, this would represent a stark difference to how Sulfolobales have traditionally been thought to grow in hot spring environments and how they are cultivated in the lab (i.e., via aerobic S^0 oxidation). Further, these observations provide additional evidence that *Stygiolobus* CP85 – 0m, and the other strains isolated in this study, can accelerate the oxidation of sulfide enzymatically and weren't simply consuming S^0 that could have been formed abiotically. Given the ubiquitous distribution of Sqr among members of the Sulfolobales, it is possible that this conclusion can be extended to other Sulfolobales as well.

To begin to probe how relevant aerobic sulfide oxidation via Sqr could be across YNP hot springs, 51 metagenomes that spanned a wide range of pH and temperature were screened for the presence of Sqr homologs. Of the 51 metagenomes, 47 included a MAG that encoded at least one Sqr homolog. The distribution of Sqr homologs (as the sum of the relative abundance of MAGs

in a metagenome) was plotted against pH and temperature (Figure 5). Although the distribution of homologs is quite variable across pH and temperature space, an increased proportion of the community members encode Sqr homologs in acidic pH (<4) and high temperature (>80°C) hot springs. The effect of pH in this distribution was more pronounced when the data from hot spring metagenomes was grouped by broad pH provinces (Figure 5B). This suggests that the Sulfolobales within YNP, the majority of which remain uncultured (e.g., Acd1) (Colman et al., 2021; Colman et al., 2022; Sims et al., 2023), can also possibly accelerate sulfide oxidation.

The majority of Sulfolobales, including all of the new YNP strains, encode the 3HP/4HB pathway of CO_2 fixation. The isolation of autotrophic strains (*Stygiolobus* CP85 – 0m, *Stygiolobus* CP85 – 9 m and *Stygiolobus* CP85 – 21 m were isolated) capable of accelerating sulfide oxidation from various depth intervals in CP, which itself exhibits increasing concentrations of dissolved sulfide with depth (Colman et al., 2022), motivated experiments to test whether cells residing in the deeper portions of CP might be actively fixing CO_2 (Figure 6). Importantly, while MAGs closely affiliated with *Stygiolobus* were not identified at depths up to 15 m in CP (21 m depth was not assayed) in a previous study of CP, they were a minor component (0.03%) of the surface (0m) planktonic communities (Colman et al., 2022). Rather, Acd1, a yet to be cultivated member of the Sulfolobales that encodes the 3HP/4HB pathway and Sqr, dominated CP communities regardless of depth. *Ex situ* ^{14}C-labeled bicarbonate activity assays revealed incorporation of $^{14}CO_2$ into biomass in planktonic communities collected from all three depth intervals assessed (0 m, 9 m, and 21 m) after 2 hr incubation. Activities dropped after 4 hr incubation, presumably due to nutrient limitation leading to cell lysis. In acidic, high temperature, and sulfur rich hot springs, the nutrient that typically becomes limiting to

autotrophs is dissolved O_2 (Boyd et al., 2009). While total dissolved inorganic carbon (DIC) could not be measured in the samples due to depressurization and degassing during sample collection with a peristaltic pump, it stands to reason that DIC would be more concentrated at depth given the propensity for CO_2 to volatilize at the surface as waters equilibrate with atmospheric CO_2 concentrations. To this end, total measured DIC activity was likely higher at depth, a finding that is consistent with the increased number of cells as a function of increasing depth in CP (Colman et al., 2022). This likely points to an active *in situ* community that is fixing CO_2. Given that autotrophic Sulfolobales that encode Sqr dominate these communities, it stands to reason that they may be driving CO_2 fixation via sulfide oxidation.

Conclusions

In this study, we investigated abiotic and biotic reactions involving sulfide oxidation at high temperature to test the hypothesis that members of the archaeal order Sulfolobales can accelerate the aerobic oxidation of sulfide and that this, alongside aerobic S^0-oxidation, contributes to the acidification of hot springs. High temperature abiotic sulfide experiments indicated that the O_2-dependent oxidation of sulfide at acidic pH was very slow or negligible, with the rate dependent on the concentration of O_2. This suggested the possibility that Sulfolobales, which universally encode Sqr, could accelerate aerobic sulfide oxidation and potentially couple this to growth. Using sulfide as electron donor and O_2 as an electron acceptor, five Sulfolobales isolates (four affiliated with *Stygiolobus* and one identifiable only to the Sulfolobaceae family level) were obtained from three springs and from multiple depths below the surface of the spring. All five strains accelerated aerobic sulfide oxidation kinetics while generating biomass and sulfate. Moreover, aerobic growth was better with sulfide when

compared to S^0-oxidation as indicated by a 4x higher cell yield, attributable in part to the 1.4x more energy released by aerobic sulfide oxidation than S^0-oxidation. However, sulfide was toxic at concentrations of >1 mM, which is above the concentration of sulfide typically measured in YNP.

Metagenomic data indicated that Sqr homologs are enriched in acidic hot springs where Sulfolobales predominate. Combined with data presented here suggesting Sulfolobales can accelerate sulfide oxidation, a new model for hot spring acidification is advocated wherein the initial O_2-dependent oxidation of sulfide is no longer considered to be an abiotic process only. Rather, Sulfolobales accelerate the O_2-dependent oxidation of sulfide that is used to drive primary production and that results in the production of acid. It is possible that O_2 limitation limits the biological capacity to oxidize sulfide in some springs or, at certain times in a given spring, it can lead to the generation of intermediate sulfur species (e.g., $S_2O_3^{2-}$) that have been measured in acidic springs, and ultimately, metastable S^0 that can precipitate and accumulate. Sulfolobales-mediated oxidation of S^0 likely further contributes to the acidification of hot spring waters. Additional research is still needed to uncover whether Sulfolobales prefer S^0 or sulfide when both substrates are present and the relative contribution of abiotic and biotic processes to sulfide oxidation and spring acidification.

Acknowledgements

This work was supported by the National Science Foundation (EAR-1820658) to DRC and ESB. MCFM is grateful to the family of Beverly Ferguson and the Molecular Bioscience Program (MBSP) for support of her graduate studies at Montana State University (MSU). The authors thank the integrated Chemical Analysis Laboratory (ICAL) at MSU for help with XRD

analyses. The authors thank Dr. Devon Payne for help with imaging at ICAL. ICAL is supported by National Science Foundation award ECCS-2025391.

References

Allen, E.T., and Day, A.L. (1935) Hot springs of the Yellowstone National Park. *Carnegie Inst Washington Pub* 466.

Amenabar, M.J., and Boyd, E.S. (2018) Mechanisms of Mineral Substrate Acquisition in a Thermoacidophile. *Applied and Environmental Microbiology* 84: e00334-00318.

Amenabar, M.J., Shock, E.L., Roden, E.E., Peters, J.W., and Boyd, E.S. (2017) Microbial substrate preference dictated by energy demand rather than supply. *Nature Geoscience* 10: 577-581.

Amend, J.P., & Shock, E. L. (2001) Energetics of overall metabolic reactions of thermophilic and hyperthermophilic Archaea and Bacteria. *FEMS Microbiology Reviews* 25: 175-243.

Atlas, R.M. (2004) *Handbook of Microbiologial Media*. Washington, D.C.: ASM Press.

Ball, J.W., McCleskey, R.B., Nordstrom, D.K., and Holloway, J.M. (2006) Water-chemistry data for selected springs, geysers, and streams in Yellowstone National Park, Wyoming, 2003–2005. In. U.S. Geological Survey Open File Report.

Beauchamp, R.O., Bus, J.S., Popp, J.A., Boreiko, C.J., Andjelkovich, D.A., and Leber, P. (1984) A Critical Review of the Literature on Hydrogen Sulfide Toxicity. *CRC Critical Reviews in Toxicology* 13: 25-97.

Boratyn, G.M., Schäffer, A.A., Agarwala, R., Altschul, S.F., Lipman, D.J., and Madden, T.L. (2012) Domain enhanced lookup time accelerated BLAST. *Biology Direct* 7: 12.

Boughanemi, S., Lyonnet, J., Infossi, P., Bauzan, M., Kosta, A., Lignon, S. et al. (2016) Microbial oxidative sulfur metabolism: biochemical evidence of the membrane-bound heterodisulfide reductase-like complex of the bacterium Aquifex aeolicus. *FEMS Microbiol Lett* 363.

Boyd, E.S., Leavitt, W.D., and Geesey, G.G. (2009) CO_2 uptake and fixation by a thermoacidophilic microbial community attached to precipitated sulfur in a geothermal spring. *Appl Environ Microbiol* 75: 4289-4296.

Boyd, E.S., Jackson, R.A., Encarnacion, G., Zahn, J.A., Beard, T., Leavitt, W.D. et al. (2007) Isolation, characterization, and ecology of sulfur-respiring crenarchaea inhabiting acid-sulfate-chloride-containing geothermal springs in Yellowstone National Park. *Appl Environ Microbiol* 73: 6669-6677.

Boyer, G. (2023) pyCHNOSZ: Python wrapper for the thermodynamic package CHNOSZ In. https://github.com/worm-portal/AqEquil.

Brito, J.A., Sousa, F.L., Stelter, M., Bandeiras, T.M., Vonrhein, C., Teixeira, M. et al. (2009) Structural and functional insights into sulfide:quinone oxidoreductase. *Biochemistry* 48: 5613-5622.

Brock, T.D. (1971) Bimodal distribution of pH values of thermal springs of the world. *Geol Soc Am Bull* 82: 1393-1394.

Brock, T.D., and Gustafson, J. (1976) Ferric iron reduction by sulfur- and iron-oxidizing bacteria. *Applied and Environmental Microbiology* 32: 567-571.

Brock, T.D., Brock, K.M., Belly, R.T., and Weiss, R.L. (1972) Sulfolobus: A New Genus of Sulfur-Oxidizing Bacteria Living at Low pH and High Temperature. *Arch Mikrobiol* 84: 14.

Chen, K.Y., and Morris, J.C. (1972) Kinetics of oxidation of aqueous sulfide by oxygen. Environmental Science & Technology. *Environ Sci Tech* 6: 8.

Colman, D.R., Amenabar, M.J., Fernandes-Martins, M.C., and Boyd, E.S. (2022) Subsurface Archaea associated with rapid geobiological change in a model Yellowstone hot spring. *Communications Earth & Environment*

Colman, D.R., Poudel, S., Hamilton, T.L., Havig, J.R., Selensky, M.J., Shock, E.L., and Boyd, E.S. (2018) Geobiological feedbacks and the evolution of thermoacidophiles. *ISME J* 12: 225-236.

Colman, D.R., Lindsay, M.R., Harnish, A., Bilbrey, E.M., Amenabar, M.J., Selensky, M.J. et al. (2021) Seasonal hydrologic and geologic forcing drive hot spring geochemistry and microbial biodiversity. *Environ Microbiol* 23: 4034-4053.

Counts, J.A., Willard, D.J., and Kelly, R.M. (2021) Life in hot acid: a genome-based reassessment of the archaeal order Sulfolobales. *Environ Microbiol* 23: 3568-3584.

Cox, A., Shock, E.L., and Havig, J.R. (2011) The transition to microbial photosynthesis in hot spring ecosystems. *Chem Geol* 280: 344-351.

Fernandes-Martins, M.C., Colman, D.R., and Boyd, E.S. (2023) Relationships between fluid mixing, biodiversity, and chemosynthetic primary productivity in Yellowstone hot springs. *Environ Microbiol*.

Fernandes-Martins, M.C., Keller, L.M., Munro-Ehrlich, M., Zimlich, K.R., Mettler, M.K., England, A.M. et al. (2021) Ecological dichotomies arise in microbial communities due to mixing of deep hydrothermal waters and atmospheric gas in a circumneutral hot spring. *Appl Environ Microbiol* 87: e01598-01521.

Fogo, J.K., and Popowsky, M. (1949) Spectrophotometric Determination of Hydrogen Sulfide. *Analytical Chemistry* 21: 732-734.

Fournier, R.O. (1989) Geochemistry and dynamics of Yellowstone hydrothermal system. *Annu Rev Earth Planet Sci* 17: 13-53.

Holland, H.D. (1965) Some applications of thermochemical data to problems of ore deposits; [Part] 2, Mineral assemblages and the composition of ore forming fluids. *Economic Geology* 60: 1101-1166.

Jiang, C.-Y., Liu, L.-J., Guo, X., You, X.-Y., Liu, S.-J., and Poetsch, A. (2014) Resolution of carbon metabolism and sulfur-oxidation pathways of Metallosphaera cuprina Ar-4 via comparative proteomics. *Journal of Proteomics* 109: 276-289.

Jiang, Z., Li, P., Jiang, D., Dai, X., Zhang, R., Wang, Y., and Wang, Y. (2016) Microbial Community Structure and Arsenic Biogeochemistry in an Acid Vapor-Formed Spring in Tengchong Geothermal Area, China. *PLOS ONE* 11: e0146331.

Kamyshny, A. (2009) Solubility of cyclooctasulfur in pure water and sea water at different temperatures. *Geochimica et Cosmochimica Acta* 73: 6022-6028.

Kawarabayasi, Y., Hino, Y., Horikawa, H., Jin-no, K., Takahashi, M., Sekine, M. et al. (2001) Complete Genome Sequence of an Aerobic Thermoacidophilic Crenarchaeon, Sulfolobus tokodaii strain7. *DNA Research* 8: 123-140.

Kletzin, A. (1989) Coupled enzymatic production of sulfite, thiosulfate, and hydrogen sulfide from sulfur: purification and properties of a sulfur oxygenase reductase from the facultatively anaerobic archaebacterium Desulfurolobus ambivalens. *Journal of Bacteriology* 171: 1638-1643.

Kletzin, A. (1992) Molecular characterization of the sor gene, which encodes the sulfur oxygenase/reductase of the thermoacidophilic Archaeum Desulfurolobus ambivalens. *Journal of Bacteriology* 174: 5854-5859.

Koch, T., and Dahl, C. (2018) A novel bacterial sulfur oxidation pathway provides a new link between the cycles of organic and inorganic sulfur compounds. *The ISME Journal* 12: 2479-2491.

Kolmert, A., Wikström, P., and Hallberg, K.B. (2000) A fast and simple turbidimetric method for the determination of sulfate in sulfate-reducing bacterial cultures. *J Microbiol Methods* 41: 179-184.

Kusakabe, M., Komoda, Y., Takano, B., and Abiko, T. (2000) Sulfur isotopic effects in the disproportionation reaction of sulfur dioxide in hydrothermal fluids: implications for the δ34S variations of dissolved bisulfate and elemental sulfur from active crater lakes. *Journal of Volcanology and Geothermal Research* 97: 287-307.

Kushkevych, I., Dordević, D., and Vítězová, M. (2019) Toxicity of hydrogen sulfide toward sulfate-reducing bacteria Desulfovibrio piger Vib-7. *Archives of Microbiology* 201: 389-397.
Kushkevych, I.V. (2013) Effect of hydrogen sulfide at differential concentrations on the process of dissimilatory sulfate reduction by the bacteria Desulfovibrio piger. *Наук зап Тернопнац пед ун-ту Сер Біол,* 4: 6.

Lencina, A.M., Ding, Z., Schurig-Briccio, L.A., and Gennis, R.B. (2013) Characterization of the Type III sulfide:quinone oxidoreductase from Caldivirga maquilingensis and its membrane binding. *Biochim Biophys Acta* 1827: 266-275.

Lewis, A.M., Recalde, A., Bräsen, C., Counts, J.A., Nussbaum, P., Bost, J. et al. (2021) The biology of thermoacidophilic archaea from the order Sulfolobales. *FEMS Microbiology Reviews* 45.

Liu, L.-J., Jiang, Z., Wang, P., Qin, Y.-L., Xu, W., Wang, Y. et al. (2021) Physiology, Taxonomy, and Sulfur Metabolism of the Sulfolobales, an Order of Thermoacidophilic Archaea. *Frontiers in Microbiology* 12.

Lv, C., Aitchison, E.W., Wu, D., Zheng, L., Cheng, X., and Yang, W. (2016) Comparative exploration of hydrogen sulfide and water transmembrane free energy surfaces via orthogonal space tempering free energy sampling. *Journal of Computational Chemistry* 37: 567-574.

McCleskey, R.B., Ball, J.W., Nordstrom, D.K., Holloway, M.J., and Taylor, E.H. (2004) Water-Chemistry Data for Selected Hot Springs, Geysers, and Streams in Yellowstone National Park, Wyoming, 2001-2002. In *Open-File Report*. Reston, VA.

McCleskey, R.B., Chiu, R.B., Nordstrom, D.K., Campbell, K.M., Roth, D.A., Ball, J.W., and Plowman, T.I. (2014) Water-chemistry data for selected springs, geysers, and streams in Yellowstone National Park, Wyoming, beginning 2009. In. U.S. Geological Survey Open File Report.

McCleskey, R.B., Roth, D.A., Nordstrom, D.K., Hurwitz, S., Holloway, J.M., Bliznik, P.A. et al. (2022) Water-Chemistry and Isotope Data for Selected Springs, Geysers, Streams, and Rivers in Yellowstone National Park, Wyoming:. In. release, U.S.G.S.d. (ed).

Morales, M., Silva, J., Morales, P., Gentina, J.C., and Aroca, G. (2012) Biofiltration of hydrogen sulfide by Sulfolobus metallicus at high temperatures. *Water Sci Technol* 66: 1958-1961.

Morales, M., Arancibia, J., Lemus, M., Silva, J., Gentina, J.C., and Aroca, G. (2011) Bio-oxidation of H2S by Sulfolobus metallicus. *Biotechnology Letters* 33: 2141-2145.

Mosser, J.L., Mosser, A.G., and Brock, T.D. (1973) Bacterial Origin of Sulfuric Acid in Geothermal Habitats. *Science* 179: 1323-1324.

Müller, F.H., Bandeiras, T.M., Urich, T., Teixeira, M., Gomes, C.M., and Kletzin, A. (2004) Coupling of the pathway of sulphur oxidation to dioxygen reduction: characterization of a novel membrane-bound thiosulphate:quinone oxidoreductase. *Molecular Microbiology* 53: 1147-1160.

Nguyen, L.T., Schmidt, H.A., von Haeseler, A., and Minh, B.Q. (2015) IQ-TREE: a fast and effective stochastic algorithm for estimating maximum-likelihood phylogenies. *Mol Biol Evol* 32: 268-274.

Nordstrom, D.K., Ball, J.W., and McCleskey, R.B. (2005) Ground water to surface water: Chemistry of thermal outflows in Yellowstone National Park. In *Geothermal Biology and Geochemistry in Yellowstone National Park*. Inskeep, W.P., and McDermott, T.R. (eds). Bozeman, MT: Thermal Biology Institute, Montana State University pp. 73-94.

Nordstrom, D.K., McCleskey, R.B., and Ball, J.W. (2009) Sulfur geochemistry of hydrothermal waters in Yellowstone National Park: IV Acid–sulfate waters. *Applied Geochemistry* 24: 191-207.

Pachmayr, F. (1960) Vorkommen und Bestimmung von Schwefelverbindungen in Mineralwasser. In.

Payne, D., Spietz, R.L., and Boyd, E.S. (2021) Reductive dissolution of pyrite by methanogenic archaea. *The ISME Journal* 15: 3498-3507.

Plumb, J.J., Haddad, C.M., Gibson, J.A.E., and Franzmann, P.D. (2007) Acidianus sulfidivorans sp. nov., an extremely acidophilic, thermophilic archaeon isolated from a solfatara on Lihir Island, Papua New Guinea, and emendation of the genus description. *Int J Syst Evol Microbiol* 57: 1418-1423.

Riahi, S., and Rowley, C.N. (2014) Why Can Hydrogen Sulfide Permeate Cell Membranes? *Journal of the American Chemical Society* 136: 15111-15113.

Sakai, H.D., and Kurosawa, N. (2017) Sulfodiicoccus acidiphilus gen. nov., sp. nov., a sulfur-inhibited thermoacidophilic archaeon belonging to the order Sulfolobales isolated from a terrestrial acidic hot spring. *International Journal of Systematic and Evolutionary Microbiology* 67: 1880-1886.

Sakai, H.D., Nakamura, K., and Kurosawa, N. (2022) Stygiolobus caldivivus sp. nov., a facultatively anaerobic hyperthermophilic archaeon isolated from the Unzen hot spring in Japan. *Int J Syst Evol Microbiol* 72.

Sayers, E.W., Bolton, E.E., Brister, J.R., Canese, K., Chan, J., Comeau, D.C. et al. (2022) Database resources of the national center for biotechnology information. *Nucleic Acids Res* 50: D20-d26.

Seemann, T. (2014) Prokka: rapid prokaryotic genome annotation. *Bioinformatics* 30: 2068-2069.

Segerer, A.H., Trincone, A., Gahrtz, M., and Stetter, K.O. (1991) Stygiolobus azoricus gen. nov., sp. nov. Represents a Novel Genus of Anaerobic, Extremely Thermoacidophilic Archaebacteria of the Order Sulfolobales. *International Journal of Systematic and Evolutionary Microbiology* 41: 495-501.

Shivvers, D.W., and Brock, T.D. (1973) Oxidation of Elemental Sulfur by Sulfolobus acidocaldarius. *Journal of Bacteriology* 114: 706-710.

Shock, E.L., Holland, M., Meyer-Dombard, D.A., Amend, J.P., Osburn, G.R., and Fischer, T.P. (2010) Quantifying inorganic sources of geochemical energy in hydrothermal ecosystems, Yellowstone National Park, USA. *Geochim Cosmochim Acta* 74: 4005-4043.

Silva, J., Ortiz-Soto, R., Morales, M., and Aroca, G. (2023) Effect of the Availability of the Source of Nitrogen and Phosphorus in the Bio-Oxidation of H2S by Sulfolobus metallicus. *Fermentation* 9: 406.

Sims, K.W.W., Messa, C.M., Scott, S.R., Parsekian, A.D., Miller, A., Role, A.L. et al. (2023) The dynamic influence of subsurface geological processes on the assembly and diversification of thermophilic microbial communities in continental hydrothermal systems. *Geochimica et Cosmochimica Acta* 362: 77-103.

Stetter, K.O., Fiala, G., Huber, G., Huber, R., and Segerer, A. (1990) Hyperthermophilic microorganisms. *FEMS Microbiology Letters* 75: 117-124.
Urbieta, M.S., González-Toril, E., Bazán, Á.A., Giaveno, M.A., and Donati, E. (2015) Comparison of the microbial communities of hot springs waters and the microbial biofilms in the acidic geothermal area of Copahue (Neuquén, Argentina). *Extremophiles* 19: 437-450.

Urich, T. (2005) The Sulfur Oxygenase Reductase from Acidianus ambivalens: Functional and structural characterization of a sulfur-disproportionating enzyme. In: Darmstadt, Techn. Univ., Diss., 2005.

Urich, T., Bandeiras, Tiago M., Leal, Sónia S., Rachel, R., Albrecht, T., Zimmermann, P. et al. (2004) The sulphur oxygenase reductase from Acidianus ambivalens is a multimeric protein containing a low-potential mononuclear non-haem iron centre. *Biochemical Journal* 381: 137-146.

Uritskiy, G.V., Diruggiero, J., and Taylor, J. (2018) MetaWRAP—a flexible pipeline for genome-resolved metagenomic data analysis. *Microbiome* 6.

Urschel, M.R., Hamilton, T.L., Roden, E.E., and Boyd, E.S. (2016) Substrate preference, uptake kinetics and bioenergetics in a facultatively autotrophic, thermoacidophilic crenarchaeote. *FEMS Microbiol Ecol* 92: fiw069.

Viollier, E., Inglett, P.W., Hunter, K., Roychoudhury, A.N., and Van Cappellen, P. (2000) The ferrozine method revisited: Fe(II)/Fe(III) determination in natural waters. *Applied Geochemistry* 15: 785-790.

Ward, L., Taylor, M.W., Power, J.F., Scott, B.J., McDonald, I.R., and Stott, M.B. (2017) Microbial community dynamics in Inferno Crater Lake, a thermally fluctuating geothermal spring. *ISME J* 11: 1158-1167.

White, D.E., Hutchinson, Roderick A., and Keith, Terry E.C. (1988) The geology and remarkable thermal activity of Norris Geyser Basin, Yellowstone National Park, Wyoming, U.S. In. U.S. Geological Survey Professional Paper p. 84.

Widdel, F. (1983) Methods for enrichment and pure culture isolation of filamentous gliding sulfate-reducing bacteria. *Archives of Microbiology* 134: 282-285.

Zeldes, B.M., Loder, A.J., Counts, J.A., Haque, M., Widney, K.A., Keller, L.M. et al. (2019) Determinants of sulphur chemolithoautotrophy in the extremely thermoacidophilic Sulfolobales. *Environmental Microbiology* 21: 3696-3710.

Zhou, Z., Tran, P., Liu, Y., Kieft, K., and Anantharaman, K. (2019) METABOLIC: A scalable high-throughput metabolic and biogeochemical functional trait profiler based on microbial genomes. *bioRxiv*: 761643.

Zimmermann, P., Laska, S., and Kletzin, A. (1999) Two modes of sulfite oxidation in the extremely thermophilic and acidophilic archaeon Acidianus ambivalens. *Archives of Microbiology* 172: 76-82.

Tables

Table 1. Location and geochemical characteristics of hot spring waters used to isolate H_2S-oxidizing members of the Sulfolobales. Samples of surface waters (0 m) from 'Realgar Pool' and Cinder Pool were collected on August 28th, 2020, and samples from depth (9 m and 21 m) at Cinder Pool were collected on June 3rd, 2021. Samples of surface waters (0 m) from 'Red Bubbler' were collected on June 13th, 2023. A more complete geochemical analysis is reported in Supp. Table 1.

Site	GPS N	GPS W	pH	Temp. (°C)	Cond. (mS)	SO_4^{2-} (mg/L)	Cl^- (mg/L)	S^{2-} (mg/L)	Fe (II) (mg/L)
'Realgar Pool'	44.73558	110.70705	3.9	85.8	4.44	420	542	0.19 ± 0.04	0.43
Cinder Pool, 0 m	44.43568	110.42351	2.6	87.8	5.88	360	579	0.06 ± 0.01	0.25
Cinder Pool, 9 m	44.43568	110.42351	2.6	88.2	5.49[a]	306[a]	NA	0.16 ± 0.03[a]	NA
Cinder Pool, 21 m	44.43568	110.42351	2.6	91.0	NA	350	NA	NA	NA
'Red Bubbler'	44.72650	110.70900	3.0	90.0	2.82	220	266	BD	5.8

BD, below detection; NA, not available; [a] Measurements from (Colman et al., 2022).

Figures

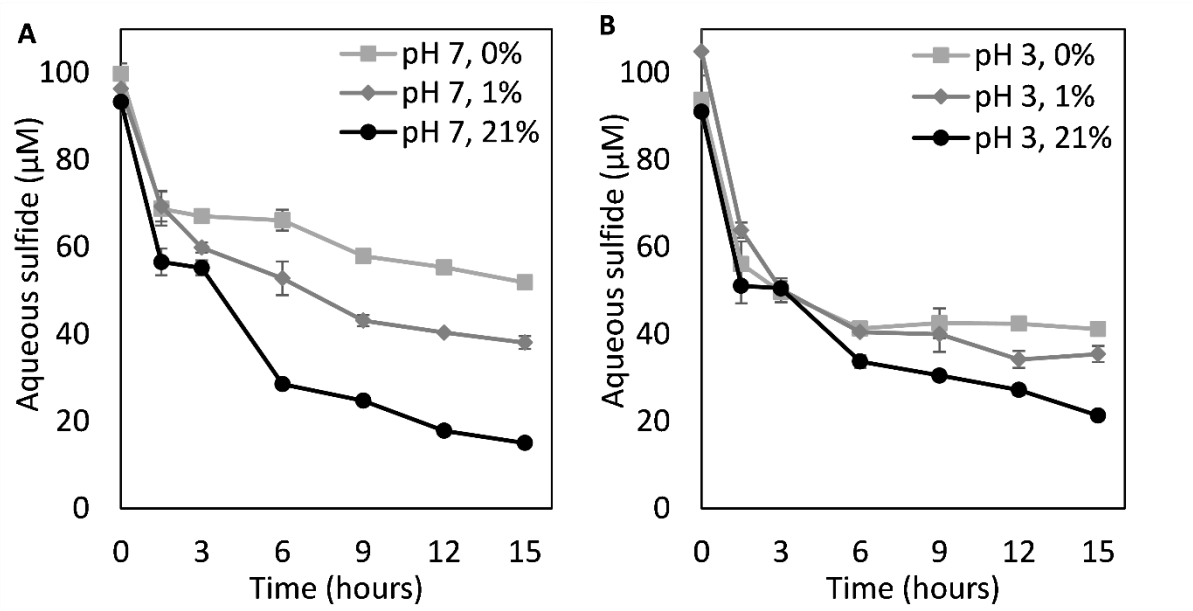

Figure 1. Kinetics of equilibration and abiotic oxidation of sulfide (added as Na_2S). Experiments were conducted in bicarbonate-buffered (1 mM; pH 7.0) Milli-Q water (A) or citric acid-buffered (0.2 mM; pH 3.0) Milli-Q water (B) in reactors with headspace O_2 concentrations of 0%, 1%, and 21% vol./vol. Reactors were incubated at 80°C and sub-samples for measurement of aqueous sulfide were taken every 3 hr over a 15 hr period. The average and standard deviation of triplicate measurements is shown; in some timeseries measurements, the standard deviation is not visible. Rates of total sulfide oxidation, which account for both aqueous and gas phase sulfide via Henry's law calculations, are presented in the text.

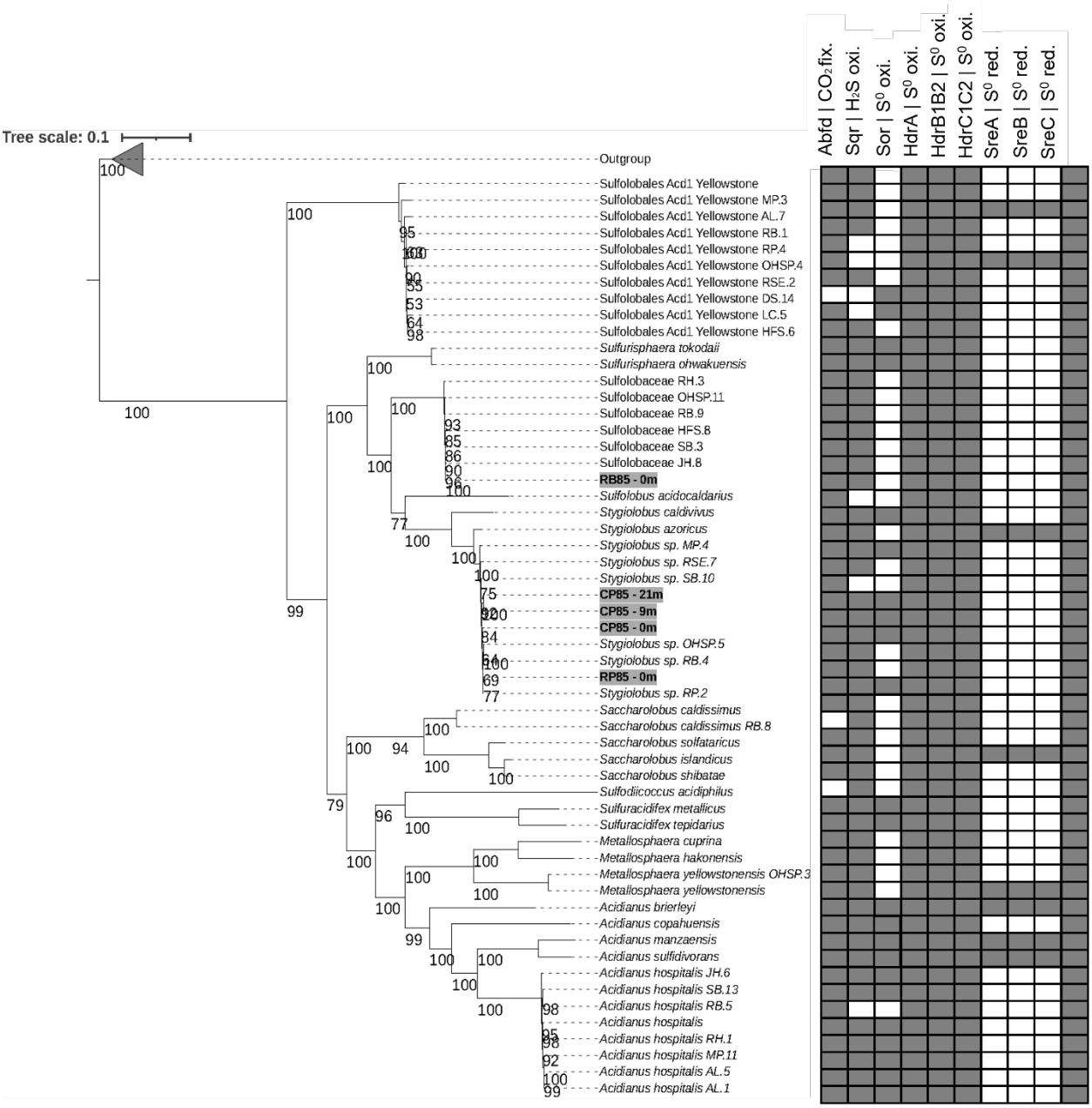

Figure 2. Phylogenomic reconstruction of representative members of the archaeal order Sulfolobales and Sulfolobales isolates recovered in this study (bold-faced and grey-shaded). The Maximum-Likelihood phylogeny was constructed using an alignment of marker genes (n = 30) and the LG substitution model. Homologs of genes encoding key sulfur-metabolizing enzymes mapped to each metagenome assembled genome or genome (grey shade indicates presence). Abbreviations: Abfd: 4-hydroxybutanoyl-CoA dehydratase; Sqr: sulfide:quinone oxidoreductase; Sor: sulfur oxidoreductase:reductase; HdrAB1B2C1C2: hetereodisulfide reductase; SreABC: sulfur/polysulfide reductase; Cox: cytochrome *c* oxidase subunit I.

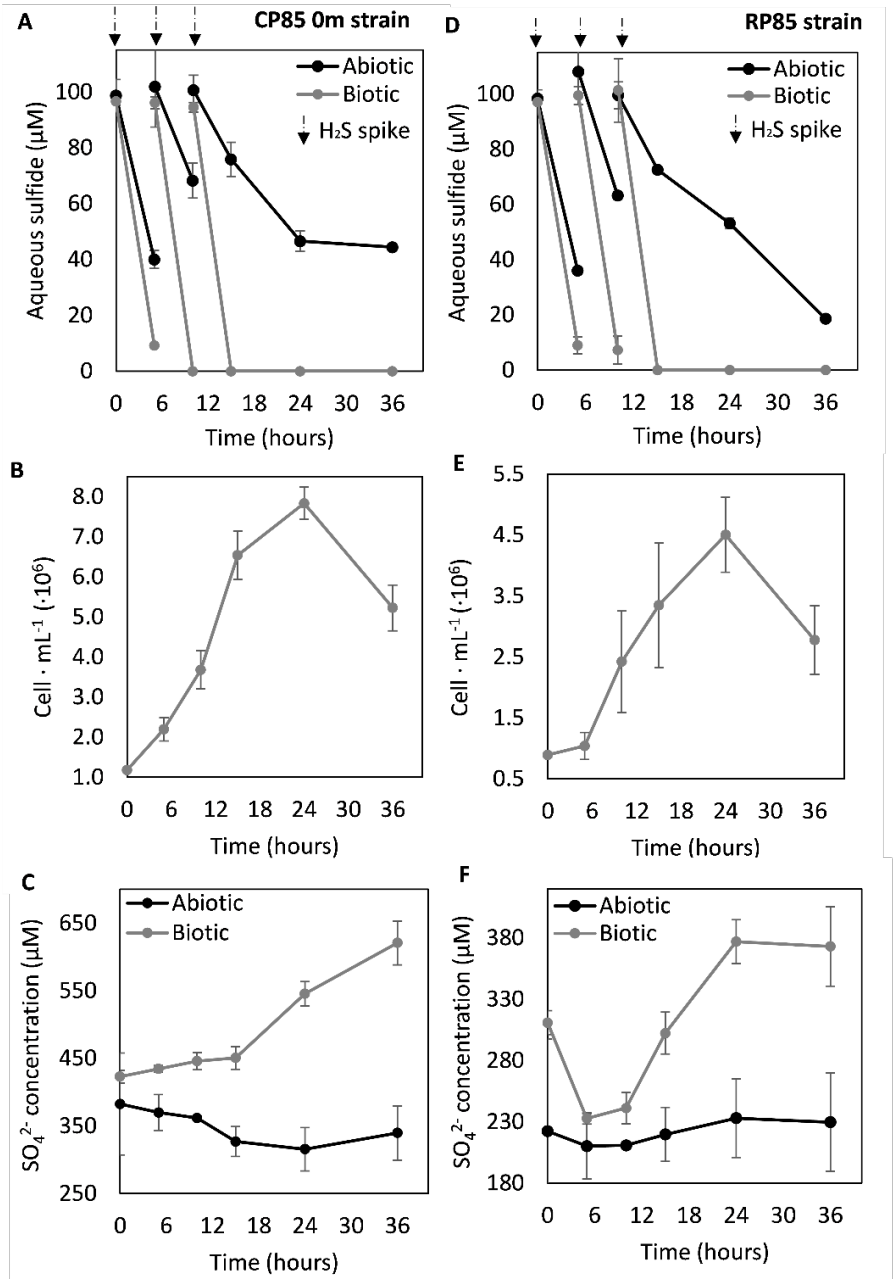

Figure 3. Depletion of aqueous sulfide, production of cells, and production of sulfate (SO_4^{2-}) in Sulfolobales isolates recovered in this study. Data are presented for cultures of *Stygiolobus* strain CP85 – 0 m grown in base salts medium with a pH of 2.6 (A-C) and in cultures of *Stygiolobus* strain RP85 – 0 m in base salts medium with a pH 4.0 (D-F) when incubated at 85°C. Data for abiotic controls are included where appropriate. Oxygen (1.5% headspace vol./vol.) was the electron acceptor and carbon dioxide (92% vol./vol.) was the carbon source. Black arrows depict additions of sulfide (added as Na_2S) to achieve ~100 µM. The average and standard deviation of triplicate measurements is shown.

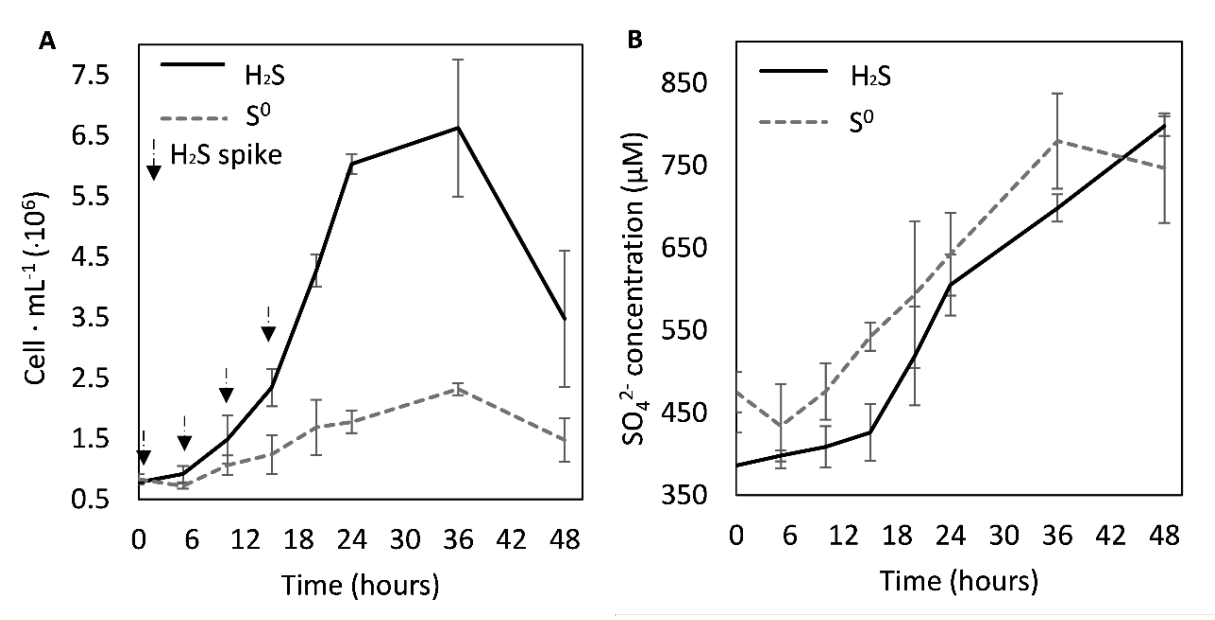

Figure 4. Production of cells (A) and sulfate (SO_4^{2-}; B) in cultures of *Stygiolobus* strain CP85 – 0 m when grown with sulfide (black solid lines) or elemental sulfur (S^0, grey dashed lines) as the electron donor. Oxygen (1.5% headspace vol./vol.) was the electron acceptor and carbon dioxide (92% vol./vol.) was the carbon source. Cultures were incubated on a shaker (50 rotations per min) at 80°C. Experiments were conducted in base salts medium with a pH of 2.6, with black arrows indicating the additions of Na_2S to achieve ~100 µM in the sulfide growth condition only. Note that the base salts medium, which contains 20% filter-sterilized water from Cinder Pool, had ~ 400 µM SO_4^{2-} at the start of the experiment. The average and standard deviation of triplicate measurements is shown.

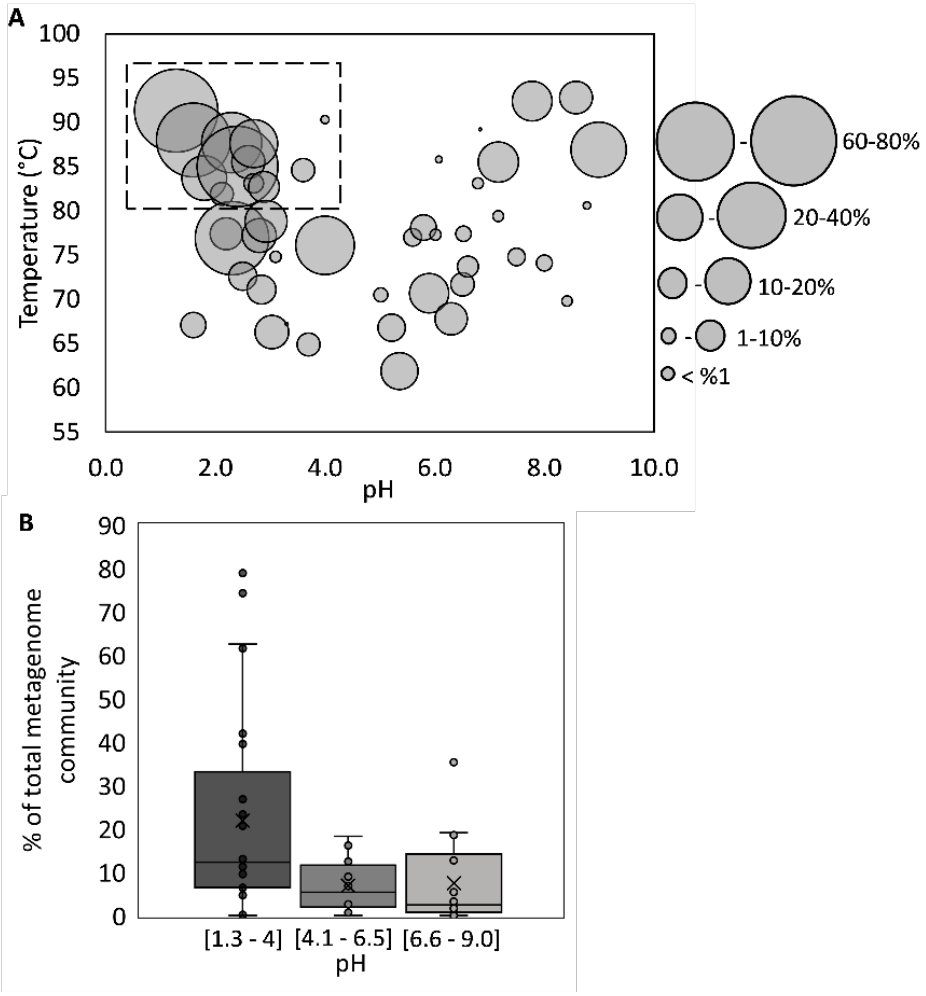

Figure 5. The distribution and relative abundance of sulfide quinone oxidoreductase (Sqr) homologs among metagenome assembled genomes (MAGs) recovered from 51 non-photosynthetic sediment communities from hot springs in Yellowstone National Park. The metagenomes are from hot springs spanning a range of pH (1.3 to 9.0) and temperature (60-93°C). (A) Each bubble represents MAGs from one metagenome, and the size represents the sum of the relative abundances of the MAGs that encode a Sqr homolog. Of the 51 metagenomes, four lacked MAGs that did not encode homologs of Sqr and these are not depicted. The box highlights the range of pH and temperature of springs where members of the order Sulfolobales predominate microbial communities (Colman et al., 2018). (B) Boxplots of the relative abundance of Sqr homologs, with the interquartile ranges of distributions denoted by the grey boxes and medians shown as black lines in the center of the boxes. Whiskers show the full ranges of the distributions. The metagenomes were grouped according to pH realms that include acidic hot springs (1.3-4.0), moderately acidic hot springs (4.1-6.5), and neutral to alkaline hot springs (6.6-9.0).

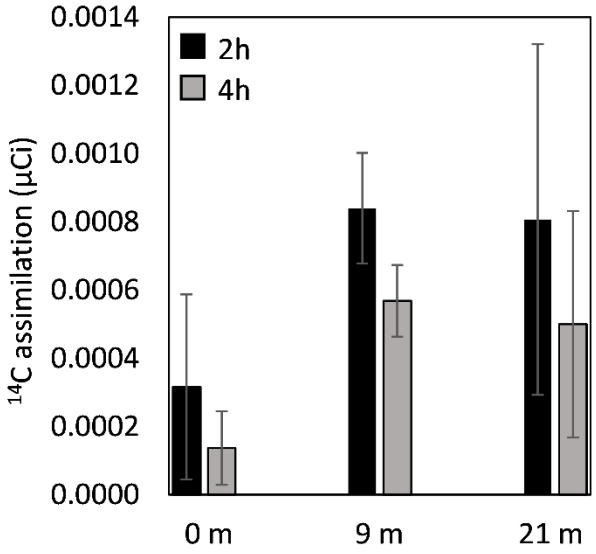

Figure 6. Assimilation of ^{14}C-labeled bicarbonate as a proxy of chemosynthetic primary production along a depth profile in Cinder Pool. Quantified activity that is attributable to cells (biotic minus abiotic controls) is plotted as the average and standard deviation of triplicates measurements. Black bars depict 2 hr of incubation while grey bars depict 4 hr of incubation. Data is not normalized to total dissolved inorganic carbon (DIC) uptake to a lack of accurate measurement of native DIC in waters due to extensive degassing from samples pumped from depth.

Supplemental Figures

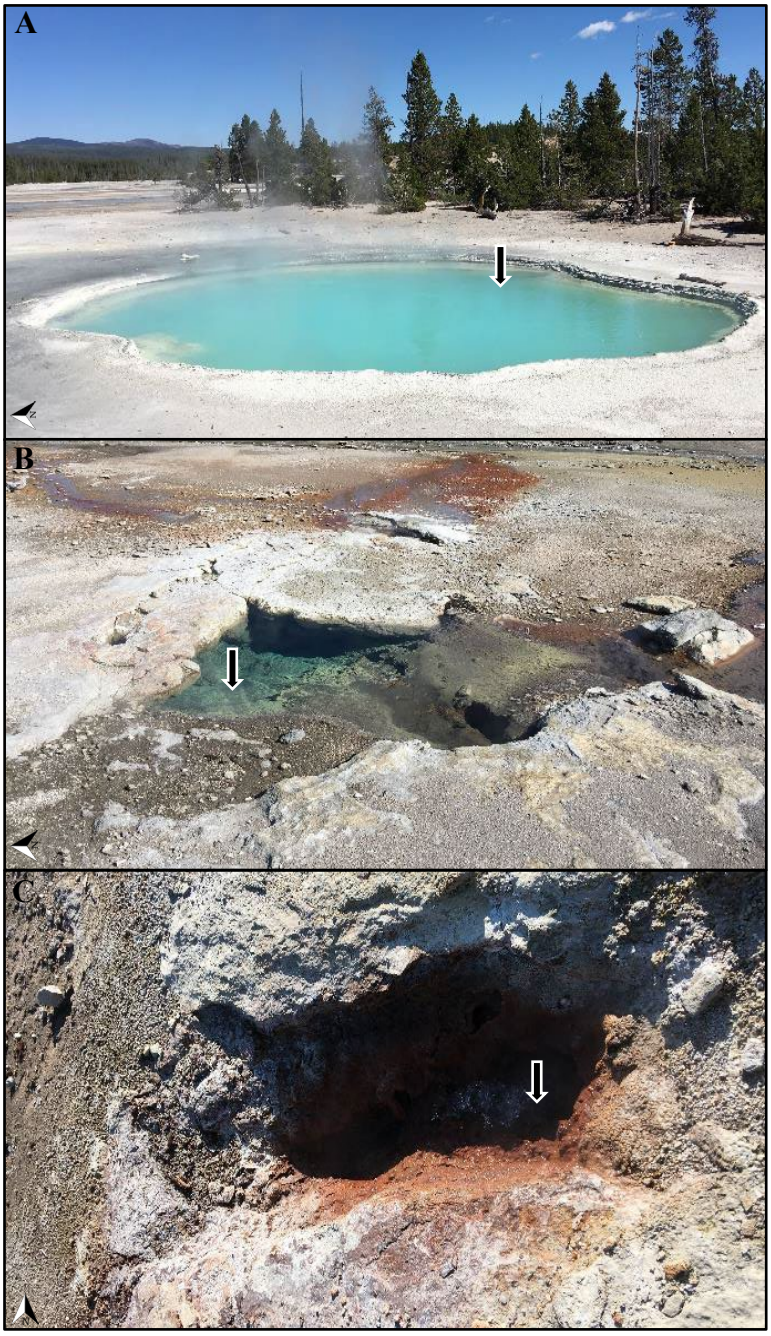

Supplemental Figure 1. Images of hot springs in Norris Geyser Basin, Yellowstone National Park where samples were collected for cultivation. The arrows denote the specific location where sediments (or waters) were collected from Cinder Pool (A), 'Realgar Pool' (B), and 'Red Bubbler' (C). The cardinal north symbol in the bottom left of each panel is shown for reference.

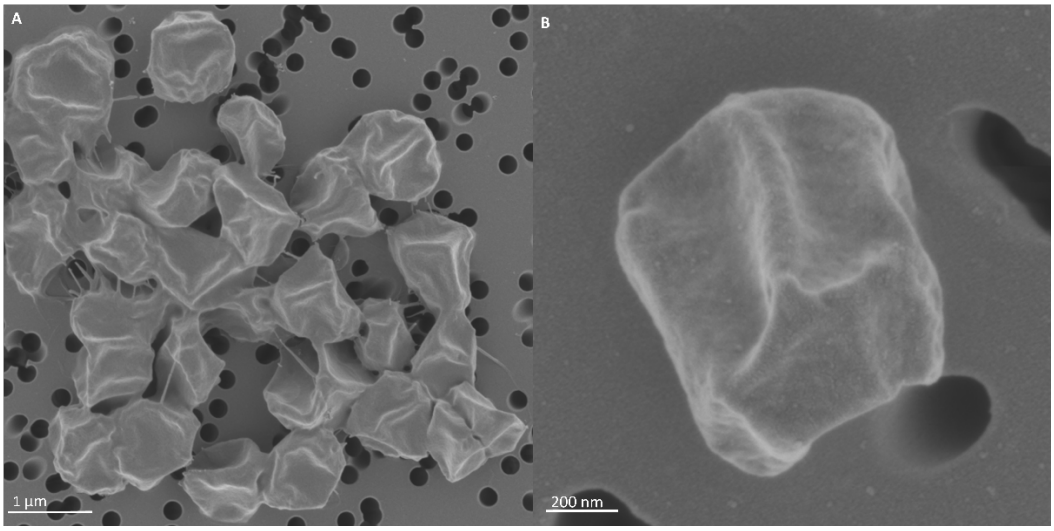

Supplemental Figure 2. Field emission-scanning electron microscopy images of *Stygiolobus* CP85 – 0m. Cells were grown with sulfide (added as Na_2S) as electron donor (total of ~280 µM), oxygen as electron acceptor (1.5% headspace vol./vol.), and carbon dioxide (92% vol./vol.) as carbon source. Cultures were grown in base salts medium with a pH of 2.6 and were incubated at 85°C. An image of a cluster of cells (A) and an image of a single cell (B) are shown.

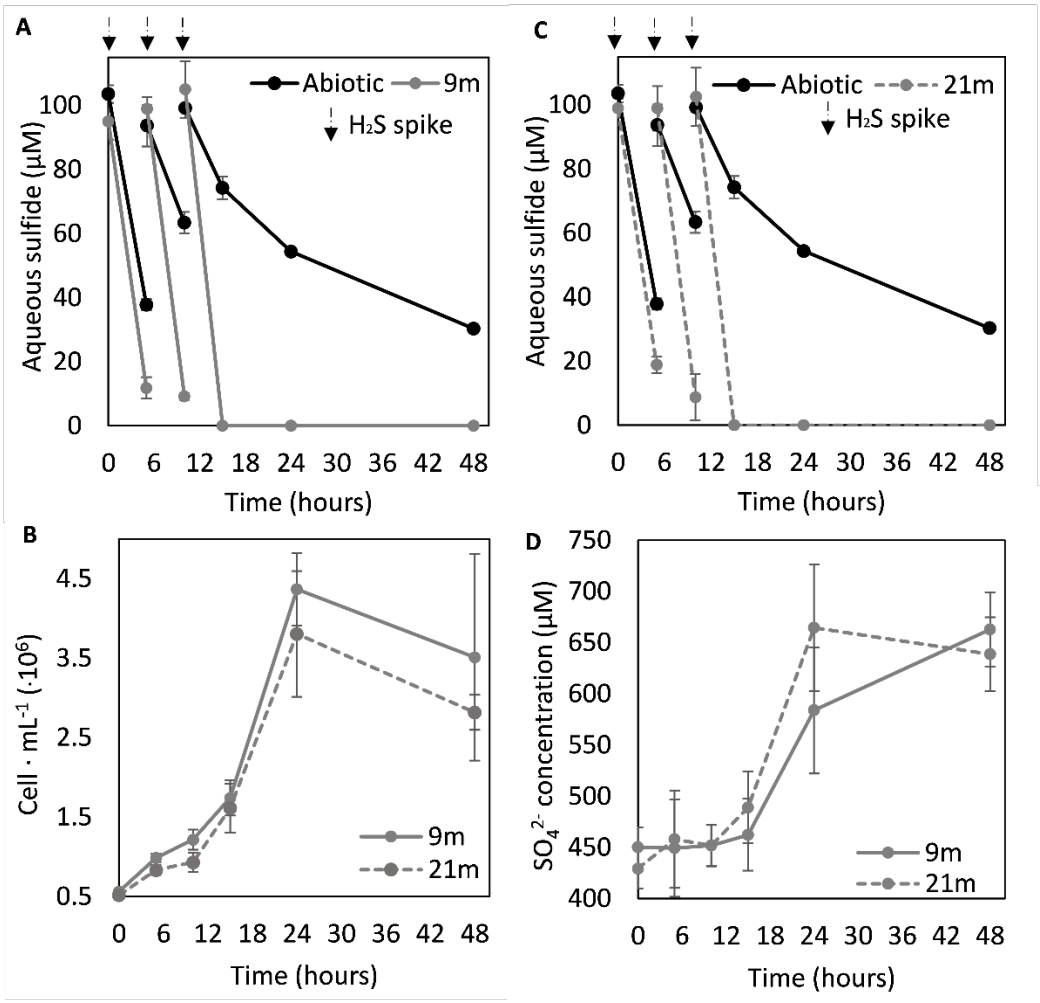

Supplemental Figure 3. Depletion of aqueous sulfide, production of cells, and production of sulfate (SO_4^{2-}) in cultures of *Stygiolobus* strain CP85 – 9 m (A, C, D) and *Stygiolobus* strain CP85 – 21 m (B, C, D). Cultures were incubated at 85°C with oxygen (1.5% headspace vol./vol.) as the electron acceptor and carbon dioxide (92% vol./vol.) as the carbon source. Experiments were conducted in base salts medium with a pH of 2.6. Black arrows depict additions of sulfide (as Na_2S) to achieve ~100 µM. The average and standard deviation of triplicate measurements is shown.

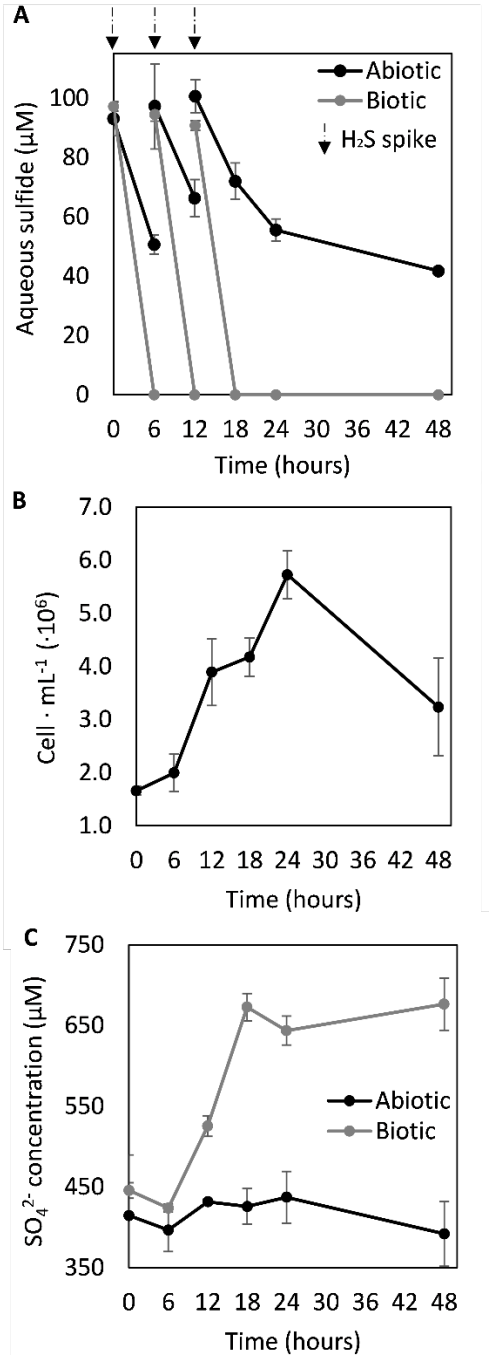

Supplemental Figure 4. Depletion of total sulfide (A), production of cells (B), and production of sulfate (SO_4^{2-}, C). Data are shown for cultures of Sulfolobales strain RB85 – 0m when incubated at 85°C. Oxygen (1.5% headspace vol./vol.) was the electron acceptor and carbon dioxide (92% vol./vol.) was the carbon source. Experiments were conducted in base salts medium with a pH of 3.0. Black arrows depict additions of Na_2S to achieve ~100 µM total sulfide. The average and standard deviation of triplicate measurements is shown.

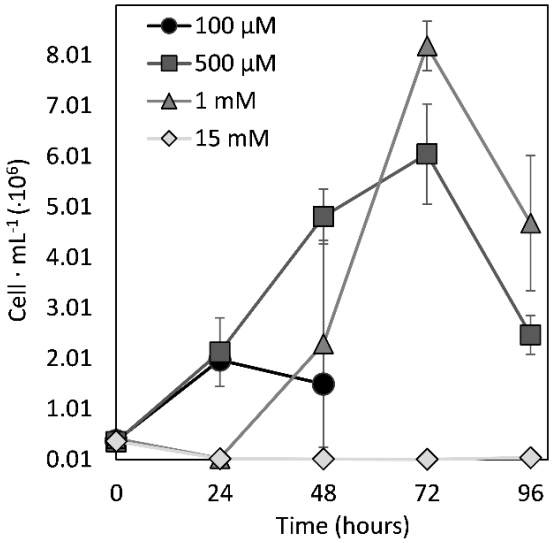

Supplemental Figure 5. Suppression of cell production in cultures of *Stygiolobus* sp. CP85 – 0 m grown in the presence of increasing concentrations of aqueous sulfide when incubated at 85°C. Sulfide was provided as the electron donor, oxygen (1.5% headspace vol./vol.) as the electron acceptor, and carbon dioxide (92% vol./vol.) as the carbon source. Experiments were conducted in base salts medium with a pH of 2.6. Sulfide (as Na_2S) was added at the start of the experiment (time 0 hr) only. Experiments were terminated for each condition after cell production ceased. The average and standard deviation of triplicate measurements is shown.

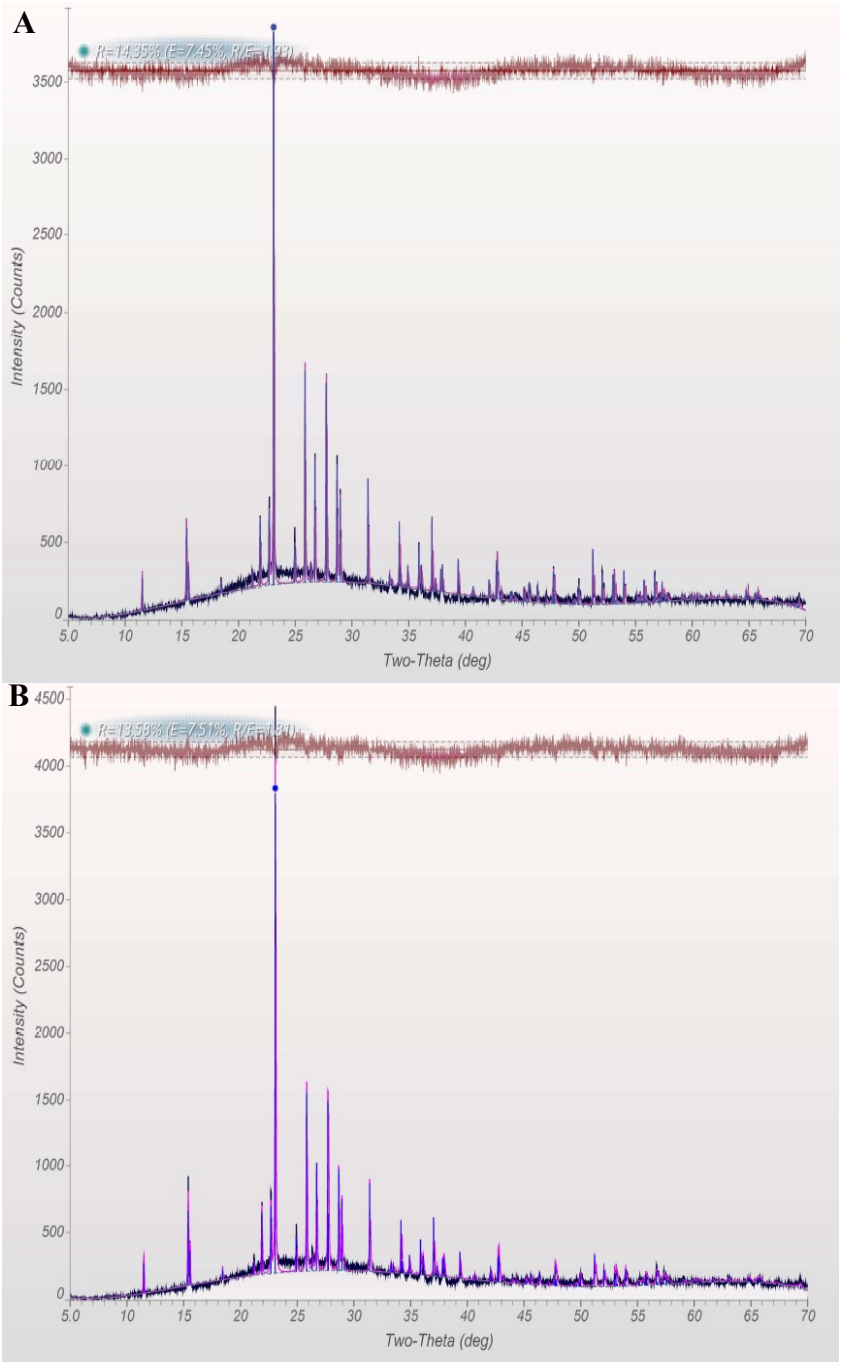

Supplemental Figure 6. X-ray diffraction (XRD) spectra of precipitates formed in abiotic vials containing ferric iron [Fe(III) added as $(Fe_2SO_4)_3$] and sulfide (added as Na_2S) (A), and in abiotic and biotic vials containing 15 mM sulfide (added as Na_2S) with 1.5% O_2 (B), at 85°C. The vials for (A) contained 100% base salt media with a pH of 2.6, whereas vials for (B) contained a 4:1 ratio of base salt media to filtered and autoclaved hot spring water, with a pH of 2.6.

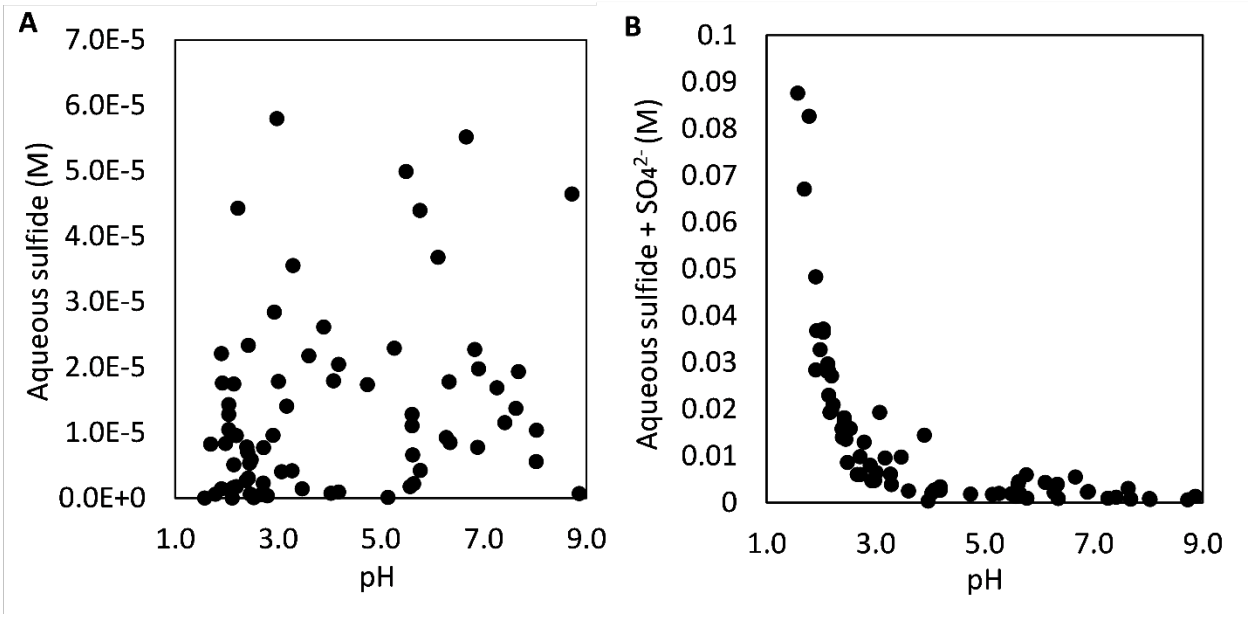

Supplemental Figure 7. Concentrations (in molar) of aqueous sulfide (A) and total sulfide plus sulfate (SO_4^{2-}) (B) in 73 hot springs in Yellowstone National Park. Data was obtained from an open file report from the United States Geological Survey (McCleskey et al., 2014) and span a range of pH (1.3-9.0) and temperature (60-95°C).

CHAPTER FOUR

ACQUISITION OF ELEMENTAL SULFUR BY SULFUR OXIDIZING SULFOLOBALES

Contribution of Authors and Co-Authors

Manuscript in Chapter 4

Author: Maria C. Fernandes-Martins

Contributions: Design the study. Conducted fieldwork. Carried out laboratory experiments and performed bioinformatics analyses. Contributed to the original writing and editing of the manuscript.

Co-Author: Carli Springer

Contributions: Conducted laboratory experiments. Contributed to the revising of the manuscript.

Co-Author: Dan R. Colman

Contributions: Conducted field work and contributed to the editing of the manuscript.

Co-Author: Eric S. Boyd

Contributions: Design the study. Conducted field work and oversaw the study. Contributed to the original writing and editing of the manuscript.

Manuscript Information

Maria C. Fernandes-Martins, Carli Springer, Dan R. Colman, and Eric S. Boyd

Environmental Microbiology

Status of Manuscript:
☐ Prepared for submission to a peer-reviewed journal
☒Officially submitted to a peer-reviewed journal
☐ Accepted by a peer-reviewed journal
☐Published in a peer-reviewed journal

Abstract

Elemental sulfur (S_8^0)-oxidizing Sulfolobales (Archaea) dominate high temperature acidic hot springs (> 80 °C, pH < 4). However, genomic analyses of S_8^0-oxidizing members of the Sulfolobales reveal a patchy distribution of genes encoding sulfur oxygenase reductase (SOR), a S_8^0 disproportionating enzyme typically attributed to S_8^0 oxidation. Here, we report the S_8^0-dependent growth of two Sulfolobales strains previously isolated from acidic hot springs in Yellowstone National Park (YNP), one of which associated with bulk S_8^0 during growth and one that did not. The genomes of each strain encoded different sulfur metabolism enzymes, with only one encoding SOR. Dialysis membrane experiments showed that direct contact is not required for S_8^0 oxidation in the SOR-encoding strain. This is attributed to the generation of sulfide (H_2S) from S_8^0 disproportionation that can solubilize bulk S_8^0 to form soluble polysulfides (S_x^{2-}) and/or S_8^0 nanoparticles that readily diffuse across dialysis membranes. The Sulfolobales strain lacking SOR required direct contact to oxidize S_8^0 which could be overcome by addition of H_2S. High concentrations of S_8^0 inhibited the growth of both strains. These results implicate alternative strategies to acquire and metabolize sulfur in Sulfolobales and have implications for their distribution and ecology in their hot spring habitats.

Introduction

Members of the archaeal order Sulfolobales dominate acidic (pH < 4.0) and high temperature (>80°C) hot springs (Urbieta et al., 2015; Jiang et al., 2016; Ward et al., 2017; Colman et al., 2018). *Sulfolobus*, the first genus of Sulfolobales described, was shown to catalyze the oxygen (O_2)-dependent oxidation of orthorhombic elemental sulfur (S_8^0), generating sulfuric

acid (H_2SO_4) as a product (Brock et al., 1972). This observation helped to explain the acidification of hot springs sourced by sulfide (H_2S)-rich volcanic gas (Brock et al., 1972; Mosser et al., 1973). More specifically, the O_2-dependent oxidation of H_2S generates thiosulfate ($S_2O_3^{2-}$), that disproportionates at acidic pH to form S_8^0 and sulfite (SO_3^{2-}), the latter of which is also unstable in the presence of O_2 and oxidizes to form SO_4^{2-}. However, these collective reactions do not generate net acidity (Nordstrom et al., 2005; Sims et al., 2023; Fernandes-Martins et al., In Review). Rather, it is the O_2-dependent oxidation of S_8^0 that generates net acidity in the form of H_2SO_4. However, S_8^0 is stable in the absence of microbial catalysts (Xu et al., 1998; Nordstrom et al., 2005). Members of the order Sulfolobales therefore became models to understand the oxidation of S_8^0 in acidic high temperature hot springs (Brock et al., 1972; Mosser et al., 1973; Shivvers and Brock, 1973; Colman et al., 2018).

After >50 years of study of Sulfolobales, several themes have emerged of their ecology, physiology, and evolution. For example, all cultivated members of Sulfolobales are thermoacidophiles that tend to be metabolically flexible, growing aerobically or anaerobically through chemoautotrophic, chemoheterotrophic, or chemolithoheterotrophic pathways (Johnson, 1998; Amenabar et al., 2018; Colman et al., 2018; Johnson and Quatrini, 2020; Counts et al., 2021; Lewis et al., 2021; Liu et al., 2021). Further, recent phylogenomic analyses suggest that Sulfolobales diversified from their neutrophilic ancestors ~1.0 – 0.6 Ma, coincident with the rise of atmospheric O_2 concentrations to near present-day levels (Colman, 2018). Yet, genomic analyses of Sulfolobales highlight many remaining unanswered questions of Sulfolobales physiology and ecology. For example, the majority of the proteins encoded by Sulfolobales have undescribed functions (Counts et al., 2021) and little is known about the feedbacks that allowed

for the diversification of Sulfolobales into the acidic habitats that they helped to create (Colman et al., 2018; Counts et al., 2021). Perhaps the largest gap in understanding is the apparent variation in the pathways of S_8^0 oxidation in Sulfolobales.

The only characterized pathway for S_8^0 oxidation in Sulfolobales starts with the O_2-dependent sulfur oxygenase reductase (SOR) enzyme that catalyzes the disproportionation of S_8^0 to form H_2S, SO_3^{2-}, and $S_2O_3^-$ in the cytoplasm (Kletzin, 1989, 1992; Urich et al., 2004; Urich et al., 2006). Surprisingly, only members of the Sulfolobales genera *Acidianus*, *Sulfurisphaera*, *Stygiolobus*, and *Sulfuricidiifex* encode SOR (Counts et al., 2021; Liu et al., 2021) while many other S_8^0-oxidizing Sulfolobales genera including *Metallosphaera*, *Sulfolobus*, and *Saccharolobus* do not encode SOR (Jiang et al., 2014; Sakai and Kurosawa, 2018; Counts et al., 2021; Liu et al., 2021). Further, many Sulfolobales genomes have been assembled from metagenomic sequence that also do not encode SOR (Colman et al., 2022; Sims et al., 2023). However, in lieu of cultivation data, it cannot be assumed that they can oxidize S_8^0. It has been suggested that sulfur dioxygenase (SDO), NADPH:sulfur oxidoreductase (NSR), or heterodisulfide reductase (HDR) may be involved in S_8^0-oxidation in members of the Sulfolobales that lack SOR (Jiang et al., 2014; Wang et al., 2020; Colman et al., 2022).

S_8^0 has a low solubility (<500 nM at 80°C; (Kamyshny, 2009)), suggesting that cells must associate with the surface of the mineral to oxidize it (Weiss, 1973) or somehow otherwise promote its solubilization. Interestingly, thermoacidophilic Archaea that reduce or disproportionate S_8^0, including a member of the Sulfolobales (*Acidianus* strain DS80) that encodes SOR, were shown to not associate with bulk S_8^0 during growth (Boyd and Druschel, 2013; Amenabar and Boyd, 2018). Rather, these cells reduced soluble nanoparticulate S_8^0 that

formed when biologically produced H_2S reacted with bulk S_8^0, generating polysulfide (S_x^{2-}) that rapidly disproportionates at acidic pH to produce soluble molecular S_8 rings. Due to their hydrophobicity, these S_8 rings rapidly aggregate to form nanoparticulate S_8^0. These collective observations raise the question of whether a similar mechanism might be involved in the solubilization of S_8^0 in SOR-encoding Sulfolobales strains and whether this might contribute differences to the respective ecologies of SOR- versus non-SOR-encoding strains, such as planktonic or mineral-surface associated growth

We previously isolated two new Sulfolobales strains capable of oxidizing S_8^0 from acidic hot springs in Yellowstone National Park, Wyoming, U.S.A. One strain, *Stygiolobus* sp. RP85, encodes SOR whereas the other strain, Sulfolobales RB85, does not encode SOR. Microscopic analyses of the two cultures grown under S_8^0-oxidizing conditions revealed that *Stygiolobus* sp. RP85 did not associate with S_8^0 whereas Sulfolobales RB85 was regularly associated with S_8^0 particles. Here, we hypothesize that SOR allows *Stygiolobus* sp. RP85 to grow without direct contact with S_8^0 since H_2S, a product of S_8^0 disproportionation, can initiate the production of S_x^{2-} and soluble nanoparticulate S_8^0, as described above. In contrast, we hypothesized that Sulfolobales RB85 would require direct contact with S_8^0 to oxidize it. The results of experiments aimed at testing these hypotheses shed new light on relevant physiological differences among members of the Sulfolobales that likely contribute to partitioning of the S_8^0 oxidation niche thereby enabling their stable co-existence.

Materials and Methods

Strain Selection

Stygiolobus sp. RP85 and Sulfolobales RB85 were isolated from "Realgar Pool" (RP; pH 3.9, T 85.8°C; 44.73558 N, 110.70705 W) and "Red Bubbler" (RB; pH 3.0, T 90°C; 44.72650 N, 110.70900 W), respectively, both located at Norris Geyser Basin, Yellowstone National Park (YNP) (Fernandes-Martins et al., In Review). *Stygiolobus* sp. RP85 was isolated under autotrophic and microaerophilic H_2S-oxidizing conditions at 85°C and pH 4.0, and it can also oxidize S_8^0. Sulfolobales RB85 was isolated under autotrophic and microaerophilic H_2S-oxidizing conditions at 85°C and pH 3.0 and can also oxidize S_8^0 and H_2 (Fernandes-Martins et al., In Review).

Culture Conditions

Stygiolobus sp. RP85 and Sulfolobales RB85 were cultivated in base salts medium amended with 20% filter-sterilized (0.22 μm) and autoclaved source water from each respective hot springs where the strains were originally isolated. For *Stygiolobus* sp. RP85, this was 'Realgar Pool' (pH 3.9, T 85.8°C) and for Sulfolobales RB85 it was 'Red Bubbler' (pH pH 3.0, T 90°C). Additional details of the springs are reported elsewhere (Fernandes-Martins et al., In Review). Base salts medium contained: NH_4Cl (0.33 g L^{-1}), KCl (0.33 g L^{-1}), $CaCl_2 \cdot 2H_2O$ (0.33 g L^{-1}), $MgCl_2 \cdot 6H_2O$ (0.33 g L^{-1}), and KH_2PO_4 (0.33 g L^{-1}) (Boyd et al., 2007). The pH of the base salts/filtered spring water medium were adjusted to the pH of the spring where the strain was isolated using 0.5 N HCl. Fifty-five mL of base salts/filtered spring water medium was dispensed into 160 mL serum bottles that were then sealed with black butyl rubber stoppers. Sealed serum bottles were autoclaved and then S_8^0 (0.16 g $\cdot$ L^{-1} and 1.6 g $\cdot$ L^{-1}; baked at 100°C, 2

hrs.) was added to the serum bottles once they cooled to below 100°C. Following addition of S_8^0 and while still hot, vials and their contents were purged for 20 min. with N_2 passed over heated (350°C) and H_2-reduced copper shavings. Next, the headspace was purged with a mixture of N_2:carbon dioxide (CO_2) (80:20) for 5 min. and vials were placed in an 80°C incubator. The headspace was equilibrated to atmospheric pressure after two hr. incubation, followed by addition of anoxic and filter-sterilized (0.22 µm) solutions of Wolfe's vitamins (Atlas, 2004) and SL-10 metals (Widdel, 1983) to final concentrations of 1 mL L^{-1} each. Oxygen (O_2) (as air) was added to the headspace to a final concentration of 2% vol./vol. The final headspace contained 78% N_2, 20% CO_2, and 2% O_2, as described above. Inocula for use in S_8^0 oxidation experiments were grown with H_2S (added as Na_2S) as an electron donor to minimize carryover of S_8^0, as previously described (Fernandes-Martins et al., In Review). Five mL (~1/10 dilution) of a log phase culture with depleted H_2S (below limit of detection of 2 µM) was used as inoculum and cultures were incubated on a shaking (50 rotations per minute) platform incubator at a temperature of 80°C.

Monitoring of Growth and Activity

The production of cells was monitored by filtering sub-samples of culture on black, 0.22 µm polycarbonate filters (Millipore Sigma, Billerica, MA), staining with DAPI (2 µg/mL final concentration) for 10 min., and enumeration on an Evos fluorescent microscope (ThermoFisher Scientific, Waltham, MA, U.S.A). The concentration of total aqueous sulfide ($H_2S/HS^-/S^{2-}$ and acid volatile metal sulfides) in cultures was quantified using the methylene blue reduction assay (Fogo and Popowsky, 1949) while the production of sulfate (SO_4^{2-}) in cultures was quantified using a barium chloride turbidity assay (Kolmert et al., 2000).

Evaluating the Requirement for Direct Contact to S_8^0 Mineral

The requirement for direct contact of *Stygiolobus* sp. RP85 and Sulfolobales RB85 cells with S_8^0 (0.16 g · L^{-1}) to catalyze the oxidation of the mineral with O_2 as the electron acceptor was investigated using dialysis membranes of 3.5 kDa pore sizes (Spectrum Laboratories, Gardena, CA). Briefly, dialysis membranes and clips were cleaned with autoclaved Milli-Q water and 50% ethanol incubation steps, as previously described (Amenabar and Boyd, 2018; Payne et al., 2021). After cleaning, dialysis membranes were kept moist and manipulated inside a UV-treated laminar flow hood. One end of each dialysis membrane was sealed with a clip so baked S_8^0 could be added, followed by 1 mL of sterile base salt medium (at the appropriate pH for each strain). Then the other end was also sealed with a clip and dialysis membranes were again rinsed with autoclaved Milli-Q to minimize potential S_8^0 contamination on the outside of the membranes.

The effect of H_2S (~15 μM added as Na_2S) amendment on the requirement for direct contact with S_8^0 to catalyze the oxidation of the mineral with O_2 as the electron acceptor was evaluated by sequestering mineral in dialysis membranes in cultures of Sulfolobales RB85. Uninoculated abiotic controls and positive controls where direct contact was allowed were conducted. Dialysis membranes and clips were included in both sets of controls.

Phylogenomic and Genomic Characterization

The partial genome sequences of *Stygiolobus* sp. RP85 and Sulfolobales RB85 are deposited under BioProject PRJNA1019763. The two partial genomes of the isolates, along with 19 type strains of the Sulfolobales order), and outgroups (*Desulfuroccocus amylolyticus*, *Desulfuroccocus mucosus*, *Thermogladius calderae*, and *Thermosphaera aggregans*) were

subjected to marker gene (n = 30) identification, alignment, and concatenation using Markerfinder (https://github.com/faylward/markerfinder#markerfinder). The resultant alignment block was subjected to phylogenomic reconstruction using the software IQ-Tree (v.1.6.11) (Nguyen et al., 2015) with the LG model specification and 1000 'ultrafast' bootstrap replicates, as previously described (Fernandes-Martins et al., In Review).

The Basic Local Alignment Search Tool (BLASTp) (Boratyn et al., 2012) was used to identify homologs involved (or proposed to be) in the first steps of dissimilatory sulfur metabolism including: Sulfide:quinone oxidoreductase, SQR; sulfur oxygenase:reductase, SOR; sulfur dioxygenase, SDO; heterodisulfide reductase, HdrAB1B2C1C2. Query sequences for use in BLASTp were homologs from the genomes of cultivars with demonstrated metabolic activity (i.e., *Acidianus ambivalens* and *Metallosphaera prunae*). An E-value cutoff of $1.0e^{-50}$, an amino acid identity of >50%, and a coverage of >60% of the query sequence were used to demarcate homologs (Supplemental Table 1).

Results and Discussion

Phylogenomic Analyses and Genomic Characterization of Sulfolobales Cultivars

A phylogenomic reconstruction of *Stygiolobus* sp. RP85 and Sulfolobales RB85, along with Sulfolobales cultivars (n = 19), was constructed, and was overlaid with experimental data compiled from the literature indicating whether the organism could oxidize S_8^0 or sulfide minerals (Fig. 1). Similarly, the presence and absence of sulfur oxidoreductase (SOR) homologs was overlaid on the phylogeny. Only two of the 22 Sulfolobales included in the phylogeny have not been experimentally shown to oxidize S_8^0 or sulfide minerals: *Stygiolobus azoricus* and

Saccharolobus caldissimus. *S. azoricus* was initially reported as a strict anaerobe that coupled H_2 oxidation with S_8^0 reduction (Segerer et al., 1991), although more recent genomic sequencing data revealed the presence of cytochrome *c* oxidase (Cox) protein homologs indicative of an ability to respire aerobically (Counts et al., 2021). Thus, it cannot be ruled out that *S. azoricus* can oxidize S_8^0. On the other hand, *S. caldissimus* is a facultatively anaerobic iron reducer that was experimentally shown not to oxidize S_8^0 when provided with O_2 (Sakai and Kurosawa, 2018).

The phylogenetic distribution of SOR, the most common enzyme attributed to S_8^0 oxidation in the Sulfolobales (Counts et al., 2021; Liu et al., 2021; Ferreira et al., 2022), among the 22 Sulfolobales genomes is also patchy and doesn't fully overlap with experimental data indicating an ability to oxidize S_8^0. Of the 20 genomes from Sulfolobales that can oxidize S_8^0 or sulfide minerals, 11 encoded homologs of Sor and these belonged to only four Sulfolobales genera (*Sulfurisphaera*, *Stygiolobus*, *Sulfuracidifex*, and *Acidianus*) (Fig. 1). Importantly, genomes affiliated with the *Sulfodiicoccus* were not included since members of this genus are inhibited by S_8^0(Sakai and Kurosawa, 2017). Similarly, members of the *Sulfurococcus* genus were not included since partial or complete genomes are not available for these strains (Liu et al., 2021) (Fig. 1). Nonetheless, these results are consistent with previous studies that have shown that nearly half of Sulfolobales do not encode homologs of SOR (Counts et al., 2021; Liu et al., 2021).

The absence of SOR in Sulfolobales strains demonstrated to oxidize S_8^0 or sulfide minerals has prompted transcriptomic or mutagenesis studies to identify alternative mechanisms (Auernik and Kelly, 2008; Jiang et al., 2014; Ai et al., 2019; Zeldes et al., 2019). These studies

have identified a complement of protein encoding genes that appear to be necessary for dissimilatory oxidative sulfur metabolism in Sulfolobales, with the presence/absence of SOR standing out among them. Intriguing, these studies also identified a potential role for sulfur dioxygenase (SDO) S_8^0 or sulfide mineral oxidation. Homologs of this enzyme tend to be present in organisms with the ability to oxidize S_8^0 or sulfide minerals but that lack SOR, with only *Metallosphaera cuprina*, *Saccharolobus solfataricus*, *Stygiolobus azoricus*, and *Sulfolobus acidocaldarius* lacking homologs of both SOR and SDO (Suppl. Table 1). To the extent that SDO may participate in S_8^0 oxidation, the observed distribution of SOR and SDO, including their near ubiquitous nature among certain Sulfolobales genera, suggests that they contribute differently to the physiology and thus ecology of these organisms.

Growth and Activity of *Stygiolobus* sp. RP85 and Sulfolobales RB85 with S_8^0

Both *Stygiolobus* sp. RP85 and Sulfolobales RB85 were grown autotrophically with 2% O_2 vol./vol. and with S_8^0 at concentrations of 0.16 g L^{-1} (5 mM) or 1.6 g L^{-1} (50 mM). For the SOR-encoding *Stygiolobus* sp. RP85, S_8^0 oxidation was coupled to growth (Fig. 2A, B). Interestingly, the growth rate and S_8^0-oxidation activity were greater in cultures provided with 0.16 g L^{-1} S_8^0 than those provided with 1.6 g L^{-1} S_8^0. Cultures provided with 0.16 g L^{-1} S_8^0 had no observed lag phase and achieved a higher cell density ($3.8 \pm 0.7 \times 10^6$ cells mL^{-1}) and a higher SO_4^{2-} concentration (1.5 ± 0.03 mM produced) than those provided with 1.6 g L^{-1} S_8^0. In cultures provided with 1.6 g L^{-1} S_8^0, the lag phase ended between 24 h and 48 h, and the cultures achieved lower cell densities ($1.1 \pm 0.02 \times 10^6$ cells mL^{-1}) and SO_4^{2-} concentrations (0.2 ± 0.06 mM produced). The metabolic coupling efficiency calculated during log phase growth in cultures

provided with 0.16 g L^{-1} S_8^0 was 0.09 cells/picomol SO_4^{2-} and in cultures provided with 1.6 g L^{-1} S_8^0 was 0.07 cells/picomol SO_4^{2-}.

The same pattern of activity was observed for the non-Sor encoding Sulfolobales RB85 strain, with the concentration of S_8^0 influenced growth activity (Fig. 2C, D). No lag phase was observed in cultures provided with 0.16 g L^{-1} S_8^0. Similarly, these cultures achieved higher cell densities ($3.6 \pm 0.9 \times 10^6$ cells mL^{-1}) and SO_4^{2-} concentrations (1.7 ± 0.28 mM total produced) than those provided with 1.6 g L^{-1} S_8^0 ($1.1 \pm 0.05 \times 10^6$ cells mL^{-1} and 0.7 ± 0.12 mM, respectively). The calculated metabolic coupling efficiency during log phase growth in cultures provided with 0.16 g L^{-1} S_8^0 was 0.05 cells/picomol SO_4^{2-} and was in cultures provided with 1.6 g L^{-1} S_8^0 was 0.03 cells/picomol SO_4^{2-}.

Interestingly, for both *Stygiolobus* sp. RP85 and Sulfolobales RB85, an increase in the concentration of S_8^0 had an inhibitory effect on growth and activity, as evidenced by a longer lag phase, slower growth rate, slower SO_4^{2-} production rate, and lower metabolic coupling efficiencies (Fig. 2). Previous studies have shown that S_8^0 can negatively influence the growth of yeast and Bacteria (Libenson et al., 1953; Cetkauskaite et al., 2004; Chen and Lin, 2004; Wang et al., 2022). While the mechanisms of toxicity are not well known, one of the prevailing hypotheses is that S_8^0, which is uncharged and is thought to freely diffuse into the cell (Boyd 2013), can generate oxidative stress once in the cytoplasm (Libenson et al., 1953; Wang et al., 2022). In this role, S_8^0 is thought to oxidize thiol (-SH) compounds (that can have antioxidant properties), leaving the cells unable to balance the redox state of the cytoplasm (Libenson et al., 1953; Wang et al., 2022). This would be particularly detrimental for a thermoacidophile considering that the combination of acidic pH and high temperature impart significant oxidative

stress (Maaty et al., 2009). It is thus possible that the higher amount of S_8^0 used herein imposed additional oxidative stress on cells, resulting in slower growth rates and lower metabolic coupling efficiencies than cultures grown with less S_8^0. Importantly, however, for this to be true an active mechanism of promoting S_8^0 solubilization must be taking place, which is discussed below. All further experiments were conducted using the lower concentration of S_8^0 (0.16 g L^{-1} or 5 mM).

While the kinetics of growth and the metabolic coupling efficiencies were similar in cultures of *Stygiolobus* sp. RP85 and Sulfolobales RB85, differences were noted in the association of cells with S_8^0 mineral regardless of the amount of S_8^0 provided. Whereas Sulfolobales RB85 cells regularly were observed in association with S_8^0 mineral, *Stygiolobus* sp. RP85 cells were rarely observed in association with S_8^0 (Fig. S1). Since the solubility of S_8^0 is low (0.5 µg L^{-1} at 80ºC (Kamyshny, 2009)), and oxidation of S_8^0 is thought to occur inside of the cell, this suggested differences in the mechanisms of accessing S_8^0 to support the metabolism of the two strains.

Requirement for Direct Contact for S_8^0 Oxidation

The qualitative observation of a difference in the association of non-SOR-encoding Sulfolobales RB85 and SOR-encoding *Stygiolobus* sp. RP85 with S_8^0 during growth prompted quantitative experiments to determine the requirement for access to the mineral to catalyze its oxidation. This was achieved by sequestering bulk S_8^0 (0.16 g L^{-1}) in dialysis membranes with pore sizes of 3.5 kDa. The SOR-encoding *Stygiolobus* sp. RP85 grew when physical access to bulk S_8^0 was restricted (Fig. 3A). Interestingly, although there was no difference in the kinetics of growth during the first 24 hr of incubation in cultures provided access to S_8^0 or when S_8^0 was

physically sequestered in dialysis membranes, cell viability was higher in the latter condition with nearly twice the number of cells remaining at the end of 96 hrs incubation ($4.7 \pm 0.2 \times 10^5$ versus $1.2 \pm 0.06 \times 10^6$ cells mL^{-1}). Moreover, production of SO_4^{2-} was much higher in cultures provided with direct access to S_8^0 for the duration of the experiment (Fig. 3B). This is reflected in metabolic coupling efficiencies of 0.07 and 0.22 cells per picomol SO_4^{2-} produced in cultures provided with direct access to S_8^0 versus those where direct access was restricted. This may point to a role for the dialysis membrane in limiting the flux of S_8^0 nanoparticles, which are known to rapidly aggregate due to their hydrophobicity once they are solubilized. In this role, the limited flux of nanoparticles that may have minimized oxidative stress, increased metabolic coupling efficiencies, and minimized cell death.

For non-SOR encoding Sulfolobales RB85, S_8^0 oxidation (as assessed via SO_4^{2-} production) was only observed in cultures when cells were allowed direct access to S_8^0, resulting in production of cells (Fig. 3C). Interestingly, while cultures of Sulfolobales RB85 did not grow when S_8^0 was sequestered in dialysis membranes, they generated ~600 μM SO_4^{2-} over the 120 hr incubation period (Fig. 3D). It is possible that the production of SO_4^{2-} was due to abiotic hydrolysis of S_8^0 ($4S + 4H_2O \rightarrow 3H_2S + H_2SO_4$ (Ellis and Giggenbach, 1971)), which can generate SO_4^{2-} and (in the presence of O_2) sulfur intermediates such as $S_2O_3^{2-}$ and $S_4O_6^{2-}$ (Xu et al., 1998), which could be soluble electron donors supporting cell metabolism. However, S_8^0 hydrolysis occurs at temperatures above the melting point of S_8^0 (~114.5°C (Steudel, 2003)) and is of neglectable importance at temperatures <105°C (Supp. Fig 2) (Xu et al., 1998). As such, S_8^0 hydrolysis cannot account for the ~600 μM SO_4^{2-} generated at 80°C. Further, if S_8^0 hydrolysis was readily occurring and intermediates like $S_2O_3^{2-}$ and $S_4O_6^{2-}$ were being generated abiotically

by O_2, then Sulfolobales RB85 wouldn't need direct contact to S_8^0 to grow. Instead, the observation that Sulfolobales RB85 does appear to need direct access to S_8^0 to grow but not to metabolize S_8^0, is interpreted to reflect the solubility of S_8^0, which while low (<500 nM at 80ºC (Kamyshny, 2009)), is not insoluble. In this model, limited S_8^0 diffused outside the membrane but the amount/flux was not sufficient to support production of cells. Consistent with this interpretation, the amount of SO_4^{2-} produced when cells were not provided direct contact with S_8^0 was ~33% of when direct contact was permitted (~1,550 µM SO_4^{2-} produced after 120 hrs incubation).

Collectively, the microscopic observation that SOR-encoding *Stygiolobus* sp. RP85 does not associate with the surface of S_8^0 and does not require direct access to the mineral during S_8^0-dependent growth and that non-SOR encoding Sulfolobales RB85 strain does associate with the surface of S_8^0 and requires direct access to the mineral during S_8^0-dependent growth points to different mechanisms of acquiring S_8^0 between the two strains. In other words, Sulfolobales that disproportionate S_8^0 appear to indirectly oxidize S_8^0 and to couple this to growth while non-SOR encoding Sulfolobales require direct contact with the S_8^0 mineral to oxidize it and couple this to growth. In support of this hypothesis, the SOR-encoding *Acidianus* strain DS80 was previously shown to grow via indirect contact while disproportioning or reducing S_8^0, presumably due to the role of H_2S in solubilizing S_8^0 as polysulfide that then disproportionated to soluble S_8^0 nanoparticles (Amenabar and Boyd, 2018). However, when cells were grown under S_8^0 oxidizing conditions with Fe(III) ions as electron acceptor, direct contact was required to oxidize the mineral, presumably due to Fe(III) ions spontaneously oxidizing H_2S thereby preventing indirect mineral solubilization (Fernandes-Martins et al., In Review).

H_2S Solubilizes S_8^0 Permitting Indirect Disproportionation/Oxidation

SOR disproportionates S_8^0 to generate H_2S/HS^-, SO_3^{2-}, and $S_2O_3^{2-}$ (Urich et al., 2004; Urich, 2005; Urich et al., 2006; Veith et al., 2011). While the actual substrate for SOR has yet to be fully resolved, it has been suggested that S_x^{2-} are the actual substrate. We were unable to measure SO_3^{2-} and $S_2O_3^{2-}$ intermediates in our studies (data not shown), which is likely due to SOR being intracellular and these products also being generated in the cytoplasm. Further, both SO_3^{2-} and $S_2O_3^{2-}$ are unstable in acidic pH (<4.0) and in the presence of O_2 (Nordstrom et al., 2005; Colman et al., 2020; Sims et al., 2023). On the other hand, H_2S/HS^- (pKa = 6.4 at 80ºC (Amend, 2001)) is likely to be protonated and uncharged/volatile at the cytoplasmic pH of ~ 5.6 measured for *Sulfolobus acidocaldarius* (Sulfolobales) (Lübben and Schäfer, 1989) and thus could freely diffuse out of the cell (Urschel et al., 2015) once it is produced and prior to its consumption via the activity of sulfide:quinone oxidoreductase (Fernandes-Martins et al., In Review).

In cultures of *Stygiolobus* sp. RP85, it was hypothesized that some H_2S diffused out of the cell and reacted with the S_8^0 inside the dialysis membranes, solubilizing it as S_x^{2-} chains. However, at the acidic pH of the growth medium (3.0 to 4.0, pending strain), S_x^{2-} is unstable and disproportionates to reform H_2S and S_8^0 nanoparticles. The S_8^0 nanoparticles are inferred to be small (<20 nm within 2 min. S_x^{2-} of acidification) during their initial formation (Boyd and Druschel, 2013) and can diffuse out of the dialysis membranes and support the growth and activity of SOR-encoding *Stygiolobus* sp. RP85 but not non-SOR-encoding Sulfolobales RB85. Indeed, cyclic voltammetry demonstrated the presence of H_2S, S_x^{2-}, and nanoparticulate S_8^0 in cultures of the thermoacidophilic archaeon *Acidilobus sulfurireducens* (Desulfurococcales) when

actively grown on S_8^0 as an electron acceptor, leading to a similar model for accessing this mineral in this organism (Boyd and Druschel, 2013).

If the model of S_8^0 solubilization that is proposed here is correct, then the addition of small amounts of H_2S should promote the growth of the non-SOR encoding Sulfolobales RB85. To test this hypothesis, the non-SOR encoding Sulfolobales RB85 strain was grown with S_8^0 sequestered in dialysis membranes (3.5 kDa pore size) with amendment of 15 μM H_2S (added as Na_2S) every 24 hr. This concentration of H_2S is known to not support growth (Fig. S3; Fig. 3C). In cultures with sequestered S_8^0 amended with H_2S, S_8^0-dependent growth was observed but was not observed in cultures not amended with H_2S (Fig. 3C). In cultures not provided direct access to S_8^0, amendment with H_2S increased the rates of cell and SO_4^{2-} production (Fig. 3C,D), presumably because the bioavailability of S_8^0 had been increased through the series of chemical reactions described above. However, both conditions achieved the same cell density, ~ 5.1 ± 0.1 x 10^6 cells mL^{-1} by the end of the log phase at 96 h. The production of SO_4^{2-} corresponded to cell growth, and both conditions achieve similar final concentrations of ~ 2 mM.

Conclusions

Sulfolobales are facultative anaerobic thermoacidophiles that inhabit sulfur-rich hot springs worldwide. Despite being remarked as organisms that oxidize S_8^0 and contribute to the formation of acidic hot spring ecosystems (Brock et al., 1972; Mosser et al., 1973; Shivvers and Brock, 1973; Colman et al., 2018), fundamental gaps in understanding of S_8^0 oxidation in these organisms remain including disparities in the distribution of SOR. The present study aimed to begin to fill this gap by identifying phenotypic and ecological differences in SOR- (*Stygiolobus* RP85) and non-SOR- (Sulfolobales RB85) encoding members. When grown with direct access

to S_8^0, both strains exhibited similar metabolic coupling efficiencies. However, SOR-encoding *Stygiolobus* RP85 did not require direct contact with S_8^0 to oxidize the mineral while the non-SOR Sulfolobales RB85 required direct contact. This was attributed to SOR generating H_2S as a product of S_8^0 disproportionation that could diffuse out of the cell and react with sequestered bulk S_8^0. Nucleophilic attack of S_8^0 by H_2S releases S_x^2, which at acidic pH disproportionates to reform H_2S and nanoparticulate S_8^0, the latter of which supports the S_8^0-dependent growth of SOR-encoding strains. The requirement for direct contact with the mineral in the non-SOR Sulfolobales RB85 could be overcome by addition of small amounts of H_2S through artificial initiation of the aforementioned reactions that increase the solubility of S_8^0. Importantly, both strains appeared to metabolize the intermediate species of sulfur (i.e., S_8^0 nanoparticles) better than bulk S_8^0. These observations highlight the need for additional investigation of S_8^0 oxidation in non-SOR-encoding Sulfolobales as well as the investigation of the potential impacts in the distribution and ecology of SOR- versus non-SOR-encoding Sulfolobales across hot springs and within-spring niche partitioning. For example, it is reasonable that the distribution and abundance of Sulfolobales in planktonic versus sediment communities can be influenced based on the requirement for direct contact (non-SOR-encoding strains) or not (SOR encoding strains). To this end, this phenotypic difference could allow for the S_8^0 oxidation niche to be partitioned to minimize overlap and enable the co-existence of SOR- and non-SOR-encoding strains, such as is hot springs in YNP (Colman et al., 2021; Colman et al., 2022). This relationship may become less pronounced in hot springs that have S_8^0 and H_2S, where the feedbacks between these chemical species can increase the bioavailability of S_8^0 and decrease the need to directly associate with the mineral. Such hypotheses should be tested in future

metagenomic/metatranscriptomic analyses of planktonic and sediment-associated communities in acid high temperature hot springs dominated by Sulfolobales.

Acknowledgements

This work was supported by the National Science Foundation (EAR-1820658) to DRC and ESB. MCFM is grateful to the family of Beverly Ferguson and the Molecular Bioscience Program (MBSP) for support of her graduate studies at Montana State University (MSU).

References

Ai, C., Yan, Z., Chai, H., Gu, T., Wang, J., Chai, L. et al. (2019) Increased chalcopyrite bioleaching capabilities of extremely thermoacidophilic Metallosphaera sedula inocula by mixotrophic propagation. *Journal of Industrial Microbiology and Biotechnology* 46: 1113-1127.

Amenabar, M.J., and Boyd, E.S. (2018) Mechanisms of Mineral Substrate Acquisition in a Thermoacidophile. *Applied and Environmental Microbiology* 84: e00334-00318.

Amenabar, M.J., Colman, D.R., Poudel, S., Roden, E.E., and Boyd, E.S. (2018) Electron acceptor availability alters carbon and energy metabolism in a thermoacidophile. *Environ Microbiol* 20: 2523-2537.

Amend, J.P., & Shock, E. L. (2001) Energetics of overall metabolic reactions of thermophilic and hyperthermophilic Archaea and Bacteria. *FEMS Microbiology Reviews* 25: 175-243.

Atlas, R.M. (2004) *Handbook of Microbiologial Media*. Washington, D.C.: ASM Press.

Auernik, K.S., and Kelly, R.M. (2008) Identification of components of electron transport chains in the extremely thermoacidophilic crenarchaeon Metallosphaera sedula through iron and sulfur compound oxidation transcriptomes. *Appl Environ Microbiol* 74: 7723-7732.

Boratyn, G.M., Schäffer, A.A., Agarwala, R., Altschul, S.F., Lipman, D.J., and Madden, T.L. (2012) Domain enhanced lookup time accelerated BLAST. *Biology Direct* 7: 12.

Boyd, E.S., and Druschel, G.K. (2013) Involvement of intermediate sulfur species in biological reduction of elemental sulfur under acidic, hydrothermal conditions. *Appl Environ Microbiol* 79: 2061-2068.

Boyd, E.S., Jackson, R.A., Encarnacion, G., Zahn, J.A., Beard, T., Leavitt, W.D. et al. (2007) Isolation, characterization, and ecology of sulfur-respiring crenarchaea inhabiting acid-sulfate-chloride-containing geothermal springs in Yellowstone National Park. *Appl Environ Microbiol* 73: 6669-6677.

Brock, T.D., Brock, K.M., Belly, R.T., and Weiss, R.L. (1972) Sulfolobus: A New Genus of Sulfur-Oxidizing Bacteria Living at Low pH and High Temperature. *Arch Mikrobiol* 84: 14.

Cetkauskaite, A., Pessala, P., and Södergren, A. (2004) Elemental sulfur: toxicity in vivo and in vitro to bacterial luciferase, in vitro yeast alcohol dehydrogenase, and bovine liver catalase. *Environ Toxicol* 19: 372-386.

Chen, S.-Y., and Lin, J.-G. (2004) Bioleaching of heavy metals from contaminated sediment by indigenous sulfur-oxidizing bacteria in an air-lift bioreactor: effects of sulfur concentration. *Water Research* 38: 3205-3214.

Colman, D.R., Amenabar, M.J., Fernandes-Martins, M.C., and Boyd, E.S. (2022) Subsurface Archaea associated with rapid geobiological change in a model Yellowstone hot spring. *Communications Earth & Environment* 3.

Colman, D.R., Poudel, S., Hamilton, T.L., Havig, J.R., Selensky, M.J., Shock, E.L., and Boyd, E.S. (2018) Geobiological feedbacks and the evolution of thermoacidophiles. *ISME J* 12: 225-236.

Colman, D.R., Lindsay, M.R., Harnish, A., Bilbrey, E.M., Amenabar, M.J., Selensky, M.J. et al. (2021) Seasonal hydrologic and geologic forcing drive hot spring geochemistry and microbial biodiversity. *Environ Microbiol* 23: 4034-4053.

Counts, J.A., Willard, D.J., and Kelly, R.M. (2021) Life in hot acid: a genome-based reassessment of the archaeal order Sulfolobales. *Environ Microbiol* 23: 3568-3584.

Fernandes-Martins, M.C., Colman, D.R., and Boyd, E.S. (2024) Sulfide oxidation by members of the Sulfolobales. *Proccedings of the National Academy of Science Nexus* In Review.

Ferreira, P., Fernandes, P.A., and Ramos, M.J. (2022) The archaeal non-heme iron-containing Sulfur Oxygenase Reductase. *Coordination Chemistry Reviews* 455: 214358.

Fogo, J.K., and Popowsky, M. (1949) Spectrophotometric Determination of Hydrogen Sulfide. *Analytical Chemistry* 21: 732-734.

Jiang, C.-Y., Liu, L.-J., Guo, X., You, X.-Y., Liu, S.-J., and Poetsch, A. (2014) Resolution of carbon metabolism and sulfur-oxidation pathways of Metallosphaera cuprina Ar-4 via comparative proteomics. *Journal of Proteomics* 109: 276-289.

Jiang, Z., Li, P., Jiang, D., Dai, X., Zhang, R., Wang, Y., and Wang, Y. (2016) Microbial Community Structure and Arsenic Biogeochemistry in an Acid Vapor-Formed Spring in Tengchong Geothermal Area, China. *PLOS ONE* 11: e0146331.

Johnson, D.B. (1998) Biodiversity and ecology of acidophilic microorganisms. *FEMS Microbiol Ecol* 27: 307-317.

Johnson, D.B., and Quatrini, R. (2020) Acidophile Microbiology in Space and Time. *Curr Issues Mol Biol* 39: 63-76.

Kamyshny, A. (2009) Solubility of cyclooctasulfur in pure water and sea water at different temperatures. *Geochimica et Cosmochimica Acta* 73: 6022-6028.

Kletzin, A. (1989) Coupled enzymatic production of sulfite, thiosulfate, and hydrogen sulfide from sulfur: purification and properties of a sulfur oxygenase reductase from the facultatively anaerobic archaebacterium Desulfurolobus ambivalens. *Journal of Bacteriology* 171: 1638-1643.

Kletzin, A. (1992) Molecular characterization of the sor gene, which encodes the sulfur oxygenase/reductase of the thermoacidophilic Archaeum Desulfurolobus ambivalens. *Journal of Bacteriology* 174: 5854-5859.

Kolmert, A., Wikström, P., and Hallberg, K.B. (2000) A fast and simple turbidimetric method for the determination of sulfate in sulfate-reducing bacterial cultures. *J Microbiol Methods* 41: 179-184.

Lewis, A.M., Recalde, A., Bräsen, C., Counts, J.A., Nussbaum, P., Bost, J. et al. (2021) The biology of thermoacidophilic archaea from the order Sulfolobales. *FEMS Microbiology Reviews* 45.

Libenson, L., Hadley, F.P., McIlroy, A.P., Wetzel, V.M., and Mellon, R.R. (1953) Antibacterial Effect of Elemental Sulfur. *The Journal of Infectious Diseases* 93: 28-35.

Liu, L.-J., Jiang, Z., Wang, P., Qin, Y.-L., Xu, W., Wang, Y. et al. (2021) Physiology, Taxonomy, and Sulfur Metabolism of the Sulfolobales, an Order of Thermoacidophilic Archaea. *Frontiers in Microbiology* 12.

Lübben, M., and Schäfer, G. (1989) Chemiosmotic energy conversion of the archaebacterial thermoacidophile Sulfolobus acidocaldarius: oxidative phosphorylation and the presence of an F0-related N,N'-dicyclohexylcarbodiimide-binding proteolipid. *Journal of Bacteriology* 171: 6106-6116.

Maaty, W.S., Wiedenheft, B., Tarlykov, P., Schaff, N., Heinemann, J., Robison-Cox, J. et al. (2009) Something old, something new, something borrowed; how the thermoacidophilic archaeon Sulfolobus solfataricus responds to oxidative stress. *PLoS One* 4: e6964.

Mosser, J.L., Mosser, A.G., and Brock, T.D. (1973) Bacterial Origin of Sulfuric Acid in Geothermal Habitats. *Science* 179: 1323-1324.

Nguyen, L.T., Schmidt, H.A., von Haeseler, A., and Minh, B.Q. (2015) IQ-TREE: a fast and effective stochastic algorithm for estimating maximum-likelihood phylogenies. *Mol Biol Evol* 32: 268-274.

Nordstrom, D.K., Ball, J.W., and McCleskey, R.B. (2005) Ground water to surface water: Chemistry of thermal outflows in Yellowstone National Park. In *Geothermal Biology and Geochemistry in Yellowstone National Park*. Inskeep, W.P., and McDermott, T.R. (eds). Bozeman, MT: Thermal Biology Institute, Montana State University pp. 73-94.

Payne, D., Spietz, R.L., and Boyd, E.S. (2021) Reductive dissolution of pyrite by methanogenic archaea. *The ISME Journal* 15: 3498-3507.

Sakai, H.D., and Kurosawa, N. (2017) Sulfodiicoccus acidiphilus gen. nov., sp. nov., a sulfur-inhibited thermoacidophilic archaeon belonging to the order Sulfolobales isolated from a terrestrial acidic hot spring. *International Journal of Systematic and Evolutionary Microbiology* 67: 1880-1886.

Sakai, H.D., and Kurosawa, N. (2018) Saccharolobus caldissimus gen. nov., sp. nov., a facultatively anaerobic iron-reducing hyperthermophilic archaeon isolated from an acidic terrestrial hot spring, and reclassification of Sulfolobus solfataricus as Saccharolobus solfataricus comb. nov. and Sulfolobus shibatae as Saccharolobus shibatae comb. nov. *International journal of systematic and evolutionary microbiology* 68: 1271-1278.

Segerer, A.H., Trincone, A., Gahrtz, M., and Stetter, K.O. (1991) Stygiolobus azoricus gen. nov., sp. nov. Represents a Novel Genus of Anaerobic, Extremely Thermoacidophilic Archaebacteria of the Order Sulfolobales. *International Journal of Systematic and Evolutionary Microbiology* 41: 495-501.

Shivvers, D.W., and Brock, T.D. (1973) Oxidation of Elemental Sulfur by Sulfolobus acidocaldarius. *Journal of Bacteriology* 114: 706-710.

Sims, K.W.W., Messa, C.M., Scott, S.R., Parsekian, A.D., Carr, B.J., Lowenstern, J.B. et al. (2023) A Tale of Two Pools: the dynamic impacts of reactive transport, phase separation and shallow mixing on the geochemistry and microbiology of a coupled Yellowstone hydrothermal system. *In Press*.

Urbieta, M.S., González-Toril, E., Bazán, Á.A., Giaveno, M.A., and Donati, E. (2015) Comparison of the microbial communities of hot springs waters and the microbial biofilms in the acidic geothermal area of Copahue (Neuquén, Argentina). *Extremophiles* 19: 437-450.

Urich, T. (2005) The Sulfur Oxygenase Reductase from Acidianus ambivalens: Functional and structural characterization of a sulfur-disproportionating enzyme. In: Darmstadt, Techn. Univ., Diss., 2005.
Urich, T., Gomes, C.M., Kletzin, A., and Frazão, C. (2006) X-ray Structure of a Self-Compartmentalizing Sulfur Cycle Metalloenzyme. *Science* 311: 996-1000.

Urich, T., Bandeiras, Tiago M., Leal, Sónia S., Rachel, R., Albrecht, T., Zimmermann, P. et al. (2004) The sulphur oxygenase reductase from Acidianus ambivalens is a multimeric protein containing a low-potential mononuclear non-haem iron centre. *Biochemical Journal* 381: 137-146.

Urschel, M.R., Kubo, M.D., Hoehler, T.M., Peters, J.W., Boyd, E.S., and Spormann, A.M. (2015) Carbon Source Preference in Chemosynthetic Hot Spring Communities. *Applied and Environmental Microbiology* 81: 3834-3847.

Veith, A., Urich, T., Seyfarth, K., Protze, J., Frazão, C., and Kletzin, A. (2011) Substrate Pathways and Mechanisms of Inhibition in the Sulfur Oxygenase Reductase of Acidianus Ambivalens. *Frontiers in Microbiology* 2.

Wang, P., Li, L.Z., Qin, Y.L., Liang, Z.L., Li, X.T., Yin, H.Q. et al. (2020) Comparative Genomic Analysis Reveals the Metabolism and Evolution of the Thermophilic Archaeal Genus Metallosphaera. *Frontiers in Microbiology* 11.

Wang, T., Yang, Y., Liu, M., Liu, H., Liu, H., Xia, Y., and Xun, L. (2022) Elemental Sulfur Inhibits Yeast Growth via Producing Toxic Sulfide and Causing Disulfide Stress. *Antioxidants (Basel)* 11.

Ward, L., Taylor, M.W., Power, J.F., Scott, B.J., McDonald, I.R., and Stott, M.B. (2017) Microbial community dynamics in Inferno Crater Lake, a thermally fluctuating geothermal spring. *ISME J* 11: 1158-1167.

Widdel, F. (1983) Methods for enrichment and pure culture isolation of filamentous gliding sulfate-reducing bacteria. *Archives of Microbiology* 134: 282-285.

Zeldes, B.M., Loder, A.J., Counts, J.A., Haque, M., Widney, K.A., Keller, L.M. et al. (2019) Determinants of sulphur chemolithoautotrophy in the extremely thermoacidophilic Sulfolobales. *Environmental Microbiology* 21: 3696-3710.

Figures

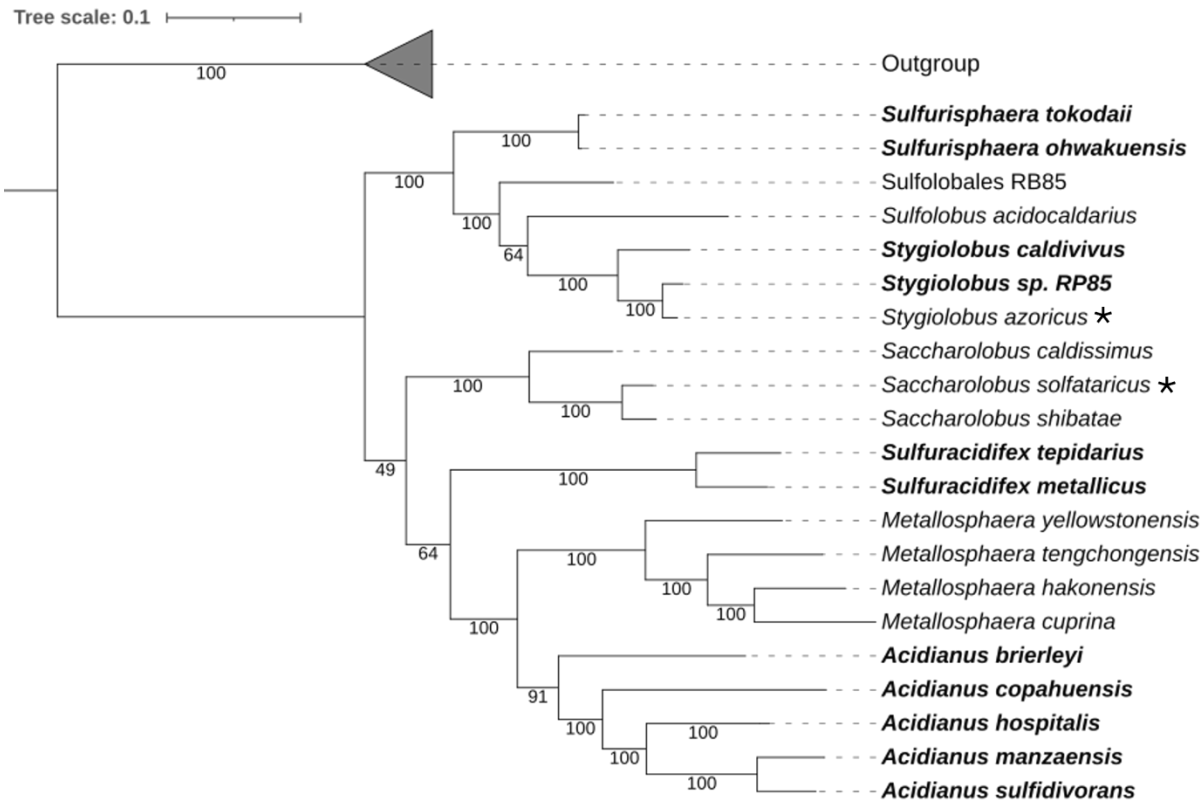

Figure 1. Phylogenomic reconstruction of Sulfolobales cultivars (n = 19) from the literature and Sulfolobales isolates used in this study (Sulfolobales RB85 and *Stygiolobus* sp. RP85). The Maximum-Likelihood phylogeny was constructed using an alignment of marker genes (n = 30) and the LG substitution model. All representative cultivars have the demonstrated ability to oxidize orthorhombic elemental sulfur (S_8^0) (Liu et al 2021), except those with an asterisk (*). Cultivars whose genomes encode for homologs of sulfur oxidoreductase (Sor) are depicted in bold-faced.

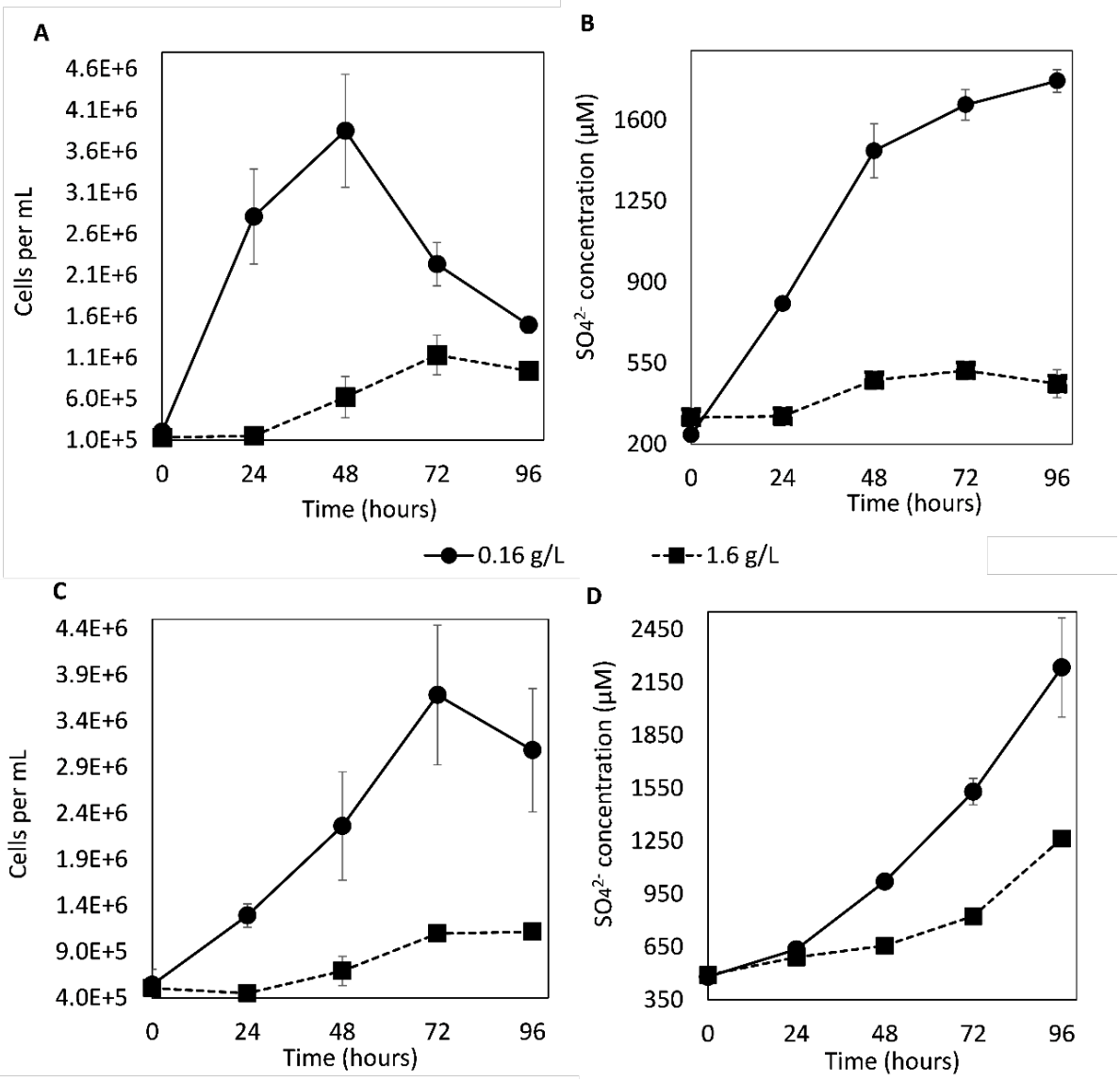

Figure 2. Production of cells and sulfate (SO_4^{2-}) in cultures of *Stygiolobus* sp. RP85 (A, B) and Sulfolobales RB85 (C, D) provided with different starting amounts of orthorhombic elemental sulfur (S_8^0). Oxygen (2% headspace vol./vol.) was the electron acceptor and carbon dioxide (20% vol./vol.) was the carbon source. Cultures were incubated on a shaker (50 rotations per min) at 80°C.

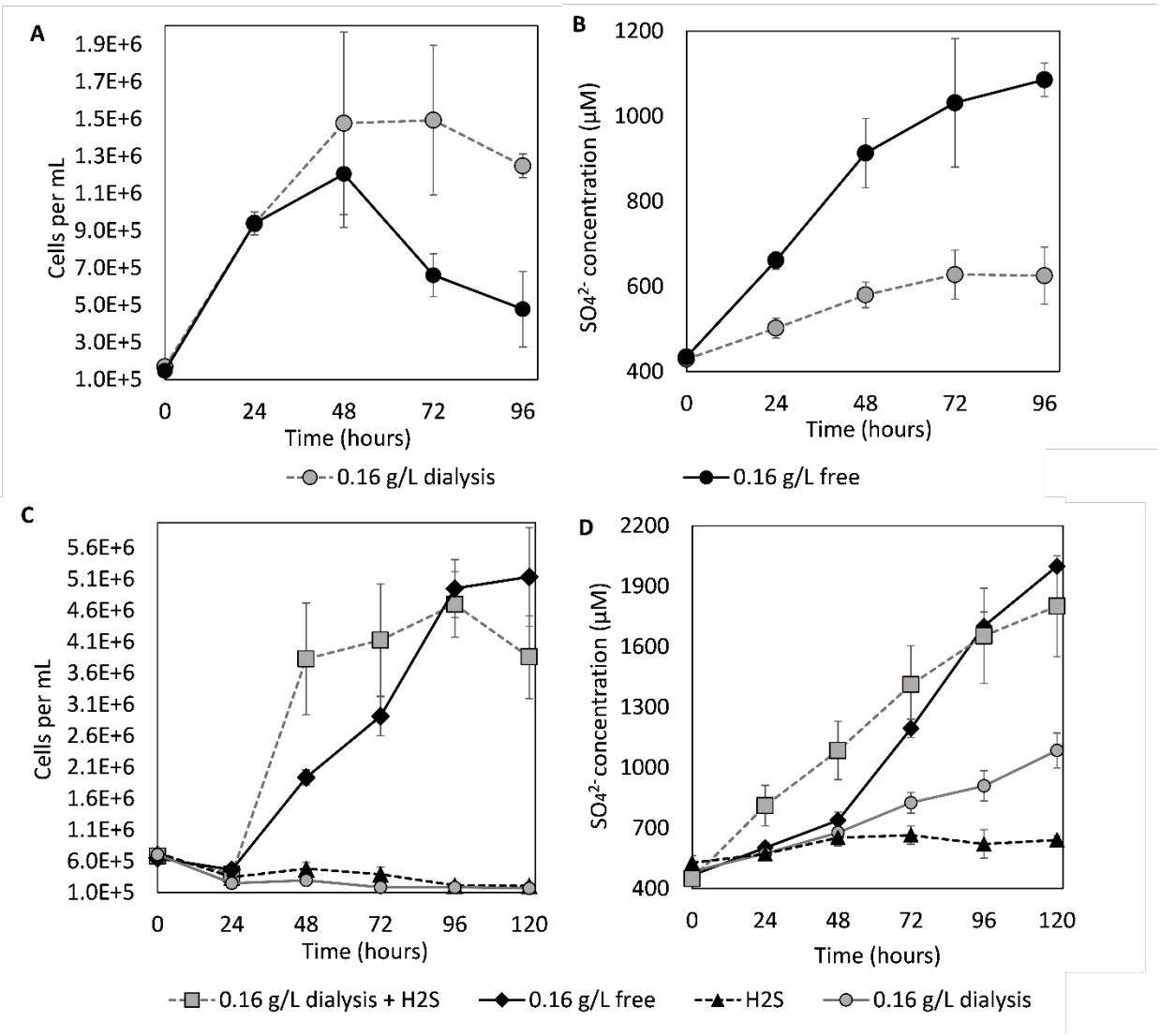

Figure 3. Production of cells and sulfate (SO_4^{2-}) in cultures of *Stygiolobus* sp. RP85 (A,B) and in cultures of Sulfolobales RB85 (C,D). Oxygen (2% headspace vol./vol.) was the electron acceptor and carbon dioxide (20% vol./vol.) was the carbon source. Cultures were incubated on a shaker (50 rotations per min) at 80°C. *Stygiolobus* sp. RP85 cultures were provided with 0.16 g/L orthorhombic elemental sulfur (S_8^0) that was either sequestered in dialysis membranes with 3.5 kDa pore sizes or that was free in solution. Sulfolobales RB85 cultures were provided with 15 µM sulfide (H_2S) only, 0.16 g/L elemental sulfur (S_8^0) only, or 15 µM H_2S and 0.16 g/L elemental sulfur (S_8^0) as electron donors. S_8^0 was either sequestered in dialysis membranes with 3.5 kDa pore sizes or was free in solution. Where indicated, cultures were amended with 15 µM H_2S (as Na_2S) every 24 hrs.

Supplemental Figures

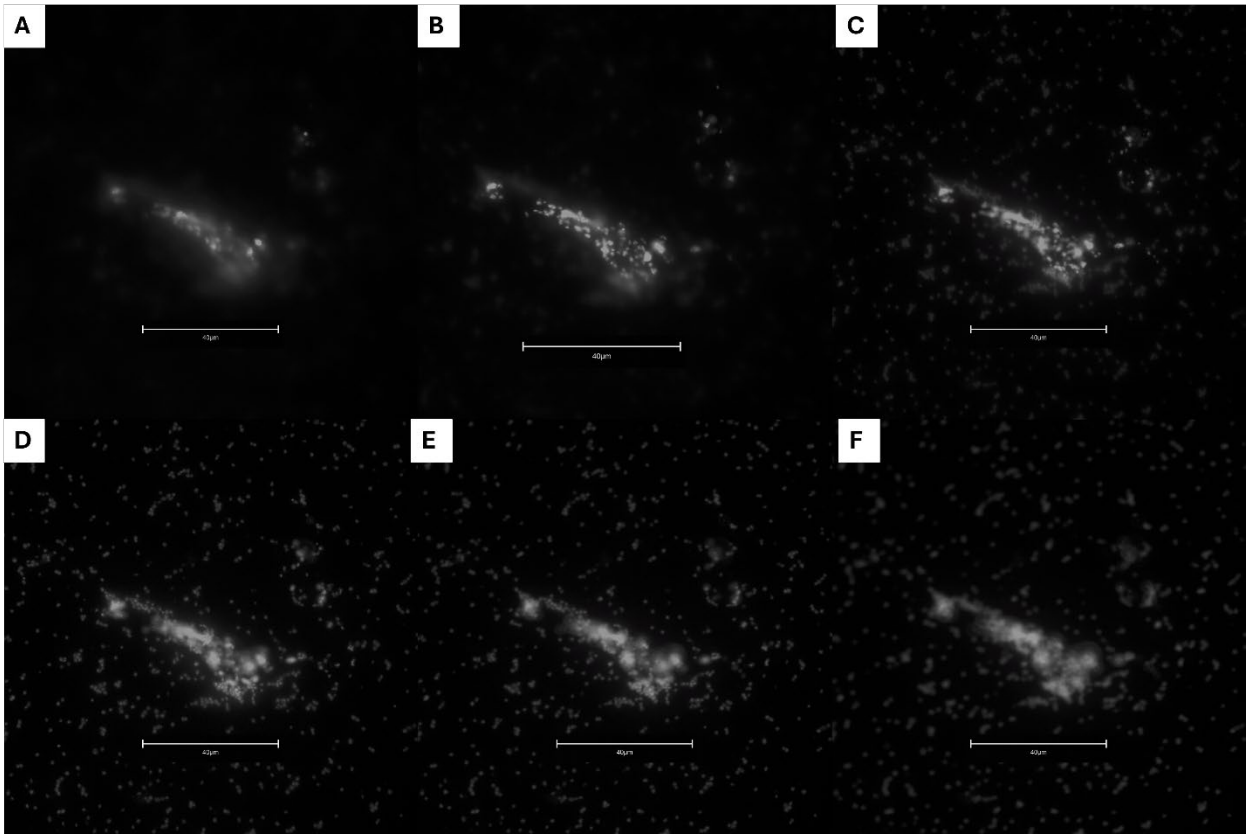

Supplemental Figure 1. Attachment of Sulfolobales RB85 to orthorhombic elemental sulfur (S_8^0). Z-stack pictures (~0.05 µm steps) (A-F) of DAPI- stained Sulfolobales RB85 (white dots) growing on S_8^0-oxidizing conditions. Pictures were obtained on a fluorescence microscope; scale is shown for reference.

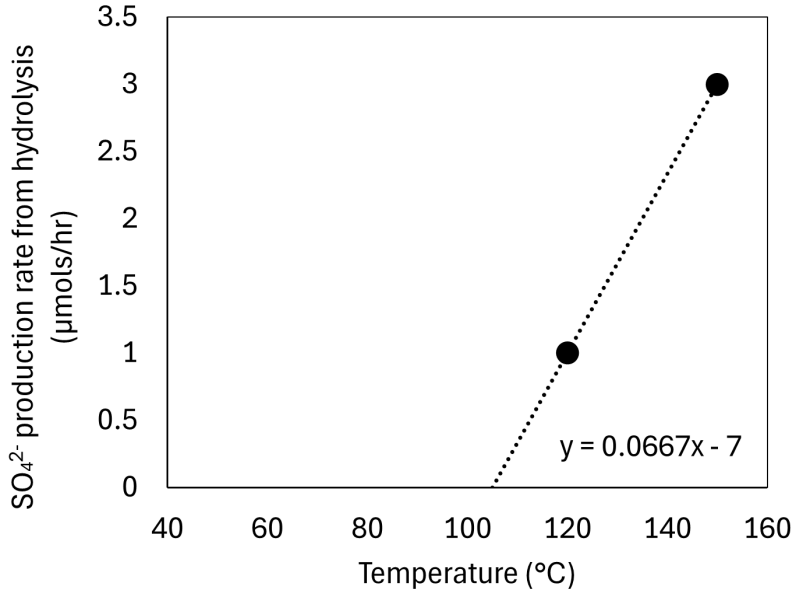

Supplemental Figure 2. Rate of sulfate (SO_4^{2-}) production from orthorhombic elemental sulfur S_8^0 hydrolysis at 120°C and 150°C, as reported previously (Xu et al., 1998). The linear relationship equation is shown, and the rates are extrapolated to the X axis intercept (104-105°C). Hydrolysis of S_8^0 occurs according to the following reaction: $4S + 4H_2O \rightarrow 3H_2S + H_2SO_4$ (Ellis and Giggenbach, 1971).

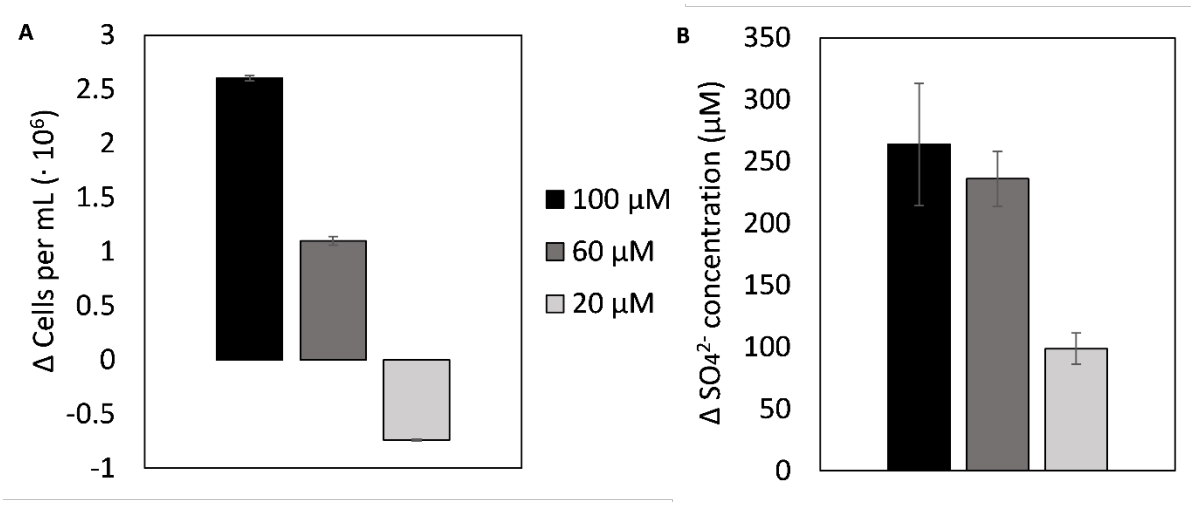

Supplemental Figure 3. Minimum amount of sulfide (added as Na_2S) to support the production of cells and sulfate (SO_4^{2-}) in cultures of Sulfolobales RB85. Sulfide was added to the specified concentration every 24 hrs for a period of 5 days. Oxygen (1.5 % headspace vol./vol.) was the electron acceptor and carbon dioxide (92% vol./vol.) was the carbon source. Cultures were incubated on a shaker (50 rotations per min) at 80°C. The plots indicate the total change (Δ) in cells (A) and SO_4^{2-} (B) after 5 days of incubation.

CHAPTER FIVE

CONCLUSIONS AND FUTURE DIRECTIONS

This thesis focused on the exploration of the feedbacks between thermophilic microorganisms and their environment that dictates their ecology and influenced their evolution, with a particular emphasis placed on members of the Sulfolobales that dominate high temperature moderately acidic to acidic communities. In Chapter 2, the focus was on how the source of fluids to hot springs (i.e., through the processes of phase separation and mixing) influence substrate availability and how this, in turn, influenced microbial community composition, diversity, and primary productivity. It was hypothesized that hot springs sourced by mixed reduced volcanic gases and liquids and oxidized near surface waters exhibit increased availability of electron donors and acceptor pairs and their disequilibrium leading to increased available niches that would select for more diverse communities that were more productive. To address this hypothesis, three co-located high temperature (precluding photosynthetic metabolism) hot springs near Nymph Lake, known as the "Roadside Springs", were studied. These three springs are examples of acidic (pH 3.2; 85.5°C), moderately acidic (pH 5.1; 86.2°C), and neutral (pH 6.6; 68.5°C) hot springs. Geochemical analyses were conducted to determine pH, temperature, dissolved gas content, ion content, and metal content. Metagenomes were generated from planktonic and sediment-associated communities, and radiolabeled CO_2-assimilation assays were performed to assess primary productivity. The results showed that the moderately acidic hot spring ("Roadside North") was sourced by reduced vapor-phase fluids mixing with a mixture of oxidized near surface groundwater and reduced liquid-phase water. The increased niche space afforded by this mixing regime supported greater taxonomic, genomic, and

phylogenetic biodiversity and primary production than for the neutral hot spring (Roadside West) and the acidic hot spring (Roadside East). These findings supported my hypothesis and provided new insights into the geobiological feedbacks controlling the assembly of these microbial communities, and potentially other similar chemosynthetic hot spring communities in YNP and elsewhere.

In Chapter 3, the focus was on acidic hot springs where microorganisms from the archaeal order Sulfolobales dominate microbial communities. Specifically, the focus was on revisiting the role of members of the Sulfolobales in the sulfur cycle and in the acidification of hot spring waters. Despite >50 years of research, fundamental gaps in the understanding of Sulfolobales physiology and ecology remain, including whether microorganisms accelerate the oxidation of H_2S given the prevalence of homologs of sulfide quinone:reductase (SQR) in the genomes of Sulfolobales. Abiotic experiments confirmed that H_2S oxidation by O_2 at acidic pH and at high temperature was kinetically slow. Five new autotrophic strains of Sulfolobales (*Stygiolobus,* and a new unnamed genus, Sulfolobales RB85) were isolated using H_2S as the electron donor and O_2 as the electron acceptor. The genomes of all five strains encoded homologs of SQR. The strains accelerated the oxidation of H_2S relative to abiotic controls and generated SO_4^{2-} and H^+ (sulfuric acid). When compared to growth with S_8^0 as the electron donor, the cell yield was higher with H_2S suggesting that cells may prefer to oxidize H_2S rather than S_8^0, the latter being considered the canonical electron donor for this group of cells. Altogether, the research outlined in Chapter 3 expands our understanding of Sulfolobales in YNP to include a role in the acceleration of H_2S oxidation that initiates the oxidative sulfur cycle and acidification of hot spring waters. These results further underscore the importance of Sulfolobales in the

landscape and biological evolution through the process collectively referred to as niche construction.

In Chapter 4, two of the five strains isolated in Chapter 3 were selected to investigate alternative mechanisms of S_8^0 oxidation. *Stygiolobus* sp. This work was motivated by the observation that members of Sulfolobales encode different complements of genes involved in the oxidative sulfur cycle, most notably homologs of sulfur oxygenase:reductase (SOR), the enzyme involved in S_8^0 disproportionation (ultimately complete oxidation of S_8^0). RP85 encoded SOR whereas Sulfolobales RB85 did not encode SOR. During growth of these two strains, it was noted through microscopic analysis that *Stygiolobus* sp. RP85 was not found in association with particles of S_8^0 while oxidizing/disproportionating the mineral while Sulfolobales RB85 was regularly found in association with S_8^0 mineral. It was hypothesized that this difference in behavior was due to the encoded pathways, since SOR is a disproportionation enzyme, it allows for the generation of intermediate species of sulfur (H_2S) that can diffuse out of the cell and react with S_8^0 ultimately increasing the solubility of the mineral through formation of S_8^0 nanoparticles. This hypothesis was tested through growth activity measurements using dialysis membranes to evaluate the requirement of direct contact to the mineral for growth and activity. The results showed that both strains had better growth and activity with lower concentrations of S_8^0, which agrees with previous suggestions of adverse effects on cell growth and activity due to intracellular oxidative stress by S_8^0 (i.e., nanoparticles). Only *Stygiolobus* sp. RP85 was able to grow without direct contact with S_8^0. Interestingly, Sulfolobales RB85 was able to grow without direct contact with S_8^0 when SOR activity was mimicked through the addition of small concentrations of H_2S to artificially initiate the reaction sequence mentioned above. These results

highlight the importance of intermediate sulfur species in the physiology and ecology of Sulfolobales in acidic hot springs and suggest the acquisition (or loss) of SOR contributes to niche partitioning allowing for the co-existence of non-SOR and SOR encoding Sulfolobales strains.

The results of this thesis work closed several gaps in understanding of hot springs geomicrobiology, in particular as it relates to Sulfolobales physiology and ecology. However, this thesis also identified numerous avenues for additional research. Future research should focus on characterizing a larger number of hot springs that fall into the three pH types (neutral to alkaline, moderately acidic, and acidic) to more firmly establish relationships between the source of fluids to springs, how this dictates hot spring geochemical compositions, and how this in turn manifests in the diversity and primary productivity of resident microbial communities. In addition, future research should be aimed at determining what specific nutrient(s) could be limiting primary productivity in each of the different systems, and if natural and local exogenous forms of nutrients such as dust and/or soil could mitigate these limitations.

While the Sulfolobales strains isolated and described in Chapter 3 were sufficient for the work described therein (as well as in Chapter 4), the original target was the abundant and early diverging Sulfolobales ("Yellowstone group Sulfolobales Acd1") that are widespread across YNP acidic hot springs in YNP. Work presented in Chapter 3 highlighted the benefits of trying to better mimic the natural habitat of target strains. While this was not quite successful in bringing Acd1 into culture, additional efforts should be made to bring this YNP cosmopolitan microorganism into culture. Such studies on this highly abundant, widespread thermoacidophilic archaeon that encodes SQR would naturally lead into the need to better characterize the

importance of H_2S oxidation *in situ* in high temperature (>80°C) acidic hot springs. In line with this, additional transcriptomic and biochemical studies are needed to fully elucidate the pathways of S_8^0 transformation in Sulfolobales. Given that only some members of the Sulfolobales are capable of disproportionation of S_8^0 via SOR, the understanding of S_8^0 oxidation in Sulfolobales is incomplete and represents a large gap in the current understanding of Sulfolobales physiology and ecology. Finally, since acidic hot springs often have co-occurring S_8^0 and H_2S, the propensity to form intermediate sulfur species (e.g., S_x^{2-}, nanoparticulate S_8^0) is high. There is a need to develop tools to measure these highly reactive species and the role of microorganisms in their interconversions in the oxidative and reductive sulfur cycles.

REFERENCES CITED

Ai, C., Yan, Z., Chai, H., Gu, T., Wang, J., Chai, L. et al. (2019) Increased chalcopyrite bioleaching capabilities of extremely thermoacidophilic Metallosphaera sedula inocula by mixotrophic propagation. *Journal of Industrial Microbiology and Biotechnology* 46: 1113-1127.

Allen, E.T., and Day, A.L. (1935) Hot springs of the Yellowstone National Park. *Carnegie Inst Washington Pub* 466.

Amenabar, M.J., and Boyd, E.S. (2018) Mechanisms of Mineral Substrate Acquisition in a Thermoacidophile. *Applied and Environmental Microbiology* 84: e00334-00318.

Amenabar, M.J., and Boyd, E.S. (2019) A review of the mechanisms of mineral-based metabolism in early Earth analog rock-hosted hydrothermal ecosystems. *World J Microbiol Biotechnol* 35: 29.

Amenabar, M.J., Urcshel, M.R., and Boyd, E.S. (2015) Metabolic and taxonomic diversification in continental magmatic hydrothermal systems. *In Microbial Evolution under Extreme Conditions ed Corien Bakermans, De Gruyter*.

Amenabar, M.J., Shock, E.L., Roden, E.E., Peters, J.W., and Boyd, E.S. (2017) Microbial substrate preference dictated by energy demand rather than supply. *Nature Geoscience* 10: 577-581.

Amenabar, M.J., Colman, D.R., Poudel, S., Roden, E.E., and Boyd, E.S. (2018) Electron acceptor availability alters carbon and energy metabolism in a thermoacidophile. *Environ Microbiol* 20: 2523-2537.

Amend, J.P., & Shock, E. L. (2001) Energetics of overall metabolic reactions of thermophilic and hyperthermophilic Archaea and Bacteria. *FEMS Microbiology Reviews* 25: 175-243.

Atlas, R.M. (2004) *Handbook of Microbiologial Media*. Washington, D.C.: ASM Press.

Auernik, K.S., and Kelly, R.M. (2008) Identification of components of electron transport chains in the extremely thermoacidophilic crenarchaeon Metallosphaera sedula through iron and sulfur compound oxidation transcriptomes. *Appl Environ Microbiol* 74: 7723-7732.

Baker-Austin, C., and Dopson, M. (2007) Life in acid: pH homeostasis in acidophiles. *Trends Microbiol* 15: 165-171.

Ball, J.W., McCleskey, R.B., Nordstrom, D.K., and Holloway, J.M. (2006) Water-chemistry data for selected springs, geysers, and streams in Yellowstone National Park, Wyoming, 2003–2005. In. U.S. Geological Survey Open File Report.

Beauchamp, R.O., Bus, J.S., Popp, J.A., Boreiko, C.J., Andjelkovich, D.A., and Leber, P. (1984) A Critical Review of the Literature on Hydrogen Sulfide Toxicity. *CRC Critical Reviews in Toxicology* 13: 25-97.
Berg, I.A. (2011) Ecological aspects of the distribution of different autotrophic CO_2 fixation pathways. *Appl Environ Microbiol* 77: 1925-1936.

Berg, I.A., Kockelkorn, D., Ramos-Vera, W.H., Say, R.F., Zarzycki, J., Hügler, M. et al. (2010) Autotrophic carbon fixation in archaea. *Nat Rev Microbiol* 8: 447-460.

Bergfeld, D., Lowenstern, J.B., Hunt, A.G., Shanks III, W.C.P., and Evans, W. (2011) Gas and isotope chemistry of thermal features in Yellowstone National Park, Wyoming. In. U.S. Geological Survey Report.

Bhattacharya, D., Friedl, T., and Schmidt, H. (1999) The Phylogeny of Thermophiles and Hyperthermophiles and the Three Domains of Life. In *Enigmatic Microorganisms and Life in Extreme Environments*. Seckbach, J. (ed). Dordrecht: Springer Netherlands, pp. 291-304.

Blank Carrine, E., Cady Sherry, L., and Pace Norman, R. (2002) Microbial Composition of Near-Boiling Silica-Depositing Thermal Springs throughout Yellowstone National Park. *Applied and Environmental Microbiology* 68: 5123-5135.

Boratyn, G.M., Schäffer, A.A., Agarwala, R., Altschul, S.F., Lipman, D.J., and Madden, T.L. (2012) Domain enhanced lookup time accelerated BLAST. *Biology Direct* 7: 12.

Boughanemi, S., Lyonnet, J., Infossi, P., Bauzan, M., Kosta, A., Lignon, S. et al. (2016) Microbial oxidative sulfur metabolism: biochemical evidence of the membrane-bound heterodisulfide reductase-like complex of the bacterium Aquifex aeolicus. *FEMS Microbiol Lett* 363.

Boyd, E.S., and Druschel, G.K. (2013) Involvement of intermediate sulfur species in biological reduction of elemental sulfur under acidic, hydrothermal conditions. *Appl Environ Microbiol* 79: 2061-2068.

Boyd, E.S., Leavitt, W.D., and Geesey, G.G. (2009) CO_2 uptake and fixation by a thermoacidophilic microbial community attached to precipitated sulfur in a geothermal spring. *Appl Environ Microbiol* 75: 4289-4296.

Boyd, E.S., Hamilton, T.L., Spear, J.R., Lavin, M., and Peters, J.W. (2010a) [FeFe]-hydrogenase in Yellowstone National Park: evidence for dispersal limitation and phylogenetic niche conservatism. *ISME J* 4: 1485-1495.

Boyd, E.S., Hamilton, T.L., Spear, J.R., Lavin, M., and Peters, J.W. (2010b) [FeFe]-hydrogenase in Yellowstone National Park: evidence for dispersal limitation and phylogenetic niche conservatism. *Isme Journal* 4: 1485-1495.

Boyd, E.S., Fecteau, K.M., Havig, J.R., Shock, E.L., and Peters, J.W. (2012) Modeling the habitat range of phototrophs in yellowstone national park: toward the development of a comprehensive fitness landscape. *Front Microbiol* 3: 221.

Boyd, E.S., Jackson, R.A., Encarnacion, G., Zahn, J.A., Beard, T., Leavitt, W.D. et al. (2007) Isolation, characterization, and ecology of sulfur-respiring crenarchaea inhabiting acid-sulfate-chloride-containing geothermal springs in Yellowstone National Park. *Appl Environ Microbiol* 73: 6669-6677.
Boyer, G. (2023) pyCHNOSZ: Python wrapper for the thermodynamic package CHNOSZ In. https://github.com/worm-portal/AqEquil.

Brierley, J.A. (1966) Contributions of chemoautotrophic bacteria to the acid thermal waters of the geyser springs group in Yellowstone National Park. In *Microbiology*. Bozeman: Montana State University

Brito, J.A., Sousa, F.L., Stelter, M., Bandeiras, T.M., Vonrhein, C., Teixeira, M. et al. (2009) Structural and functional insights into sulfide:quinone oxidoreductase. *Biochemistry* 48: 5613-5622.

Brock, T.D. (1967) Life at High Temperatures. *Science* 158: 1012-1019.

Brock, T.D. (1971) Bimodal distribution of pH values of thermal springs of the world. *Geol Soc Am Bull* 82: 1393-1394.

Brock, T.D., and Freeze, H. (1969) Thermus aquaticus gen. n. and sp. n., a nonsporulating extreme thermophile. *J Bacteriol* 98: 289-297.

Brock, T.D., and Gustafson, J. (1976) Ferric iron reduction by sulfur- and iron-oxidizing bacteria. *Applied and Environmental Microbiology* 32: 567-571.

Brock, T.D., Brock, K.M., Belly, R.T., and Weiss, R.L. (1972) Sulfolobus: A New Genus of Sulfur-Oxidizing Bacteria Living at Low pH and High Temperature. *Arch Mikrobiol* 84: 14.

Brun, P., Zimmermann, N.E., Graham, C.H., Lavergne, S., Pellissier, L., Münkemüller, T., and Thuiller, W. (2019) The productivity-biodiversity relationship varies across diversity dimensions. *Nat Commun* 10: 5691.

Cavicchioli, R., Ripple, W.J., Timmis, K.N., Azam, F., Bakken, L.R., Baylis, M. et al. (2019) Scientists' warning to humanity: microorganisms and climate change. *Nat Rev Microbiol* 17: 569-586.

Cetkauskaite, A., Pessala, P., and Södergren, A. (2004) Elemental sulfur: toxicity in vivo and in vitro to bacterial luciferase, in vitro yeast alcohol dehydrogenase, and bovine liver catalase. *Environ Toxicol* 19: 372-386.

Chafetz, H.S., and Guidry, S.A. (2003) Deposition and diagenesis of Mammoth Hot Springs travertine, Yellowstone National Park, Wyoming, U.S.A.1. *Canadian Journal of Earth Sciences* 40: 1515-1529.

Chapelle, F.H., Vroblesky, D.A., Woodward, J.C., and Lovley, D.R. (1997) Practical considerations for measuring hydrogen concentrations in groundwater. *Environ Sci Tech* 31: 2873–2877.

Chapin, F.S.l., Matson, P.A., and Vitousek, P. (2011) *Principles of Terrestrial Ecosystem Ecology*: New York, NY: Springer Science & Business Media.

Chen, K.Y., and Morris, J.C. (1972) Kinetics of oxidation of aqueous sulfide by oxygen. Environmental Science & Technology. *Environ Sci Tech* 6: 8.
Chen, S.-Y., and Lin, J.-G. (2004) Bioleaching of heavy metals from contaminated sediment by indigenous sulfur-oxidizing bacteria in an air-lift bioreactor: effects of sulfur concentration. *Water Research* 38: 3205-3214.

Chien, A., Edgar, D.B., and Trela, J.M. (1976) Deoxyribonucleic acid polymerase from the extreme thermophile Thermus aquaticus. *Journal of bacteriology* 127: 1550-1557.

Christiansen, R.L. (2001) The quarternary and pliocene Yellowstone plateau volcanic field of Wyoming, Idaho, and Montana. In. U.S. Geological Survey Professional Paper 729-G.

Christiansen, R.L., Lowenstern, J.B., Smith, R.B., Heasler, H.P., Morgan, L.A., Manuel et al. (2007) Preliminary Assessment of Volcanic and Hydrothermal Hazards in Yellowstone National Park and Vicinity. In.

Christner, B.C., Priscu, J.C., Achberger, A.M., Barbante, C., Carter, S.P., Christianson, K. et al. (2014) A microbial ecosystem beneath the West Antarctic ice sheet. *Nature* 512: 310-313.

Ciccarelli, F.D., Doerks, T., von Mering, C., Creevey, C.J., Snel, B., and Bork, P. (2006) Toward Automatic Reconstruction of a Highly Resolved Tree of Life. *Science* 311: 1283-1287.

Clum, A., Huntemann, M., Bushnell, B., Foster, B., Foster, B., Roux, S. et al. (2021) DOE JGI Metagenome Workflow. *mSystems* 6: e00804-00820.

Colman, D.R., Lindsay, M.R., and Boyd, E.S. (2019a) Mixing of meteoric and geothermal fluids supports hyperdiverse chemosynthetic hydrothermal communities. *Nat Commun* 10: 681.

Colman, D.R., Lindsay, M.R., Amenabar, M.J., and Boyd, E.S. (2019b) The Intersection of Geology, Geochemistry, and Microbiology in Continental Hydrothermal Systems. *Astrobiology* 19: 1505-1522.

Colman, D.R., Amenabar, M.J., Fernandes-Martins, M.C., and Boyd, E.S. (2022) Subsurface Archaea associated with rapid geobiological change in a model Yellowstone hot spring. *Communications Earth & Environment* 3.

Colman, D.R., Poudel, S., Stamps, B.W., Boyd, E.S., and Spear, J.R. (2017) The deep, hot biosphere: Twenty-five years of retrospection. *Proc Natl Acad Sci U S A* 114: 6895-6903.

Colman, D.R., Feyhl-Buska, J., Robinson, K.J., Fecteau, K.M., Xu, H., Shock, E.L., and Boyd, E.S. (2016) Ecological differentiation in planktonic and sediment-associated chemotrophic microbial populations in Yellowstone hot springs. *FEMS Microbiol Ecol* 92.

Colman, D.R., Poudel, S., Hamilton, T.L., Havig, J.R., Selensky, M.J., Shock, E.L., and Boyd, E.S. (2018) Geobiological feedbacks and the evolution of thermoacidophiles. *ISME J* 12: 225-236.

Colman, D.R., Lindsay, M.R., Harnish, A., Bilbrey, E.M., Amenabar, M.J., Selensky, M.J. et al. (2021) Seasonal hydrologic and geologic forcing drive hot spring geochemistry and microbial biodiversity. *Environ Microbiol* 23: 4034-4053.
Counts, J.A., Willard, D.J., and Kelly, R.M. (2021) Life in hot acid: a genome-based reassessment of the archaeal order Sulfolobales. *Environ Microbiol* 23: 3568-3584.

Cox, A., Shock, E.L., and Havig, J.R. (2011) The transition to microbial photosynthesis in hot spring ecosystems. *Chem Geol* 280: 344-351.

Craig, H., Gordon, L.I., and Horibe, Y. (1963) Isotopic exchange effects in the evaporation of water. *J Geophys Res* 68: 5079-5087.

D'Imperio, S., Lehr, C.R., Breary, M., and McDermott, T.R. (2007) Autecology of an arsenite chemolithotroph: sulfide constraints on function and distribution in a geothermal spring. *Appl Environ Microbiol* 73: 7067-7074.

D'Imperio, S., Lehr, C.R., Oduro, H., Druschel, G., Kuhl, M., and McDermott, T.R. (2008) Relative importance of H2 and H2S as energy sources for primary production in geothermal springs. *Appl Environ Microbiol* 74: 5802-5808.

Davis, B.M. (1897) The Vegetation of the Hot Springs of Yellowstone Park. *Science* 6: 145-157.

Dunham, E.C., Dore, J.E., Skidmore, M.L., Roden, E.E., and Boyd, E.S. (2021) Lithogenic hydrogen supports microbial primary production in subglacial and proglacial environments. *Proc Natl Acad Sci U S A* 118: e2007051117.

Falkowski, P.G., Fenchel, T., and Delong, E.F. (2008) The microbial engines that drive Earth's biogeochemical cycles. *Science* 320: 1034-1039.

Farrell, J., Smith, R.B., Husen, S., and Diehl, T. (2014) Tomography from 26 years of seismicity revealing that the spatial extent of the Yellowstone crustal magma reservoir extends well beyond the Yellowstone caldera. *Geophysical Research Letters* 41: 3068-3073.

Fernandes-Martins, M.C., Colman, D.R., and Boyd, E.S. (2023) Relationships between fluid mixing, biodiversity, and chemosynthetic primary productivity in Yellowstone hot springs. *Environ Microbiol*.

Fernandes-Martins, M.C., Colman, D.R., and Boyd, E.S. (In Review) Sulfide oxidation by members of the Sulfolobales. *Proccedings of the National Academy of Science Nexus*.

Fernandes-Martins, M.C., Keller, L.M., Munro-Ehrlich, M., Zimlich, K.R., Mettler, M.K., England, A.M. et al. (2021) Ecological dichotomies arise in microbial communities due to mixing of deep hydrothermal waters and atmospheric gas in a circumneutral hot spring. *Appl Environ Microbiol* 87: e01598-01521.

Ferreira, P., Fernandes, P.A., and Ramos, M.J. (2022) The archaeal non-heme iron-containing Sulfur Oxygenase Reductase. *Coordination Chemistry Reviews* 455: 214358.

Fogo, J.K., and Popowsky, M. (1949) Spectrophotometric Determination of Hydrogen Sulfide. *Analytical Chemistry* 21: 732-734.
Fones, E.M., Templeton, A.S., Mogk, D.W., and Boyd, E.S. (2022) Transformation of low-molecular-weight organic acids by microbial endoliths in subsurface mafic and ultramafic igneous rock. *Environ Microbiol*.

Fouke, B.W. (2011) Hot-spring Systems Geobiology: abiotic and biotic influences on travertine formation at Mammoth Hot Springs, Yellowstone National Park, USA. *Sedimentology* 58: 170-219.

Fournier, R.O. (1989) Geochemistry and dynamics of Yellowstone hydrothermal system. *Annu Rev Earth Planet Sci* 17: 13-53.

Gibson, M.L., and Hinman, N.W. (2013) Mixing of hydrothermal water and groundwater near hot springs, Yellowstone National Park (USA): hydrology and geochemistry. *Hydrogeology Journal* 21: 919-933.

Giggenbach, W.F. (1978) The isotopic composition of waters from the El Tatio geothermal field, northern Chile. *Geochim Cosmochim Acta* 42: 979-988.

Giulio, M.D. (2003) The Universal Ancestor was a Thermophile or a Hyperthermophile: Tests and Further Evidence. *Journal of Theoretical Biology* 221: 425-436.

Goordial, J., D'Angelo, T., Labonté, J.M., Poulton, N.J., Brown, J.M., Stepanauskas, R. et al. (2021) Microbial diversity and function in shallow subsurface sediment and oceanic lithosphere of the Atlantis Massif. *mBio* 12: e00490-00421.

Grace, J.B., Anderson, T.M., Seabloom, E.W., Borer, E.T., Adler, P.B., Harpole, W.S. et al. (2016) Integrative modelling reveals mechanisms linking productivity and plant species richness. *Nature* 529: 390-393.

Hamamura, N., Macur, R.E., Korf, S., Ackerman, G., Taylor, W.P., Kozubal, M. et al. (2009) Linking microbial oxidation of arsenic with detection and phylogenetic analysis of arsenite oxidase genes in diverse geothermal environments. *Environmental Microbiology* 11: 421-431.

Hamilton, T.L., Boyd, E.S., and Peters, J.W. (2011) Environmental constraints underpin the distribution and phylogenetic diversity of nifH in the Yellowstone geothermal complex. *Microb Ecol* 61: 860-870.

Hamilton, T.L., Vogl, K., Bryant, D.A., Boyd, E.S., and Peters, J.W. (2012) Environmental constraints defining the distribution, composition, and evolution of chlorophototrophs in thermal features of Yellowstone National Park. *Geobiology* 10: 236-249.

Hamilton, T.L., Koonce, E., Howells, A., Havig, J.R., Jewell, T., Torre, J.R.d.l. et al. (2014) Competition for Ammonia Influences the Structure of Chemotrophic Communities in Geothermal Springs. *Applied and Environmental Microbiology* 80: 653-661.

Heasler, H.P., Jaworowski, C., Foley, D., Young, R., and Norby, L. (2009) Geothermal systems and monitoring hydrothermal features. In *Geological Monitoring*: Geological Society of America, p. 0.

Holland, H.D. (1965) Some applications of thermochemical data to problems of ore deposits; [Part] 2, Mineral assemblages and the composition of ore forming fluids. *Economic Geology* 60: 1101-1166.

Huang, H.-H., Lin, F.-C., Schmandt, B., Farrell, J., Smith, R.B., and Tsai, V.C. (2015) The Yellowstone magmatic system from the mantle plume to the upper crust. *Science* 348: 773-776.

Huber, J.A., Butterfield, D.A., and Baross, J.A. (2002) Temporal changes in archaeal diversity and chemistry in a mid-ocean ridge subseafloor habitat. *Appl Environ Microbiol* 68: 1585-1594.

Huber, J.A., Butterfield, D.A., and Baross, J.A. (2003) Bacterial diversity in a subseafloor habitat following a deep-sea volcanic eruption. *FEMS Microbiol Ecol* 43: 393-409.

Huber, R., and Eder, W. (2006) Aquificales. In *The Prokaryotes*: Springer New York, pp. 925-938.

Huber, R., Eder, W., Heldwein, S., Wanner, G., Huber, H., Rachel, R., and Stetter, K.O. (1998) Thermocrinis ruber gen. nov., sp. nov., A pink-filament-forming hyperthermophilic bacterium isolated from yellowstone national park. *Appl Environ Microbiol* 64: 3576-3583.

Hurwitz, S., and Lowenstern, J.B. (2014) Dynamics of the Yellowstone hydrothermal system. *Rev Geophys* 52: 375-411.

Inskeep, W.P., Jay, Z.J., Tringe, S.G., Herrgard, M.J., Rusch, D.B., Committee, Y.N.P.M.P.S., and Working Group, M. (2013) The YNP metagenome project: environmental parameters responsible for microbial distribution in the Yellowstone geothermal ecosystem. *Front Microbiol* 4: 67.

Inskeep, W.P., Rusch, D.B., Jay, Z.J., Herrgard, M.J., Kozubal, M.A., Richardson, T.H. et al. (2010) Metagenomes from high-temperature chemotrophic systems reveal geochemical controls on microbial community structure and function. *PLoS One* 5: e9773.

Ishino, S., and Ishino, Y. (2014) DNA polymerases as useful reagents for biotechnology - the history of developmental research in the field. *Front Microbiol* 5: 465.

Jay, Z.J., Beam, J.P., Kozubal, M.A., Jennings, R.d., Rusch, D.B., and Inskeep, W.P. (2016) The distribution, diversity and function of predominant Thermoproteales in high-temperature environments of Yellowstone National Park. *Environmental Microbiology* 18: 4755-4769.

Jay, Z.J., Beam, J.P., Dohnalkova, A., Lohmayer, R., Bodle, B., Planer-Friedrich, B. et al. (2015) Pyrobaculum yellowstonensis strain WP30 respires on elemental sulfur and/or arsenate in circumneutral sulfidic geothermal sediments of Yellowstone National Park. *Applied and environmental microbiology* 81: 5907-5916.

Jennings, R.d.M., Moran, J.J., Jay, Z.J., Beam, J.P., Whitmore, L.M., Kozubal, M.A. et al. (2017) Integration of Metagenomic and Stable Carbon Isotope Evidence Reveals the Extent and Mechanisms of Carbon Dioxide Fixation in High-Temperature Microbial Communities. *Frontiers in Microbiology* 8.

Jiang, C.-Y., Liu, L.-J., Guo, X., You, X.-Y., Liu, S.-J., and Poetsch, A. (2014) Resolution of carbon metabolism and sulfur-oxidation pathways of Metallosphaera cuprina Ar-4 via comparative proteomics. *Journal of Proteomics* 109: 276-289.

Jiang, Z., Li, P., Jiang, D., Dai, X., Zhang, R., Wang, Y., and Wang, Y. (2016) Microbial Community Structure and Arsenic Biogeochemistry in an Acid Vapor-Formed Spring in Tengchong Geothermal Area, China. *PLOS ONE* 11: e0146331.

Johnson, D.B. (1998) Biodiversity and ecology of acidophilic microorganisms. *FEMS Microbiol Ecol* 27: 307-317.

Johnson, D.B., and Quatrini, R. (2020) Acidophile Microbiology in Space and Time. *Curr Issues Mol Biol* 39: 63-76.

Kamyshny, A. (2009) Solubility of cyclooctasulfur in pure water and sea water at different temperatures. *Geochimica et Cosmochimica Acta* 73: 6022-6028.

Kanehisa, M., and Goto, S. (2000) KEGG: Kyoto Encyclopedia of Genes and Genomes. *Nucleic Acids Res* 28: 27-30.

Kawarabayasi, Y., Hino, Y., Horikawa, H., Jin-no, K., Takahashi, M., Sekine, M. et al. (2001) Complete Genome Sequence of an Aerobic Thermoacidophilic Crenarchaeon, Sulfolobus tokodaii strain7. *DNA Research* 8: 123-140.

Kawasumi, T., Igarashi, Y., Kodama, T., and Minoda, Y. (1984) Hydrogenobacter thermophilus gen. nov., sp. nov., an extremely thermophilic, aerobic, hydrogen-oxidizing bacterium. *International Journal of Systematic and Evolutionary Microbiology* 34: 5-10.

Kembel, S.W., Cowan, P.D., Helmus, M.R., Cornwell, W.K., Morlon, H., Ackerly, D.D. et al. (2010) Picante: R tools for integrating phylogenies and ecology. *Bioinformatics* 26: 1463-1464.

Kharaka, Y.K., Thordsden, J.J., and White, L.D. (2002) Isotope and chemical compositions of meteoric and thermalwaters and snow from the greater Yellowstone NationalPark region. In. U.S. Geological Survey Open File Report.

Kletzin, A. (1989) Coupled enzymatic production of sulfite, thiosulfate, and hydrogen sulfide from sulfur: purification and properties of a sulfur oxygenase reductase from the facultatively anaerobic archaebacterium Desulfurolobus ambivalens. *Journal of Bacteriology* 171: 1638-1643.

Kletzin, A. (1992) Molecular characterization of the sor gene, which encodes the sulfur oxygenase/reductase of the thermoacidophilic Archaeum Desulfurolobus ambivalens. *Journal of Bacteriology* 174: 5854-5859.

Koch, T., and Dahl, C. (2018) A novel bacterial sulfur oxidation pathway provides a new link between the cycles of organic and inorganic sulfur compounds. *The ISME Journal* 12: 2479-2491.

Kolmert, A., Wikström, P., and Hallberg, K.B. (2000) A fast and simple turbidimetric method for the determination of sulfate in sulfate-reducing bacterial cultures. *J Microbiol Methods* 41: 179-184.

Kozubal, M.A., Macur, R.E., Jay, Z.J., Beam, J.P., Malfatti, S.A., Tringe, S.G. et al. (2012) Microbial iron cycling in acidic geothermal springs of yellowstone national park: integrating molecular surveys, geochemical processes, and isolation of novel fe-active microorganisms. *Front Microbiol* 3: 109.

Kusakabe, M., Komoda, Y., Takano, B., and Abiko, T. (2000) Sulfur isotopic effects in the disproportionation reaction of sulfur dioxide in hydrothermal fluids: implications for the δ34S variations of dissolved bisulfate and elemental sulfur from active crater lakes. *Journal of Volcanology and Geothermal Research* 97: 287-307.

Kushkevych, I., Dordević, D., and Vítězová, M. (2019) Toxicity of hydrogen sulfide toward sulfate-reducing bacteria Desulfovibrio piger Vib-7. *Archives of Microbiology* 201: 389-397.

Kushkevych, I.V. (2013) Effect of hydrogen sulfide at differential concentrations on the process of dissimilatory sulfate reduction by the bacteria Desulfovibrio piger. *Наук зап Тернопнац пед ун-ту Сер Біол,* 4: 6.

Laliberté, E., and Legendre, P. (2010) A distance-based framework for measuring functional diversity from multiple traits. *Ecology* 91: 299-305.

Lencina, A.M., Ding, Z., Schurig-Briccio, L.A., and Gennis, R.B. (2013) Characterization of the Type III sulfide:quinone oxidoreductase from Caldivirga maquilingensis and its membrane binding. *Biochim Biophys Acta* 1827: 266-275.

Lewis, A.M., Recalde, A., Bräsen, C., Counts, J.A., Nussbaum, P., Bost, J. et al. (2021) The biology of thermoacidophilic archaea from the order Sulfolobales. *FEMS Microbiology Reviews* 45.

Liang, J., Crowther, T.W., Picard, N., Wiser, S., Zhou, M., Alberti, G. et al. (2016) Positive biodiversity-productivity relationship predominant in global forests. *Science* 354: 12.

Liang, M., Liu, X., Parker, I.M., Johnson, D., Zheng, Y., Luo, S. et al. (2019) Soil microbes drive phylogenetic diversity-productivity relationships in a subtropical forest. *Sci Adv* 5: 8.

Libenson, L., Hadley, F.P., McIlroy, A.P., Wetzel, V.M., and Mellon, R.R. (1953) Antibacterial Effect of Elemental Sulfur. *The Journal of Infectious Diseases* 93: 28-35.

Lindsay, M.R., Amenabar, M.J., Fecteau, K.M., Debes, R.V., 2nd, Fernandes Martins, M.C., Fristad, K.E. et al. (2018) Subsurface processes influence oxidant availability and chemoautotrophic hydrogen metabolism in Yellowstone hot springs. *Geobiology* 16: 674-692.

Lindsay, M.R., Colman, D.R., Amenabar, M.J., Fristad, K.E., Fecteau, K.M., Debes, R.V., 2nd et al. (2019) Probing the geological source and biological fate of hydrogen in Yellowstone hot springs. *Environ Microbiol* 21: 3816-3830.

Liu, L.-J., Jiang, Z., Wang, P., Qin, Y.-L., Xu, W., Wang, Y. et al. (2021) Physiology, Taxonomy, and Sulfur Metabolism of the Sulfolobales, an Order of Thermoacidophilic Archaea. *Frontiers in Microbiology* 12.

Lowenstern, J.B., Bergfeld, D., Evans, W.C., and Hurwitz, S. (2012) Generation and evolution of hydrothermal fluids at Yellowstone: insights from the Heart Lake Geyser Basin. *Geochem, Geophys Geosyst* 13.

Lowenstern, J.B., Bergfeld, D., Evans, W.C., and Hunt, A.G. (2015) Origins of geothermal gases at Yellowstone. *J Volcanol Geotherm Res* 302: 87-101.

Lübben, M., and Schäfer, G. (1989) Chemiosmotic energy conversion of the archaebacterial thermoacidophile Sulfolobus acidocaldarius: oxidative phosphorylation and the presence of an F0-related N,N'-dicyclohexylcarbodiimide-binding proteolipid. *Journal of Bacteriology* 171: 6106-6116.

Lv, C., Aitchison, E.W., Wu, D., Zheng, L., Cheng, X., and Yang, W. (2016) Comparative exploration of hydrogen sulfide and water transmembrane free energy surfaces via orthogonal space tempering free energy sampling. *Journal of Computational Chemistry* 37: 567-574.

Maaty, W.S., Wiedenheft, B., Tarlykov, P., Schaff, N., Heinemann, J., Robison-Cox, J. et al. (2009) Something old, something new, something borrowed; how the thermoacidophilic archaeon Sulfolobus solfataricus responds to oxidative stress. *PLoS One* 4: e6964.

Marais, D.J.D. (2000) When did photosynthesis emerge on Earth? *Science* 289: 2.

McCleskey, R.B., Ball, J.W., Nordstrom, D.K., Holloway, M.J., and Taylor, E.H. (2004) Water-Chemistry Data for Selected Hot Springs, Geysers, and Streams in Yellowstone National Park, Wyoming, 2001-2002. In *Open-File Report*. Reston, VA.

McCleskey, R.B., Chiu, R.B., Nordstrom, D.K., Campbell, K.M., Roth, D.A., Ball, J.W., and Plowman, T.I. (2014) Water-chemistry data for selected springs, geysers, and streams in Yellowstone National Park, Wyoming, beginning 2009. In. U.S. Geological Survey Open File Report.

McCleskey, R.B., Roth, D.A., Nordstrom, D.K., Hurwitz, S., Holloway, J.M., Bliznik, P.A. et al. (2022) Water-Chemistry and Isotope Data for Selected Springs, Geysers, Streams, and Rivers in Yellowstone National Park, Wyoming:. In. release, U.S.G.S.d. (ed).

Mehta, R., Singhal, P., Singh, H., Damle, D., and Sharma, A.K. (2016) Insight into thermophiles and their wide-spectrum applications. *3 Biotech* 6: 81.

Meuser, J.E., Baxter, B.K., Spear, J.R., Peters, J.W., Posewitz, M.C., and Boyd, E.S. (2013) Contrasting patterns of community assembly in the stratified water column of Great Salt Lake, Utah. *Microb Ecol* 66: 268-280.

Meyer-Dombard, D.A.R., Swingley, W., Raymond, J., Havig, J., Shock, E.L., and Summons, R.E. (2011) Hydrothermal ecotones and streamer biofilm communities in the Lower Geyser Basin, Yellowstone National Park. *Environmental Microbiology* 13: 2216-2231.
Meyer-Dombard, D.R., Shock, E.L., and Amend, J.P. (2005) Archaeal and bacterial communities in geochemically diverse hot springs of Yellowstone National Park, USA. *Geobiology* 3: 211-227.

Miller-Coleman, R.L., Dodsworth, J.A., Ross, C.A., Shock, E.L., Williams, A.J., Hartnett, H.E. et al. (2012) Korarchaeota diversity, biogeography, and abundance in Yellowstone and Great Basin hot springs and ecological niche modeling based on machine learning. *PLoS One* 7: e35964.

Morales, M., Silva, J., Morales, P., Gentina, J.C., and Aroca, G. (2012) Biofiltration of hydrogen sulfide by Sulfolobus metallicus at high temperatures. *Water Sci Technol* 66: 1958-1961.

Morales, M., Arancibia, J., Lemus, M., Silva, J., Gentina, J.C., and Aroca, G. (2011) Bio-oxidation of H2S by Sulfolobus metallicus. *Biotechnology Letters* 33: 2141-2145.

Moriya, Y., Itoh, M., Okuda, S., Yoshizawa, A.C., and Kanehisa, M. (2007) KAAS: an automatic genome annotation and pathway reconstruction server. *Nucleic Acids Res* 35: W182-W185.

Mosser, J.L., Mosser, A.G., and Brock, T.D. (1973) Bacterial Origin of Sulfuric Acid in Geothermal Habitats. *Science* 179: 1323-1324.

Müller, F.H., Bandeiras, T.M., Urich, T., Teixeira, M., Gomes, C.M., and Kletzin, A. (2004) Coupling of the pathway of sulphur oxidation to dioxygen reduction: characterization of a novel membrane-bound thiosulphate:quinone oxidoreductase. *Molecular Microbiology* 53: 1147-1160.

Müller, W.J., Tlalajoe, N., Cason, E.D., Litthauer, D., Reva, O., Brzuszkiewicz, E., and Van Heerden, E. (2016) Whole genome comparison of *Thermu*s sp. NMX2.A1 reveals principal carbon metabolism differences with closest relation *Thermus scotoductus* SA-01. *G3-Genes Genom Genet* 6: 2791-2797.

Munster, M.J., Munster, A.P., Woodrow, J.R., and Sharp, R.J. (1986) Isolation and Preliminary Taxonomic Studies of Thermus Strains Isolated from Yellowstone National Park, USA. *Microbiology* 132: 1677-1683.

Nakagawa, S., Shtaih, Z., Banta, A., Beveridge, T.J., Sako, Y., and Reysenbach, A.-L. (2005a) Sulfurihydrogenibium yellowstonense sp. nov., an extremely thermophilic, facultatively heterotrophic, sulfur-oxidizing bacterium from Yellowstone National Park, and emended descriptions of the genus Sulfurihydrogenibium, Sulfurihydrogenibium subterraneum and Sulfurihydrogenibium azorense. *International Journal of Systematic and Evolutionary Microbiology* 55: 2263-2268.

Nakagawa, S., Takai, K., Inagaki, F., Chiba, H., Ishibashi, J.-I., Kataoka, S. et al. (2005b) Variability in microbial community and venting chemistry in a sediment-hosted backarc hydrothermal system: impacts of subseafloor phase-separation. *FEMS Microbiol Ecol* 54: 141-155.

Nguyen, L.T., Schmidt, H.A., von Haeseler, A., and Minh, B.Q. (2015) IQ-TREE: a fast and effective stochastic algorithm for estimating maximum-likelihood phylogenies. *Mol Biol Evol* 32: 268-274.

Nordstrom, D.K., Ball, W.J., and McCleskey, R.B. (2005a) Ground water to surface water, chemistry of thermal outflows in Yellowstone National Park. In *Geothermal Biology and Geochemistry in Yellowstone National Park*. Inskeep, W.P., and McDermott, T. (eds). Bozeman, MT: Thermal Biology Institute, Montana State University, pp. 73-94.

Nordstrom, D.K., Ball, J.W., and McCleskey, R.B. (2005b) Ground water to surface water: Chemistry of thermal outflows in Yellowstone National Park. In *Geothermal Biology and Geochemistry in Yellowstone National Park*. Inskeep, W.P., and McDermott, T.R. (eds). Bozeman, MT: Thermal Biology Institute, Montana State University pp. 73-94.

Nordstrom, D.K., McCleskey, R.B., and Ball, J.W. (2009a) Sulfur geochemistry of hydrothermal waters in Yellowstone National Park: IV Acid-sulfate waters. *Appl Geochem* 24: 191-207.

Nordstrom, D.K., McCleskey, R.B., and Ball, J.W. (2009b) Sulfur geochemistry of hydrothermal waters in Yellowstone National Park: IV Acid–sulfate waters. *Applied Geochemistry* 24: 191-207.

Ogawa, Y., and Ichimura, S. (1984) Phytoplankton diversity in inland waters of different trophic status. *Japanese J Limnology* 45: 173-177.

Pace, N.R. (1997) A molecular view of microbial diversity and the biosphere. *Science* 276: 734-740.

Pachmayr, F. (1960) Vorkommen und Bestimmung von Schwefelverbindungen in Mineralwasser. In.

Parks, D.H., Imelfort, M., Skennerton, C.T., Hugenholtz, P., and Tyson, G.W. (2015) CheckM: assessing the quality of microbial genomes recovered from isolates, single cells, and metagenomes. *Genome Res* 25: 1043-1055.

Payne, D., Spietz, R.L., and Boyd, E.S. (2021) Reductive dissolution of pyrite by methanogenic archaea. *The ISME Journal* 15: 3498-3507.

Plumb, J.J., Haddad, C.M., Gibson, J.A.E., and Franzmann, P.D. (2007) Acidianus sulfidivorans sp. nov., an extremely acidophilic, thermophilic archaeon isolated from a solfatara on Lihir

Island, Papua New Guinea, and emendation of the genus description. *Int J Syst Evol Microbiol* 57: 1418-1423.

Porter, M.L., Engel, A.S., Kane, T.C., and Kinkle, B.K. (2009) Productivity-diversity relationships from chemolithoautotrophically based sulfidic karst systems. *Int J Speleol* 38: 13.

Prosser, J.I., Bohannan, B.J.M., Curtis, T.P., Ellis, R.J., Firestone, M.K., Freckleton, R.P. et al. (2007) The role of ecological theory in microbial ecology. *Nat Rev Microbiol* 5: 384-392.

Reysenbach, A.-L., Ehringer, M., and Hershberger, K. (2000) Microbial diversity at 83°C in Calcite Springs, Yellowstone National Park: Another environment where the Aquificales and "Korarchaeota" coexist. *Extremophiles* 4: 61-67.

Reysenbach, A.-L., Banta, A., Civello, S., Daly, J., Mitchell, K., Lalonde, S., and al., e. (2005) Aquificales in Yellowstone National Park. In *Geothermal biology and geochemistry in Yellowstone National Park*. W. P. Inskeep, and McDermott, T.R. (eds). Bozeman: Montana State University Thermal Biology Institute, pp. 129-142.
Reysenbach, A.-L., St. John, E., Meneghin, J., Flores, G.E., Podar, M., Dombrowski, N. et al. (2020) Complex subsurface hydrothermal fluid mixing at a submarine arc volcano supports distinct and highly diverse microbial communities. *Proc Natl Acad Sci U S A* 117: 32627-32638.

Reysenbach, A.L., Wickham, G.S., and Pace, N.R. (1994) Phylogenetic analysis of the hyperthermophilic pink filament community in Octopus Spring, Yellowstone National Park. *Appl Environ Microbiol* 60: 2113-2119.

Riahi, S., and Rowley, C.N. (2014) Why Can Hydrogen Sulfide Permeate Cell Membranes? *Journal of the American Chemical Society* 136: 15111-15113.

Rika E., A., Mónica T., B., Steven J., H., and John A., B. (2013) Microbial community structure across fluid gradients in the Juan de Fuca Ridge hydrothermal system. *FEMS Microbiol Ecol* 83: 324-339.

Rodriguez, R.L., Gunturu, S., Tiedje, J.M., Cole, J.R., and Konstantinidis, K.T. (2018) Nonpareil 3: Fast Estimation of Metagenomic Coverage and Sequence Diversity. *mSystems* 3.

Rye, R.O., and Truesdell, A.H. (1993) The question of recharge to the deep thermal reservoir underlying the geysers and hot springs of Yellowstone National Park. In. U.S. Geological Survey Open File Report Vol. 1993.

Saiki, R.K., Scharf, S., Faloona, F., Mullis, K.B., Horn, G.T., Erlich, H.A., and Arnheim, N. (1985) Enzymatic amplification of β-globin genomic sequences and restriction site analysis for diagnosis of sickle cell anemia. *Science* 230: 1350-1354.

Sakai, H.D., and Kurosawa, N. (2017) Sulfodiicoccus acidiphilus gen. nov., sp. nov., a sulfur-inhibited thermoacidophilic archaeon belonging to the order Sulfolobales isolated from a terrestrial acidic hot spring. *International Journal of Systematic and Evolutionary Microbiology* 67: 1880-1886.

Sakai, H.D., and Kurosawa, N. (2018) Saccharolobus caldissimus gen. nov., sp. nov., a facultatively anaerobic iron-reducing hyperthermophilic archaeon isolated from an acidic terrestrial hot spring, and reclassification of Sulfolobus solfataricus as Saccharolobus solfataricus comb. nov. and Sulfolobus shibatae as Saccharolobus shibatae comb. nov. *International journal of systematic and evolutionary microbiology* 68: 1271-1278.

Sakai, H.D., Nakamura, K., and Kurosawa, N. (2022) Stygiolobus caldivivus sp. nov., a facultatively anaerobic hyperthermophilic archaeon isolated from the Unzen hot spring in Japan. *Int J Syst Evol Microbiol* 72.

Sato, Y., Kanbe, H., Miyano, H., Sambongi, Y., Arai, H., Ishii, M., and Igarashi, Y. (2012) Transcriptome analyses of metabolic enzymes in thiosulfate- and hydrogen-grown Hydrogenobacter thermophilus cells. *Biosci Biotechnol Biochem* 76: 1677-1681.

Sayers, E.W., Bolton, E.E., Brister, J.R., Canese, K., Chan, J., Comeau, D.C. et al. (2022) Database resources of the national center for biotechnology information. *Nucleic Acids Res* 50: D20-d26.

Schoen, R. (1969) Rate of Sulfuric Acid Formation in Yellowstone National Park. *GSA Bulletin* 80: 643-650.

Schrenk, M.O., Kelley, D.S., Delaney, J.R., and Baross, J.A. (2003) Incidence and diversity of microorganisms within the walls of an active deep-sea sulfide chimney. *Appl Environ Microbiol* 69: 3580-3592.

Schwartzman, D.W., and Lineweaver, C.H. (2004) The hyperthermophilic origin of life revisited. *Biochem Soc Trans* 32: 168-171.

Sébastien, V. (2008) New multidimensional functional diversity indices for a multifaceted framework in functional ecology. *Ecology* v. 89: pp. 2290-2301-2008 v.2289 no.2298.

Seemann, T. (2014) Prokka: rapid prokaryotic genome annotation. *Bioinformatics* 30: 2068-2069.

Segerer, A.H., Trincone, A., Gahrtz, M., and Stetter, K.O. (1991) Stygiolobus azoricus gen. nov., sp. nov. Represents a Novel Genus of Anaerobic, Extremely Thermoacidophilic Archaebacteria of the Order Sulfolobales. *International Journal of Systematic and Evolutionary Microbiology* 41: 495-501.

Setchell, W.A. (1903) The Upper Temperature Limits of Life. *Science* 17: 934-937.

Shivvers, D.W., and Brock, T.D. (1973) Oxidation of Elemental Sulfur by Sulfolobus acidocaldarius. *Journal of Bacteriology* 114: 706-710.

Shock, E.L., and Holland, M.E. (2007) Quantitative Habitability. *Astrobiology* 7: 839-851.

Shock, E.L., Holland, M., Meyer-Dombard, D.A., Amend, J.P., Osburn, G.R., and Fischer, T.P. (2010) Quantifying inorganic sources of geochemical energy in hydrothermal ecosystems, Yellowstone National Park, USA. *Geochim Cosmochim Acta* 74: 4005-4043.

Silva, J., Ortiz-Soto, R., Morales, M., and Aroca, G. (2023) Effect of the Availability of the Source of Nitrogen and Phosphorus in the Bio-Oxidation of H2S by Sulfolobus metallicus. *Fermentation* 9: 406.

Sims, K.W.W., Messa, C.M., Scott, S.R., Parsekian, A.D., Miller, A., Role, A.L. et al. (2023) The dynamic influence of subsurface geological processes on the assembly and diversification of thermophilic microbial communities in continental hydrothermal systems. *Geochimica et Cosmochimica Acta* 362: 77-103.

Smith, R.B., Jordan, M., Steinberger, B., Puskas, C.M., Farrell, J., Waite, G.P. et al. (2009) Geodynamics of the Yellowstone hotspot and mantle plume: Seismic and GPS imaging, kinematics, and mantle flow. *Journal of Volcanology and Geothermal Research* 188: 26-56.

Smith, V.H. (2007) Microbial diversity-productivity relationships in aquatic ecosystems. *FEMS Microbiol Ecol* 62: 181-186.

Spear, J.R., Waker, J.J., McCollom, T.M., and Pace, N.R. (2005) Hydrogen and bioenergetics in the Yellowstone geothermal ecosystem. *Proc Natl Acad Sci U S A* 102: 2555-2560.

Stefánsson, A., Keller, N.S., Robin, J.G., Kaasalainen, H., Björnsdóttir, S., Pétursdóttir, S. et al. (2016) Quantifying mixing, boiling, degassing, oxidation and reactivity of thermal waters at Vonarskard, Iceland. *Journal of Volcanology and Geothermal Research* 309: 53-62.

Stetter, K.O., Fiala, G., Huber, G., Huber, R., and Segerer, A. (1990) Hyperthermophilic microorganisms. *FEMS Microbiology Letters* 75: 117-124.

Sturchio, N.C., Bohlke, J.K., and Markun, F.J. (1993) Radium isotope geochemistry of thermal waters, Yellowstone National Park, Wyoming, USA. *Geochimica et Cosmochimica Acta* 57: 1203-1214.

Suzuki, M., Hirai, T., Arai, H., Ishii, M., and Igarashi, Y. (2006) Purification, characterization, and gene cloning of thermophilic cytochrome cd1 nitrite reductase from Hydrogenobacter thermophilus TK-6. *J Biosci Bioeng* 101: 391-397.

Takacs-vesbach, C., Inskeep, W.P., Jay, Z.J., Herrgard, M.J., Rusch, D.B., Tringe, S.G. et al. (2013) Metagenome Sequence Analysis of Filamentous Microbial Communities Obtained from Geochemically Distinct Geothermal Channels Reveals Specialization of Three Aquificales Lineages. *Frontiers in Microbiology* 4.

Team, R.C. (2018) R: A language and environment for statistical computing. *R Foundation for Statistical Computing, Vienna, Austria*.

Thauer, R.K., Jungermann, K., and Decker, K. (1977) Energy conservation in chemotrophic anaerobic bacteria. *Bacteriological reviews* 41: 100-180.

Tilman, D., Reich, P.B., and Isbell, F. (2012) Biodiversity impacts ecosystem productivity as much as resources, disturbance, or herbivory. *Proc Natl Acad Sci U S A* 109: 10394-10397.

Truesdell, A.H., and Fournier, R.O. (1976) Conditions in the deeper parts of the hot spring systems of Yellowstone National Park, Wyoming. In. U.S. Geological Survey Open-File Report 76-428.

Truesdell, A.H., Nathenson, M., and Rye, R.O. (1977) The effects of subsurface boiling and dilution on the isotopic compositions of Yellowstone thermal waters. *J Geophys Res* 82: 3694-3704.

Urbieta, M.S., González-Toril, E., Bazán, Á.A., Giaveno, M.A., and Donati, E. (2015) Comparison of the microbial communities of hot springs waters and the microbial biofilms in the acidic geothermal area of Copahue (Neuquén, Argentina). *Extremophiles* 19: 437-450.

Urich, T. (2005) The Sulfur Oxygenase Reductase from Acidianus ambivalens: Functional and structural characterization of a sulfur-disproportionating enzyme. In: Darmstadt, Techn. Univ., Diss., 2005.

Urich, T., Gomes, C.M., Kletzin, A., and Frazão, C. (2006) X-ray Structure of a Self-Compartmentalizing Sulfur Cycle Metalloenzyme. *Science* 311: 996-1000.
Urich, T., Bandeiras, Tiago M., Leal, Sónia S., Rachel, R., Albrecht, T., Zimmermann, P. et al. (2004) The sulphur oxygenase reductase from Acidianus ambivalens is a multimeric protein containing a low-potential mononuclear non-haem iron centre. *Biochemical Journal* 381: 137-146.

Uritskiy, G.V., Diruggiero, J., and Taylor, J. (2018) MetaWRAP—a flexible pipeline for genome-resolved metagenomic data analysis. *Microbiome* 6.

Urschel, M.R., Hamilton, T.L., Roden, E.E., and Boyd, E.S. (2016) Substrate preference, uptake kinetics and bioenergetics in a facultatively autotrophic, thermoacidophilic crenarchaeote. *FEMS Microbiol Ecol* 92: fiw069.

Urschel, M.R., Kubo, M.D., Hoehler, T.M., Peters, J.W., Boyd, E.S., and Spormann, A.M. (2015) Carbon Source Preference in Chemosynthetic Hot Spring Communities. *Applied and Environmental Microbiology* 81: 3834-3847.

Veith, A., Urich, T., Seyfarth, K., Protze, J., Frazão, C., and Kletzin, A. (2011) Substrate Pathways and Mechanisms of Inhibition in the Sulfur Oxygenase Reductase of Acidianus Ambivalens. *Frontiers in Microbiology* 2.

Viollier, E., Inglett, P.W., Hunter, K., Roychoudhury, A.N., and Van Cappellen, P. (2000) The ferrozine method revisited: Fe(II)/Fe(III) determination in natural waters. *Applied Geochemistry* 15: 785-790.

Vitale, M.V., Gardner, P., and Hinman, N.W. (2008) Surface water-groundwater interaction and chemistry in a mineral-armored hydrothermal outflow channel, Yellowstone National Park, USA. *Hydrogeology Journal* 16: 1381-1393.

Wang, P., Li, L.Z., Qin, Y.L., Liang, Z.L., Li, X.T., Yin, H.Q. et al. (2020) Comparative Genomic Analysis Reveals the Metabolism and Evolution of the Thermophilic Archaeal Genus Metallosphaera. *Frontiers in Microbiology* 11.

Wang, T., Yang, Y., Liu, M., Liu, H., Liu, H., Xia, Y., and Xun, L. (2022) Elemental Sulfur Inhibits Yeast Growth via Producing Toxic Sulfide and Causing Disulfide Stress. *Antioxidants (Basel)* 11.

Ward, L., Taylor, M.W., Power, J.F., Scott, B.J., McDonald, I.R., and Stott, M.B. (2017) Microbial community dynamics in Inferno Crater Lake, a thermally fluctuating geothermal spring. *ISME J* 11: 1158-1167.

White, D.E., Hutchinson, Roderick A., and Keith, Terry E.C. (1988) The geology and remarkable thermal activity of Norris Geyser Basin, Yellowstone National Park, Wyoming, U.S. In. U.S. Geological Survey Professional Paper p. 84.

Widdel, F. (1983) Methods for enrichment and pure culture isolation of filamentous gliding sulfate-reducing bacteria. *Archives of Microbiology* 134: 282-285.

Williams, R.A.D., and Da Costa, M.S. (1992) The Genus *Thermus* and Related Microorganisms. In *The Prokaryotes*: Springer, New York, NY., pp. 3745-3753.
Willig, M.R. (2011) Biodiversity and productivity. *Science* 333: 1709-1710.

Zeldes, B.M., Loder, A.J., Counts, J.A., Haque, M., Widney, K.A., Keller, L.M. et al. (2019) Determinants of sulphur chemolithoautotrophy in the extremely thermoacidophilic Sulfolobales. *Environmental Microbiology* 21: 3696-3710.

Zhou, Z., Tran, P., Liu, Y., Kieft, K., and Anantharaman, K. (2019) METABOLIC: A scalable high-throughput metabolic and biogeochemical functional trait profiler based on microbial genomes. *bioRxiv*: 761643.

Zimmermann, P., Laska, S., and Kletzin, A. (1999) Two modes of sulfite oxidation in the extremely thermophilic and acidophilic archaeon Acidianus ambivalens. *Archives of Microbiology* 172: 76-82.